Examining the role of Myt3 in beta-cell function and survival

by

BRYAN RUTHVEN TENNANT

B.Sc., The University of British Columbia, 2006
M.Sc., Simon Fraser University, 2009

A DISSERTATION SUBMITTED IN PARTIAL FULFILLMENT OF

THE REQUIREMENTS FOR THE DEGREE OF

DOCTOR OF PHILOSOPHY

in

THE FACULTY OF GRADUATE AND POSTDOCTORAL STUDIES

(Cell and Developmental Biology)

THE UNIVERSITY OF BRITISH COLUMBIA

(Vancouver)

December 2015

Abstract

Diabetes is a chronic disease that results from the body's inability to properly control circulating blood glucose levels. The loss of glucose homeostasis can arise either from a loss of β-cell mass because of immune-cell mediated attack, as in T1D, and/or from dysfunction of individual β-cells (in conjunction with target organ insulin resistance), as in T2D. Despite advances in current therapies to treat diabetes we are still far from a cure, and a greater understanding of the transcriptional pathways regulating islet development, function and survival will be critical if we are to achieve this goal. The aims of this dissertation were to delineate the role of the transcription factor *Myt3* in β-cell function and survival. To this end we first examined the regulatory mechanisms involved in the control of *Myt3* expression. We demonstrate that *Myt3* expression is dependent on important islet transcription factors, including Foxa2, Pdx1 and Neurod1. We further established that *Myt3* expression is regulated both developmentally, likely by the aforementioned factors, and by external stimuli including glucose and cytokines. From these early results we explored the effect of *Myt3* suppression on the function and survival of β-cells. Our data show that reduced levels of *Myt3* impair the ability of β-cells to migrate, which has potential implications for islet formation during development and compensatory islet neogenesis during diabetes progression, and leads to increased apoptosis. Lastly, to confirm these effects *in vivo* we studied the effects of *Myt3* suppression in syngeneic islet transplants. Our data show that reduced *Myt3* results in increased cell death in the grafts. Collectively, the data presented in this dissertation are an important step in clarifying the regulatory networks responsible for β-cell development, function and survival, and point to *Myt3* as a potential therapeutic target for improving functional β-cell mass.

Preface

All studies in this thesis were conceived and designed by BR Tennant and BG Hoffman.

Studies from Chapter 2 are published in the following article: Tennant BR, Islam R, Kramer MM, Merkulova Y, Kiang RL, Whiting CJ, Hoffman BG. (2012) The transcription factor *Myt3* acts as a pro-survival factor in β-cells. *PloS one*. 7(12):e51501. BR Tennant wrote this work with revisions by BG Hoffman. BR Tennant, R Islam, MM Kramer, Y Merkulova, RL Kiang, CJ Whiting, and BG Hoffman performed experiments. BR Tennant performed data analysis. BG Hoffman generated the data in figures 1 and 2, and made the figures.

Studies from Chapter 3 are published in the following article: Tennant BR, Chen J, Shih AZL, Luciani DS, Hoffman BG. (2015) *Myt3* mediates laminin-V/integrin-β1 induced islet-cell migration via *Tgfbi*. *Molecular Endocrinology*. 29(9): 1254-1268. BR Tennant wrote this work with revisions by DS Luciani and BG Hoffman. BR Tennant, J Chen, AZL Shih and DS Luciani performed experiments. BR Tennant, AZL Shih and BG Hoffman performed data analysis.

BR Tennant performed studies from Chapter 4 with assistance from J Dhillon. D Dai and G Soukhatcheva performed islet transplants. BR Tennant wrote this chapter.

This dissertation was written by BR Tennant with editing provided by BG Hoffman. The University of British Columbia Animal Care Committee approved all animal studies described in this thesis (Certificates # A14-0173, A14-0032 and A00-0033).

Table of Contents

List of Tables

List of Figures

List of Abbreviations

Ad	Adenovirus Serotype V
Akt (Pkb)	Protein Kinase B
ATP	Adenosine Triphosphate
αTC1	AlphaTumour Cell 1
Bak	Bcl2 Homolgous Antagonist/Killer 1
Bax	BCL Associated X Protein
Bcl2	B-Cell CLL/Lymphoma 2
bHLH	Basic Helix Loop Helix
Bid	BH3 Interacting Domain Death Agonist
βGal	Beta Galactosidase
CD45	Lymphocyte Common Antigen
CDA	Canadian Diabetes Association
Cdc42	Cell Division Cycle 42
Cdh1	Epithelial Cadherin
cDNA	Complementary Deoxyribonucleic Acid
ChIP	Chromatin Immunoprecipitation
ChIP-seq	Chromatin Immunoprecipitation Sequencing
Chop (Ddit3)	DNA Damage Inducible Transcript 3
CHX	Cycloheximide
cIap2 (Birc3)	Baculoviral IAP Repeat Containing 3
CNS	Central Nervous System
Cre	Enterobacteriophage P1 Recombinase
CreER	Oestrogen Receptor Coupled Cre
Ctnnb1	Cadherin Associated Protein Beta 1
CVD	Cardiovascular Disease
DIG-UTP	Digoxigenin Uracil Triphosphate
DMEM	Dulbecco's Modified Eagle Medium
DMSO	Dimethyl Sulphoxide
DNA	Deoxyribonucleic Acid
E8.5	Embryonic Day 8.5
ECM	Extracellular Matrix
Egfr	Epidermal Growth Factor Receptor
ELISA	Enzyme Linked Immunosorbent Assay
FACs	Fluorescence Activated Cell Sorting
Fak	Focal Adhesion Kinase
Fasl	FAS Ligand
FBS	Foetal Bovine Serum
Foxa2	Forkhead Box A2
Gadd34	Protein Phosphatase 1 Regulatory Subunit 15A
Gapdh	Glyceraldehyde 3 Phosphate Dehydrogenase
GEO	Gene Expression Omnibus

GFP	Green Fluorescent Protein
Glp-1	Glucagon Like Peptide 1
Glut2	Glucose Transporter 2
GTPase	Guanosine Triphosphate Hydrolase
H3K27ac	Histone 3 Lysine 27 Acetylation
H3K27me3	Histone 3 Lysine 27 Tri-methylation
H3K4me1	Histone 3 Lysine 4 Mono-methylation
H3K4me3	Histone 3 Lysine 4 Tri-methylation
Hex	Beta Hexosamine
Hnf1α	Hepatocyte Nuclear Factor 1 Alpha
Hnf1β	Hepatocyte Nuclear Factor 1 Beta
Hnf4α	Hepatocyte Nuclear Factor 4 Alpha
Iap	Inhibitor of Apoptosis
IAPP	Islet Amyloid Polypeptide
Ifnγ	Interferon Gamma
Igfr1	Insulin Growth Factor Receptor 1
IgG	Immunoglobulin G
Il-1rn	Interleukin 1 Receptor Antagonist
Il-1α	Interleukin 1 Alpha
Il-1β	Interleukin 1 Beta
Il-6	Interleukin 6
iNos	Induced Nitric Oxide Synthase
Ins1	Insulin 1
Ins2	Insulin 2
Insm1	Insulinoma Associated 1
Irf3	Interferon Regulatory Factor 3
Isl1	ISL LIM Homeobox 1
Itga1	Integrin Alpha 1
Itgb3	Integrin Beta 3
KRB	Kreb's Ringer Buffer
Mafa	Musculoaponeurotic Fibrosarcoma Oncogene Homolog A
Mapk	Mitogen Activated Kinase Like Protein
MCF-7	Michigan Cancer Foundation 7
MIN6	Mouse Insulinoma 6
MIP	Mouse Insulin Promoter
miR	Micro RNA
mM	millimolar
MODY	Maturity Onset Diabetes of the Young
MOI	Multiplicity of Infection
mPAC	Mouse Pancreatic Adenocarcinoma
Myt	Myelin Transcription Factor
Neurod1	Neurogenic Differentiation 1
Nfκb	Nuclear Factor Kappa B

Ngn3	Neurogenin 3
NIH	National Institutes of Health
NOD	Non Obese Diabetic
OMM	Outer Mitochondrial Membrane
Pak1	p21 Protein Activated Kinase 1
PCR	Polymerase Chain Reaction
Pdx1	Pancreatic and Duodenal Homeobox 1
PFA	Paraformaldehyde
PFU	Plaque Forming Units
Pik3	Phosphatidylinositol-4,5-bisphosphate 3 Kinase
PP	Pancreatic Polypeptide
Ptf1a	Pancreas Specific Transcription Factor 1A
Ptk2	Protein Tyrosine Kinase 2
Pxn	Paxilin
qPCR	Quantitative Polymerase Chain Reaction
Rac1	Ras-related C3 Botulinum Toxin Substrate 1
Raf1	RAF Proto-oncogene Serine Threonine Protein Kinase
Ras	Rat Sarcoma
Rhoa	RAS Homolog Family Member A
RIPA	Radioimmunoprecipitation assay buffer
RNA	Ribonucleic Acid
Rock	Rho Kinase
RPMI	Roswell Park Memorial Institute Medium
SAGE	Serial Analysis of Gene Expression
SD	Standard Deviation
SEM	Standard Error of the Mean
shRNA	Short Hairpin Ribonucleic Acid
Sin3b	SIN3 Transcription Regulator Family Member B
siRNA	Small Interfering Ribonucleic Acid
Sox9	SRY-related HMG-box 9
St18	Suppressor of Tumourogenicity 18
STZ	Streptozotocin
T1D	Type 1 Diabetes
T2D	Type 2 Diabetes
Tgfbi	Transforming Growth Factor Beta Induced
Tle3	Transducin Like Enhancer of Split 3
Tnfα	Tumour Necrosis Factor Alpha
Trail	Tumour Necrosis Factor Related Apoptosis Inducing Ligand
TSS	Transcription Start Sight
TUNEL	Terminal Deoxynucleotidyl Transferase dUTP Nick End Labeling
UCSC	Univeristy of California, Santa Cruz
Wasf1	WAS Protein Family Member 1

Wasl	Wiskott-Aldrich Syndrome Like
Wnt5a	Wingless Type MMTV Integration Site Family Member 5A
Xbp1	X-Box Binding Protein 1
Xiap	X-Linked Inhibitor of Apoptosis

Acknowledgements

I would like to thank my supervisor Dr. Brad Hoffman for giving me the opportunity to undertake my PhD in his lab. I had initially been looking for work as a lab technician and he saw in me the potential to become an independent researcher and offered for me to become his first graduate student. Over the past five years Brad has provided me with continuous support, guiding me through the experimental design process, improving my writing skills and allowing me to discuss science with him and challenge his ideas to strengthen my reasoning skills. I would also like to thank my supervisory committee, Dr. Bruce Verchere, Dr. Francis Lynn and Dr. Jim Johnson for their ongoing support and encouragement during the past five years. Thank you for your thoughtful discussions about my research and for keeping my research focused and on track.

I would like to thank Cheryl Whiting, Stephanie Campbell and Peter Hurley for always being willing to listen to my complaints, to talk about science and helping with experiments on weekends when I couldn't make it in. A big thank you to Derek Dai and Galina Soukhatcheva for all the work you put in on the transplant studies. I also had the pleasure of working with some very talented students over the years and I can't thank them enough for all the work that they put in. Ada Kim, Marabeth Kramer, Yulia Merkulova, Jenny Chen and Jasmine Dhillon all contributed to the completion of this thesis and they helped me tremendously, not only with experiments, but also to become a better mentor.

I would also like to acknowledge the financial support I received during my degree. I was lucky enough to receive salary support from Dr. Hoffman when I first started in the lab and was later the recipient of salary awards from the CIHR Training Program in

Transplantation, the Child and Family Research Institute and the Canadian Diabetes Association.

Thank you to my family and friends for being so understanding of my long days in the lab and the numerous weekends that I had to bail on due to having mice to monitor or cells to maintain. Hopefully we can make up for lost time in the very near future. A big thank you to my parents, you have supported every decision I have made in getting to this point and have given me every opportunity to excel. Mom, you may not have always understood everything that I was talking about but you were also willing to listen, even if it was just to let me vent. You always had an encouraging word when I was down and were quick to praise my every achievement.

Last, but definitely not least, I would like to thank my wife Jasna. You have supported me throughout this arduous journey and have put up with my many ups and downs along the way. You have encouraged me to pursue my dreams, you have tolerated my busy schedule and you have challenged me to be a better person and researcher. I truly appreciate all the scientific discussions we have had and cannot think of any person I would rather have shared this journey with.

In loving memory of Peter Tennant

Chapter 1: Introduction

1.1 Dissertation overview

Type 1 diabetes (T1D) and type 2 diabetes (T2D) inherently result from an insufficient capacity of the body's β-cells to secrete sufficient insulin to maintain glucose homeostasis [1, 2]. In the case of T1D this deficiency is the result of immune mediated β-cell dysfunction and apoptosis [3], while in T2D, insulin resistance, β-cell dysfunction, and β-cell loss all play important roles [4] and can lead to insulin dependence in many patients. In both cases, it is clear that prevention of diabetes depends on maintenance of β-cell mass and insulin secretory capacity. For this reason, a great deal of recent effort has focused on finding ways to enhance β-cell survival, prevent β-cell death and stimulate β-cell mass replacement. Additional work is being done to generate glucose-responsive insulin-secreting cells from more abundant cell types like embryonic stem cells and hepatocytes [5, 6]. Despite these efforts, to date, these approaches have met with limited success. To develop better strategies it is necessary to improve our understanding of how β-cells are specified, how they mature, and how they respond to immune attack as in T1D and nutrient stress associated with T2D.

The transcriptional networks governing β-cell genesis, function and survival have been intensively studied to identify novel targets for diabetes therapies [7-10] but despite this, our understanding of these transcriptional networks is still far from complete and further investigations are necessary to fill in the gaps. Our laboratory previously determined that Myelin transcription factor 3 (*Myt3*), also known as *Suppressor of tumourigenicity 18* (*St18*), is highly expressed in pancreatic islets [8]. In addition, *Myt3* is a target and mediator of cytokine signalling in both islets and fibroblasts, and was demonstrated to compensate for the

loss of *Myt1* in regulating islet function [11-13], as such this body of work is designed to establish the role of *Myt3* in β-cell function and survival.

1.2 Diabetes mellitus

1.2.1 Prevalence, diagnosis and complications

Diabetes mellitus is a complex metabolic disorder that has been broadly classified into four general categories: type 1, type 2, gestational, and monogenic diabetes. Type 1 diabetes accounts for 5-10% of all cases, monogenic forms a further 1-2%, and type 2 diabetes accounting for the remainder [14]. Gestational diabetes, while transient, affects about 2-4% of all pregnancies in the general population [15]. Currently there are an estimated 382 million people living with diabetes worldwide and this is projected to reach 592 million people by 2035 [15]. Staggeringly, there are a further 319 million individuals around the world who are classified as having impaired glucose tolerance, many of whom will go on to develop frank diabetes [15]. Within Canada the situation is no less dire with 2009 data suggesting that approximately 2.4 million people in Canada are living with diabetes, with that number expected to grow to 3.7 million by 2019 [16].

The microvascular (retinopathy, nephropathy and neuropathy) and macrovascular (stroke and cardiovascular disease) disorders that are associated with diabetes add another layer of complexity to the management of the disease and can have severe impacts on the quality of life and longevity of diabetic patients. The major determinant of macrovascular complications in diabetic patients is increased circulating free fatty acids associated with insulin resistance while hyperglycaemia is the major contributor to microvascular disease, primarily through the generation of advanced glycation end-products (AGEs) [17]. Current

data indicates that diabetic patients have a cardiovascular disease (CVD) risk of greater than 20% and a 2- to 5-fold increased risk of ischemic stroke [16], while diabetic nephropathy is the leading cause of end stage renal disease. Diabetic neuropathy on the other hand is thought to affect 50% of diabetic patients and is a leading cause of limb amputation which occurs in approximately 1-2% of patients [18]. In all cases intensive therapy to prevent hyperglycaemia is known to significantly improve health outcomes associated with these complications [16].

It is clear that diabetes is having a significant impact on the quality of life and longevity of patients, not only as a direct result of trying to manage the disease but also due to the debilitating complications that are associated with poor glycaemic control. This impact is not only on patients, but is also a drain on the global economy. Approximately 10.8% of all health expenditures were related to diabetes and its complications, amounting to $581 billion globally [15]. In Canada, total economic costs have never been accurately determined in part due to varying definitions of direct, indirect and induced costs. The Canadian Diabetes Association has however developed a Diabetes Cost Model that estimated the economic burden for 2010 to be $12.2 billion and projected a further increase of $4.7 billion by 2020 [16].

1.2.2 Type 1 diabetes

T1D is defined by autoimmune destruction of β-cells presenting early in post-natal development with two clear incidence peaks centering around 5-7 years of age and again near puberty [19]. One of the proposed disease models is that individuals with a genetic predisposition for aberrant antigen presentation or impaired immune development undergo an

initiating insult resulting in the release and presentation of islet auto-antigens. Subsequent immune mediated destruction of β-cells ultimately results in the loss of insulin secretion, hyperglycaemia and overt diabetes [3, 19, 20].

It is now well established that in the absence of genetic susceptibility the likelihood of developing T1D is negligible. To date, over 40 genetic loci have been associated with T1D; however, only four of these have a significant impact on the incidence of diabetes with the most highly associated locus being the human leukocyte antigen (HLA) region, although polymorphisms in the insulin promoter are also highly associated with T1D [1, 20]. HLA class II proteins are heterodimers comprised of structurally similar, cell-surface proteins that bind and present antigenic peptides to maturing T-cells in the thymus. During the thymic education process T-cells that have a weak association with self-antigens presented by HLA class II proteins are positively selected while those that exhibit robust association are negatively selected against. Polymorphisms in HLA that are associated with diabetes disrupt this process interfering with the negative selection of self-reactive T-cells which are then allowed to enter circulation [3, 20-22]. The second component to the initiation of auto-immunity is the breakdown of peripheral tolerance and auto-antibody generation [21]. There are four primary auto-antibodies that are used as diagnostic and prognostic tools including insulin, glutamic acid decarboxylase 65 (GAD65), insuloma-associated protein 2 (IAP2) and zinc transporter 8 (SLC30A8). There is some debate however as to the contribution auto-antibodies make to disease progression and it has been suggested that self-antigen presentation by B-cells is the pathogenic process contributing to diabetes onset [1, 21-23]. Studies in non-obese diabetic (NOD) mice, a mouse model of T1D, have shown that the presentation of self-antigens by dendritic cells (DCs) in the draining pancreatic lymph node

(LN) leads to the activation of both CD8+ and CD4+ T-cells which are responsible for the targeted destruction of β-cells [21, 24].

The question remains, however, as to the initial source of the auto-antigens that are available for presentation. One promising hypothesis to account for the rising incidence of T1D, especially in developed countries is the hygiene hypothesis [25]. This theory, which lacks any definitive clinical evidence, is based on observations that infections early on in life, as well as certain vaccination programs have provided protection against diabetes. Furthermore, some have suggested that antigen competition between strong antigens carried by infectious agents and weak self-antigens may contribute to protection against diabetes. Studies in NOD mice have also shown that stimulation by TLR agonists prevented diabetes onset likely through modulation of immunoregulatory cytokines [25]. From this it has been inferred that the increased cleanliness of environments in developed countries, along with stringent hygiene practices, is preventing immune challenge resulting in a skewing of the immune system to a more auto-immune status leading to a higher incidence of T1D [25]. Conversely, virus exposure has been posited as a precipitating event in the onset of diabetes. Various reports have documented a seasonal synchronization to diabetes diagnosis providing the basis for this hypothesis. There is a large body of evidence to support this hypothesis, including the association of many viruses with the disease but, for a number of different reasons, definitive proof of a causal link is lacking [1, 19, 26, 27]. Enteroviruses, and more specifically Coxsackievirus infections, have been correlated with increased incidences of diabetes with one study showing that 44 of 72 new-onset diabetic patients harboured enteroviruses in their pancreata while only 3 of 50 controls showed signs of viral infection [28]. It is evident that our understanding of the mechanisms underlying initiation of diabetes

and how these signals are processed and propagated by the immune system is improving but is still far from complete. It is clear though that type 1 diabetes is dependent on both genetic and environmental factors, and the specific interactions between these components dictates the progression of the disease.

Regardless of the mechanisms underlying the loss of β-cells, it is the loss of β-cells and the subsequent hyperglycaemia that needs to be treated at a clinical level following diagnosis. Current treatment options for T1D are limited, with best medical practice being the administration of exogenous insulin, via subcutaneous injection, which was pioneered by Banting and Best at the University of Toronto [29]. Advancements have been made, however, with the development of artificial pancreas systems that rely on constant glucose monitoring and automatic insulin administration [30, 31]. Another option for the treatment of diabetes with long-term insulin independence is the transplantation of cadaveric islets using the Edmonton Protocol, which was developed at the University of Alberta [32]. This option is limited to a subset of patients, however, and while initially capable of reversing diabetes patients ultimately return to insulin dependence, albeit with lower insulin requirements [32, 33]. One of the major drawbacks to the transplant of islets is the lack of donor tissue, as such a substantial amount of research is focused on increasing the supply of transplantable cells [5, 34, 35]. These treatments, however, remain primarily a stopgap until a cure for the disease can be found. As such, research is ongoing with the goal of identifying patients while they still have sufficient numbers of functional β-cells to maintain normoglycaemia, to then prevent the immune assault that is driving the disease, and to restore functional β-cell mass in these patients [36-38].

1.2.3 Monogenic diabetes

Monogenic diabetes results from a genetic mutation in a single gene leading to inappropriate glucose homeostasis. These rare forms of diabetes are typically diagnosed in early childhood and present with varying age of onset, level of hyperglycaemia and severity of complications [14]. The age at onset is used to classify the monogenic forms of diabetes with diagnosis prior to six months of age being defined as neonatal diabetes [39, 40], and diagnosis between six months and 25 years as maturity onset diabetes of the young (MODY) [41-45]. Mutations in the MODY genes are inherited in an autosomal dominant manner and result in defects in β-cell development, maturation or function. There are currently 13 forms of MODY affecting: insulin secretion (BLK, ABCC8 and KCNJ11), glucose sensitivity (KLF11 and GCK), pancreas development (HNF4α, HNF1α, HNF1β, PDX1), or endocrine-cell maturation (NEUROD1), with mutations in the insulin gene also giving rise to MODY [46]. The correct diagnosis of MODY is key to the treatment of, and prognosis for, patients. It is currently estimated that approximately 80% of patients with MODY are misdiagnosed as having T1D. This deficit needs to be addressed as glycaemic control and quality of life are dramatically improved in patients that receive appropriate treatment, for example in patients with mutations in ABCC8 and KCNJ11, both of which affect insulin secretion, switching to oral sulfonylureas allows patients to discontinue exogenous insulin [46].

1.2.4 Type 2 diabetes

Type 2 diabetes is characterised by the combined contribution of insulin resistance, and α- and β-cell dysfunction [14, 47-50]. Similar to T1D and monogenic forms of diabetes, T2D has a genetic component that underlies susceptibility to disease. Genome wide association

studies have identified close to 75 genes associated with T2D but all of these loci only affect disease susceptibility to a marginal extent [51-53]. The largest positive association with T2D however is obesity [14, 47, 48]. Obesity results in the accumulation of fat in traditional fat depots but also in β-cells, muscle and liver. The excess accumulation of fat in these tissues induces the activation of PKCs which reduces tyrosine, and increases serine, phosphorylation of IRS1 interfering with its ability to bind the insulin receptor [54]. This disrupts normal insulin signalling, inhibiting the translocation of glucose transporters to the plasma membrane resulting in peripheral insulin resistance [14, 47, 48, 55]. The importance of ectopic fat accumulation to the development of T2D is highlighted by a recent study examining Vegfb, which regulates fatty acid uptake and transport into heart and skeletal muscle [56]. Ablation of Vegfb signalling in *db/db* mice prevented lipid accumulation in muscle and in islets, instead shunting it to traditional fat pads. The result is mice that are significantly heavier than controls, but with improved glucose homeostasis driven by increased glucose uptake in muscles. Interestingly, inhibition of Vegfb in already diabetic mice also reduced ectopic fat accumulation, improved glucose tolerance and limited disease progression [56].During early disease progression the β-cells are able to compensate for this obesity induced insulin resistance through islet hypertrophy and hyperplasia [57].

While many studies have shown that obesity is one of the predominant risk factors associated with T2D, a 24 year study of 515 patients demonstrated that hyperinsulinemia has a significant association with the development of T2D [58] and a recent study in $Ins1^{+/-}$:$Ins2^{-/-}$ mice showed that these mice are protected from diet-induced obesity suggesting that hyperinsulinemia is also a major driving force in T2D development [59]. Regardless, as the disease progresses, β-cell dysfunction increases and β-cells are no longer

able to compensate for the continued insulin resistance [48]. This ultimately results in increased apoptosis, with the final outcome being insulin dependent T2D [4, 14, 47, 48, 55, 60].

The β-cell dysfunction that precedes β-cell loss results from a combination of hyperglycaemia, hyperlipidemia, ER- and oxidative-stress, islet amyloid polypeptide (IAPP) accumulation and inflammation. Chronically elevated levels of glucose and fatty acids independently have detrimental effects on islets and act synergistically to further impair islet function. Chronic hyperglycaemia generates excessive levels of reactive oxygen species (ROS) leading to cellular damage, Nlrp3 inflammasome activation and enhanced Nfκb activity [61, 62]. Hyperglycaemia also causes a loss of *Ins* gene expression via a post-transcriptional arrest in *Pdx1,* a reduction in the expression of Neurod1, and ubiquitin-mediated Mafa degradation [63-65]. Lipid accumulation on the other hand causes an accumulation of long-chain acyl-CoA that can inhibit glucose-stimulated insulin secretion through interactions with potassium channels and by increasing Ucp-2 expression, which will reduce cellular ATP levels [4, 66]. In the context of T2D however, there is a combination of both hyperglycaemia and hyperlipidemia that act synergistically to inhibit β-cell function. Under these conditions excess glucose leads to an elevation in malonyl-CoA, which inhibits free fatty acid (FFA) oxidation. This results in the accumulation of fatty acid acyl-CoAs in the cytoplasm exacerbating the effects of hyperglycaemia [67]. Further β-cell dysfunction is induced by IAPP, a peptide co-secreted with insulin [68, 69] that can aggregate to form pathogenic fibrils that are found in most T2D patients [70]. IAPP has been proposed to directly induce β-cell dysfunction through interaction with, and disruption of, β-cell

membranes [71], as well as by activating the Nlrp3 inflammasome in resident macrophages leading to a self-propagating inflammatory response [72-75].

It is evident that T2D is a complex disorder that is the result of an accumulation of insults that intersect to drive the progressive nature of the disease. The contribution of inflammation to the progression of T2D cannot be ignored however, and the signalling cascades that are involved in this process will be discussed in greater detail below.

1.2.5 Gestational diabetes

As the name implies gestational diabetes (GDM) is a condition that is defined by insulin resistance and hyperglycaemia during pregnancy. GDM typically occurs around the 24th week of gestation with 3-20% of pregnant women being affected [15, 16]. Due to the late gestational age of GDM onset there is not a significant developmental risk to the child; however, foetuses can become significantly larger than average resulting in complications during the birthing process. The condition also has negative outcomes for the mother with increased prevalence of GDM in subsequent pregnancies and a higher probability of developing T2D later in life [15].

1.3 Inflammation in diabetes

Despite exhibiting similar characteristics, many aspects of T1D and T2D are distinct, including the aetiology of disease onset and the inflammatory mechanisms driving β-cell dysfunction and apoptosis.

In the case of T1D, activation of auto-reactive T-cells targeting β-cells is the primary inflammatory process driving the disease [24, 76, 77]. As discussed earlier viral infection of

islets can initiate the activation of T-cells leading to auto-immunity [28]. Viral dsRNA upregulates Tlr3, Rig-I and Mda-5 expression in β-cells and ligand binding to these pattern recognition receptors (PRRs) induces the activation of Nfκb and Irf-3, which is followed by the production of Ifnα and Ifnβ. These cytokines then activate the transcription factor Stat1, a process leading to the production of pro-inflammatory chemokines (Cxcl10, Ccl2 and Ccl20) and cytokines (Ifnα, Ifnβ and Il-15) [77-80]. This virus-induced secretion of chemokines by β-cells acts to recruit pro-inflammatory immune cells to the islets [1, 77]. Recruited immune cells secrete Il-1β, Tnfα, and Ifnγ that bind to receptors on the surface of β-cells leading to activation of downstream signalling cascades inducing changes in β-cell gene expression (Figure 1.1).

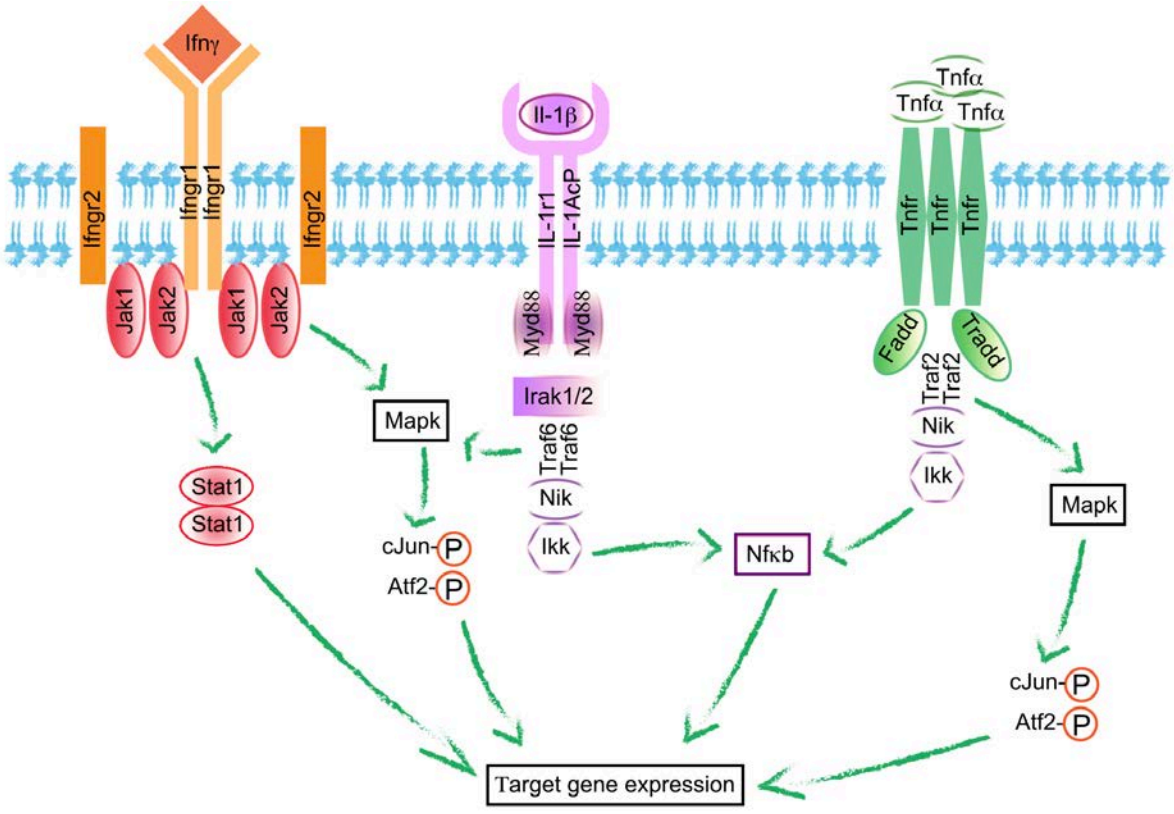

Figure 1.1: Ifnγ, Il-1β and Tnfα act synergistically to alter gene expression in β-cells
Ifnγ, Il-1β and Tnfα all signal through Mapk, while Il-1β and Tnfα additionally signal through Nfκb. Ifnγ also signals through the Jak/Stat pathway. Figure adapted from [81].

Il-1β binds to the Il-1 receptor promoting Myd88-dependent recruitment of the Il-1r1-activated kinase (Irak) [82]. Irak interacts with Tnf-receptor-associated factor (Traf) 6 which is implicated in Nfκb activation through Nfκb inducing kinase (Nik) mediated activation of inhibitory κb (Iκb) kinase (ikk) and Iκb degradation [83]. Tnfα binding to the p60 Tnf receptor induces receptor trimerization promoting association with Tnf receptor associated death domain and Fas-associated death domain proteins. Next, Traf2 and receptor interacting protein are recruited to the complex followed by Nik, Pkc, Jnk and Pkr binding. Nik once again promotes the activation of Nfκb [84]. Ifnγ primarily signals through the Jak/Stat pathway downstream of Ifnγ receptor 1 (IfnγR1) dimerization and IfnγR2 recruitment. Jak1/2 are activated by auto- and trans-phosphorylation leading to phosphorylation of the IfnγR, docking of two Stat1 molecules and their activation by Jak2. Phosphorylation of Stat1 induces homodimerization and translocation to the nucleus [85]. Together these pathways act synergistically to induce β-cell dysfunction and apoptosis [78, 86, 87]. This synergistic activity is the result of the intersection of signalling pathways initiated by Il-1β, Tnfα, and Ifnγ (Figure 1.1). Il-1β signalling activates mitogen-activated kinases (Mapk) [82] and Pik3 [88] which intersects with Jak activation of Mapk and Pik3 downstream of Ifnγ [89]. Tnfα signalling intersects with Ifnγ through the Mapk kinase cascade and with Il-1β through both Mapk and Nik mediated Nfκb activation [82, 84, 89, 90].

The activation of the Stat1, Mapk and Nfκb transcription factors results in significant changes in the transcription of genes that are necessary for the maintenance of β-cell function and survival [13, 81, 87]. Stat1 was initially thought to promote apoptosis via Irf1, which activates caspases and iNos [78], but Irf1 knock-out mice suggested this pathway was not involved in mediating β-cell death [81]. An essential role for Stat1 in β-cell death was

elegantly shown using Stat1 null mice on a NOD background. The authors showed that Stat1 deletion prevented the inhibition of X-linked inhibitor of apoptosis (Xiap) expression, iNos induction and nitric oxide (NO) production [80]. The primary effect of Mapk is thought to be the activation of Nfκb and also augmentation of Nfκb binding via regulation of activating transcription factor 2 (Atf2) and Ap1 [81].

Nfκb regulates a host of genes that have disparate roles in the regulation of β-cell function and survival. The Nfκb family of transcription factors is comprised of five members that form homo- or heterodimers. Prior to stimulation, inhibitory Iκb proteins bind Nfκb dimers, sequestering the complexes in the cytoplasm. Stimulus coupled Iκb phosphorylation results in its degradation allowing Nfκb to translocate to the nucleus where it can activate gene transcription programs that initiate pro-apoptotic signalling cascades [91-93]. The target genes that are regulated by Nfκb are extensive and the expression pattern of these genes is dependent on the stimulus and the cell type that is being targeted [13, 87, 91, 94]. In the case of cytokine stimulation, Nfκb regulates the production of both pro- and anti-apoptotic genes including genes involved in β-cell repair and function (*MnSod, Hsp70, Iκbα, Pdx1, Neurod1, Ins*, *Glut2* and *Isl1*), chemokines and cytokines (*Il-15*, *Ip-10* and *Mcp1*), iNos and many other genes including *Myt3* [13], which is the focus of this thesis.

Type 2 diabetes on the other hand results from chronic low level islet inflammation activated by IAPP, glucose, free fatty acids and resident macrophages (Figure 1.2) [95-101]. IAPP aggregates in islets are phagocytosed by resident macrophages leading to activation of the Nlrp3 inflammasome, which results in activation of caspase-1, cleavage of pro-Il-1β and release of mature Il-1β [72]. IAPP also induces Tnfα production in a Myd88 dependent manner, and increases the levels of several other cytokines and chemokines including Il-1α,

Il-6, Ccl2 and Cxcl2 [72]. Elevated blood glucose induces the activation of Nlrp3 in β-cells through the generation of reactive oxygen species (ROS) and the accumulation of advanced glycation end products (AGEs) both of which lead to enhanced Nfκb activity independently of Nlrp3 activation. Nlrp3 activation in β-cells leads to the release of mature Il-1β in the same manner as in macrophages (Figure 1.2) [62, 102, 103]. Il-1β subsequently acts in an autocrine/paracrine fashion to further stimulate Nfκb activation enhancing inflammatory signalling. Similarly, free fatty acids engage Tlr2 and Tlr4 facilitating receptor dimerization and recruitment of the adapter protein Myd88. Downstream signalling causes the phosphorylation and degradation of Iκb and the activation of Nfκb (Figure 1.2) [104, 105].

In addition to increases in β-cell apoptosis, loss of β-cell functional maturity in response to cellular stresses associated with T2D, including inflammatory signalling, is becoming widely recognized as a significant contributor to the development of T2D [106-109]. β-cell specific ablation of Foxo1 along with lineage tracing demonstrated that under stress conditions the loss of mature β-cells resulted from the loss of Pdx1, Mafa and insulin as opposed to reduction in β-cell mass [106]. This loss of functional maturity was further demonstrated in mice expressing ATP-insensitive Kir6.2, in which hyperglycaemia induced a loss of insulin along with a concomitant increase in Ngn3 production in transgenic β-cells [110]. The effects of oxidative stress and cytokine exposure on β-cell maturity in *ex vivo* islets [108, 111], both of which are features of T1D and T2D, suggests that the loss of functional β-cell maturity is likely a contributing factor in the early stages of T1D development as well.

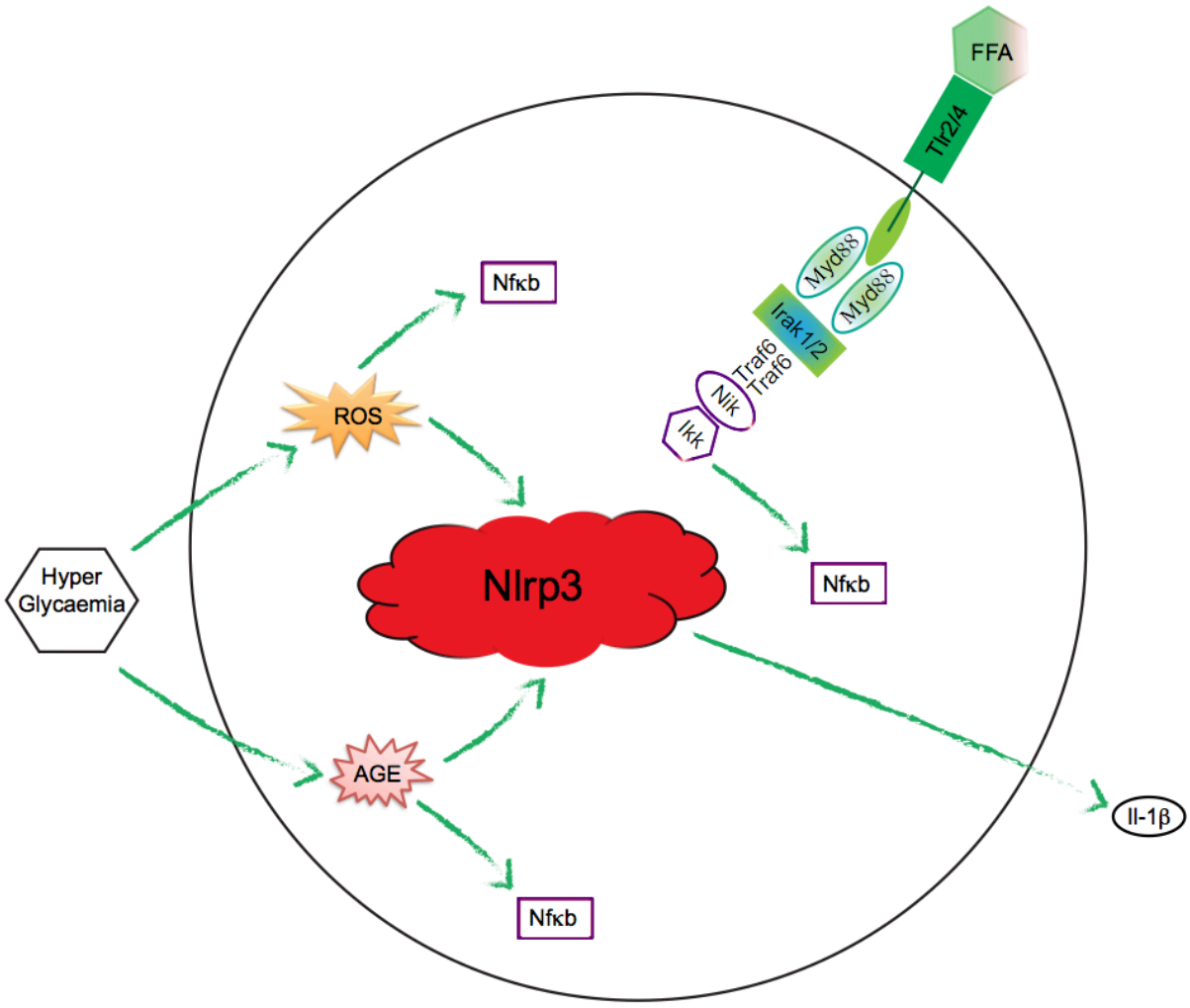

Figure 1.2: Inflammatory signalling in Type 2 diabetes
Schematic representation of glucose and free fatty acid induced inflammation in T2D. Chronically elevated levels of circulating glucose induce the formation of reactive oxygen species and advanced glycation end products both of which activate the inflammasome and Nfκb. Nlrp3 activation leads to Il-1β production that further induces Nfκb activation. Free fatty acids activate pattern recognition receptors leading to the activation of Nfκb.

1.4 Apoptosis

The inflammation that is present in both T1D and T2D ultimately feeds into cell death pathways that cause the loss of functional β-cell mass. There are three distinct apoptotic pathways that are responsible for the eventual activation of caspase-3, namely the extrinsic, intrinsic and perforin/granzyme pathways (Figure 1.3) [112, 113]. The extrinsic pathway

involves activation of death receptors by Fasl and Tnfα, which induces receptor clustering, and cleavage of procaspase-8. Active caspase-8 then acts via the pro-apoptotic Bcl2 family member, Bid, to induce mitochondrial permeabilisation, cytochrome c release, and caspase-3 activation (Figure 1.3).

Cytotoxic T-cells can induce apoptosis in target cells through the secretion of the pore forming protein perforin and the subsequent transfer of granzyme A and B. Granzyme A induces caspase independent apoptosis by cleaving the SET complex leading to DNA degradation, while granzyme B cleaves procaspase-10 and Bid, and can also directly activate caspase-3 (Figure 1.3) [112].

Lastly, The intrinsic pathway is initiated via receptor independent mechanisms but intersects with the extrinsic pathway in that the signalling events initiated by hypoxia, ER-stress, removal of growth factors and other cellular insults leads to disruption of mitochondrial potential and release of cytochrome c and other mitochondrial proteins. These mitochondrial proteins function to promote activation of the apoptosome and inhibition of Inhibitor of Apoptosis (Iap) activity. The majority of the effects of the activation of the intrinsic pathway are mediated through a balancing act between the pro- and anti-apoptotic Bcl family members [81, 112-114]. The release of cytochrome c from mitochondria is a result of oligomerisation of, and subsequent pore formation by, the pro-apoptotic Bax and Bak proteins. Bak is constitutively inserted into the outer mitochondrial membrane (OMM) while Bax is translocated from the cytosol. Accumulation of Bax in the OMM is prevented by the pro-survival protein Bcl2l1 which retro-translocates Bax from the OMM to the cytosol and Bcl2 binds to other BH3-only proteins preventing their activation [115-119]. This event is antagonised by the BH3-only Bid and Bim proteins, which induce a conformational change

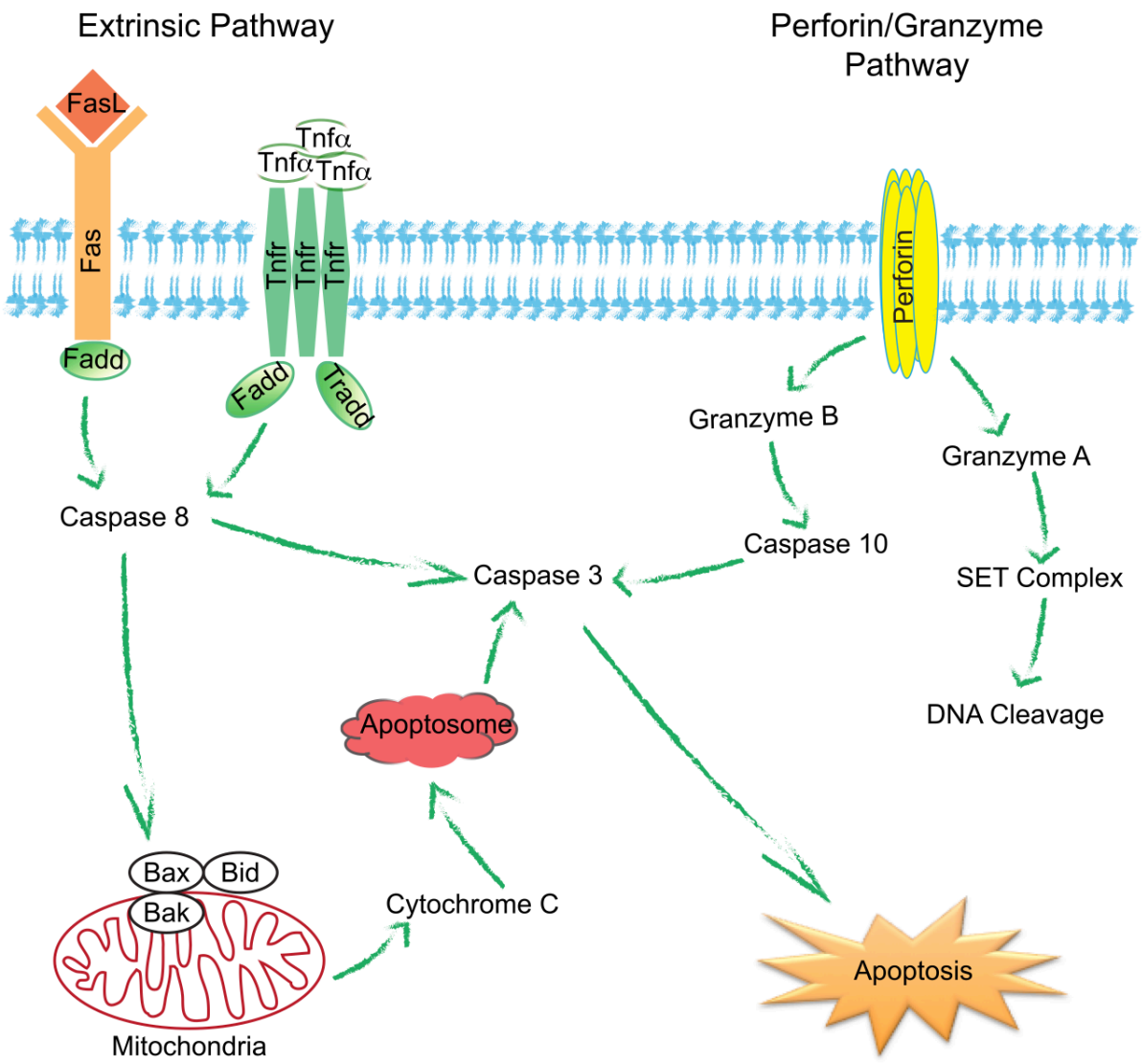

Figure 1.3: Extrinsic and granzyme apoptotic pathways
The extrinsic pathway is induced by activation of death receptors by Fas ligand or Tnfα that induces the cleavage of procaspase-8 to its mature form leading to the activation of Bid, translocation of Bax/Bak to mitochondria and release of cytochrome c. The perforin/granzyme pathway induces DNA damage and the activation of caspase-10. Caspase-8, caspase-10 and cytochrome c activates the effector caspase, caspase-3.

in Bax, facilitating insertion into the OMM (Figure 1.4) [115-119]. In addition to the pro-survival Bcl2 family there are several additional mechanisms that exist to inhibit apoptosis. These mechanisms include inhibitor of apoptosis proteins such as Xiap, as well as the Pik3/Akt, Ras-Raf and Mapk signalling pathways [81, 120-122].

Islet transplants [32, 123] face similar immune assault due to alloimmune rejection. In T1D patients this rejection is augmented by residual host immune responses targeting β-cell specific antigens such as insulin. In all cases it is clear that immune mediated cytokine production plays a pivotal role in the induction of diabetes regardless of the underlying cause of the immune cell infiltration.

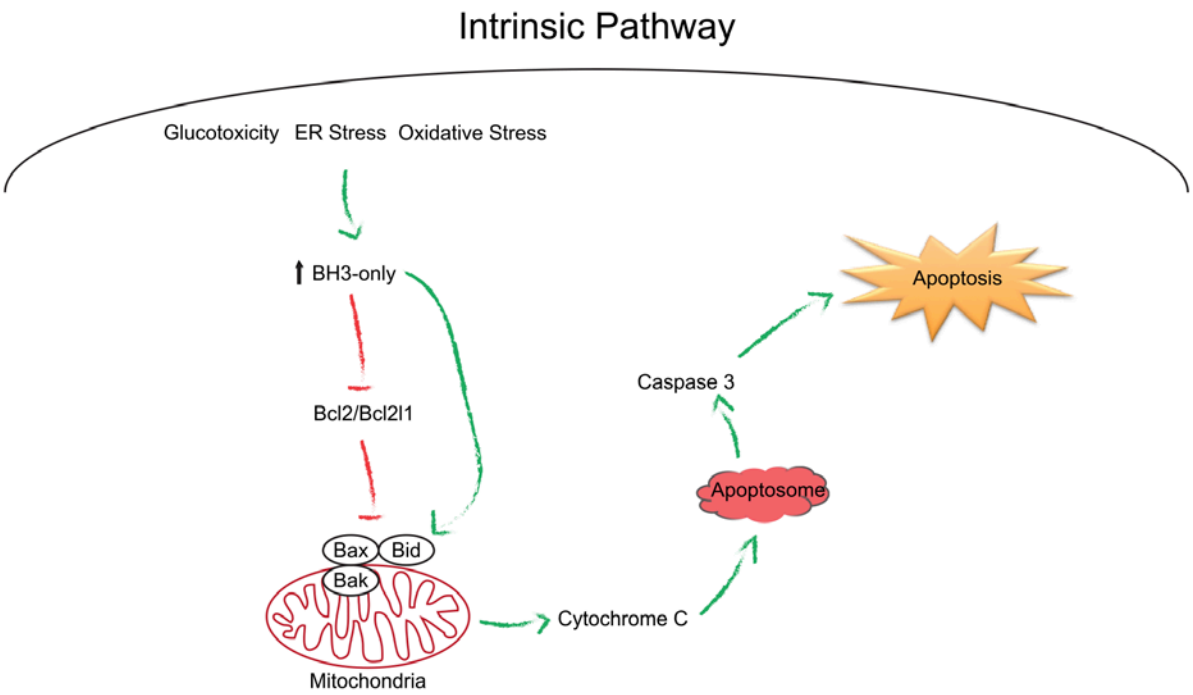

Figure 1.4: Intrinsic apoptotic signalling in diabetes
The intrinsic pathway is receptor independent and inhibits the pro-survival activity of Bcl2 and Bcl2l1, while inducing the expression and activity of pro-apoptotic BH3-only proteins leading to the release of cytochrome c and the activation of caspase-3.

1.5 Pancreas development

The pancreas is a multifunctional glandular organ comprised of an exocrine compartment that secretes digestive enzymes via a comprehensive network of ducts, and an endocrine compartment that secretes glucose regulating hormones into the circulatory system [7, 124, 125]. Pancreas development (Figure 1.5) is initiated at around embryonic day 9.5 (E9.5) in a subset of cells in the posterior foregut endoderm defined both dorsally and ventrally by Tgif2 inhibition of *Hex* [7, 124, 125]. Blocking *Hex* activation results in the activation of *Pdx1* and induction of pancreatic development. In conjunction with the regulation of *Pdx1* expression several extracellular signals derived from adjacent tissues promote pancreas development through suppression of sonic hedgehog (Shh) expression [7, 124, 125]. Subsequently, the pancreas cells adopt a "protodifferentiated" state in which cells become irreversibly committed to a pancreatic fate and undergo an initial proliferative wave. It is at this time, in mice, that the first wave of endocrine cells arise, comprised primarily of glucagon positive cells with a few interspersed glucagon/insulin co-positive and insulin positive cells [124]. The contribution of these early endocrine cells to the formation of mature islets is unclear at this time [126-130] but there is some evidence to suggest that the glucagon positive cells may contribute to α-cell mass in mature islets [126, 131]. During this early phase of pancreas expansion, termed the primary transition (~E9.5-E12.5), cells undergo linked programs of proliferation and morphogenesis to allow for the expansion of the progenitor pool and the adoption of an arbour structure. Wnt, FGF and Notch signalling determine the size of this progenitor pool and disruption of epithelial/mesenchymal cross-talk during this period, either through removal of the mesenchyme, or inhibition of signalling, results in a skewing towards differentiation rather than proliferation giving rise to organ hypoplasia [7, 124, 125].

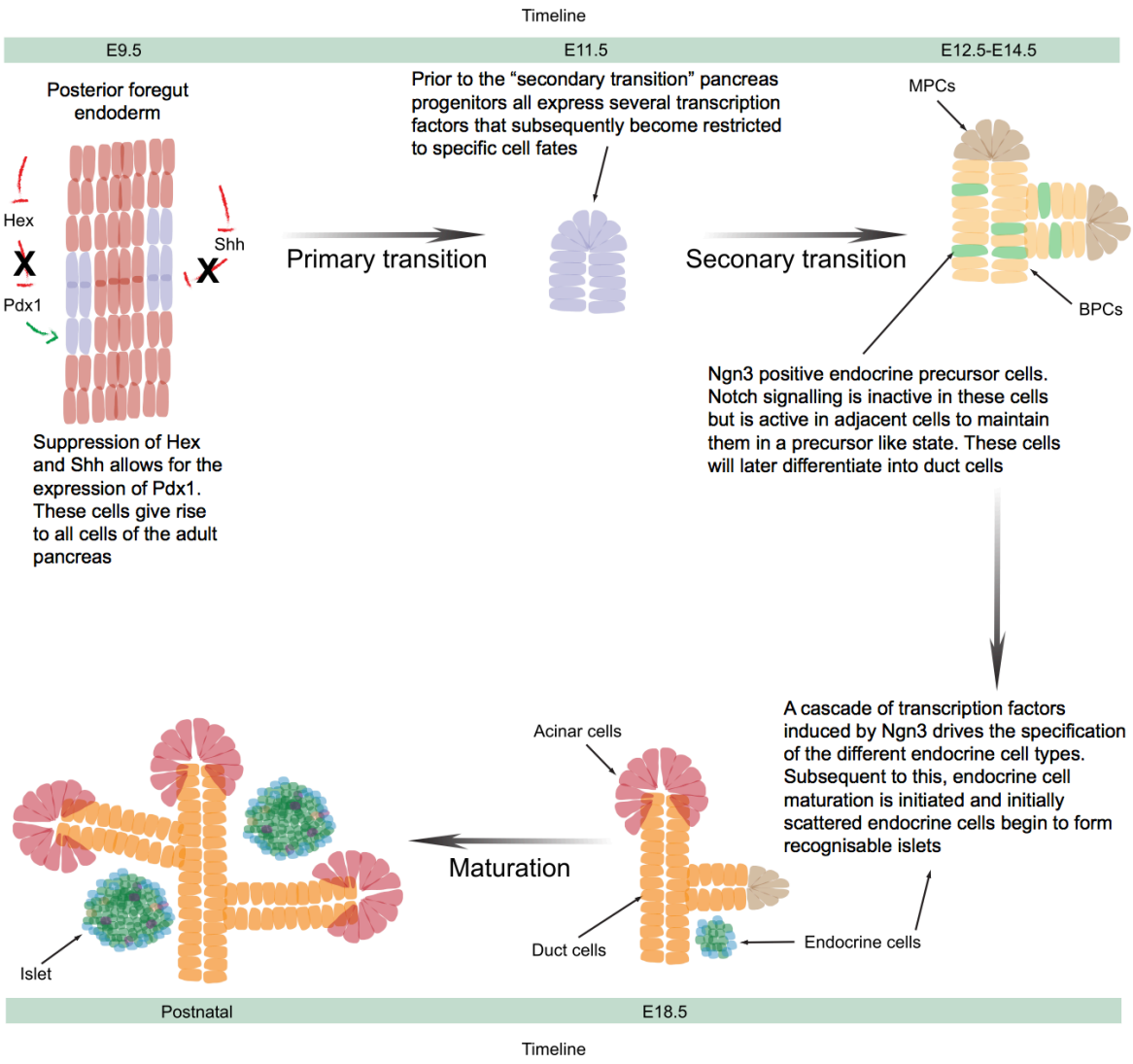

Figure 1.5: Pancreas development
Pancreas progenitors (purple) are specified at E9.5 and expand during the primary transition. During the secondary transition the pancreas undergoes branching morphogenesis due to the asymmetric division of multipotent progenitor cells (brown) at the tips of the branches. A subset of bipotent progenitor cells (beige) turns on Ngn3 expression (green) ultimately giving rise to mature endocrine cells (blue/green). As development proceeds the MPCs differentiate into acinar cells (red), while the BPCs differentiate into duct cells (orange).

During the secondary transition (~E13.5-E14.5), multipotent progenitor cells (MPCs) at the tips of the branching pancreatic epithelium begin to drive a profound remodelling of the epithelium resulting in an expansion of the branching pancreatic tree (Figure 1.5). Asymmetric division at the base of the tip domain results in the formation of bipotent

progenitor cells that will ultimately give rise to ductal and endocrine cells, while the MPCs at the crown of the tip domain continue to divide and over time differentiate into acinar cells [7, 124, 125]. A subset of the bipotent progenitor cells turn on *Ngn3* expression, which is induced by the synergistic activities of the transcription factors Sox4, Sox9, Hnf1α, Foxa2, Hnf6 and Pdx1 [132-136]. The *Ngn3* expressing endocrine precursors down-regulate the apical marker aPKC promoting delamination from the Sox9 positive pancreas progenitor layer [137]. These cells maintain the expression of E-cadherin indicating that they remain epithelial at this point and have yet to complete the epithelial-to-mesenchymal transition (EMT) and escape from the epithelium. Subsequent to this initial delamination endocrine precursor cells start to differentiate and hormone positive endocrine cells begin to break down the basal lamina, induce the expression of the mesenchymal markers vimentin and N-cadherin while down-regulating E-cadherin [137]. The EMT process in endocrine cells and the escape from the epithelium is dependent on the induction of *Snail2* expression by Ngn3 [138].

Ngn3 induces endocrine precursor differentiation through the induction of a transcriptional cascade that gives rise to the five endocrine cell lineages. Disruption of any of the transcription factors immediately downstream of Ngn3, including *Neurod1, Insm1*, *Rfx6,* and *Isl1* causes significantly reduced numbers of different endocrine cell populations or impairment in their differentiation into hormone producing cells [124, 125, 139]. For example, the deletion of *Neurod1* leads to an arrest in endocrine development around the secondary transition [140].

The differentiation of the specific hormone producing endocrine cells is controlled by the coordinated expression of several transcription factors that become successively more restricted to individual endocrine cell types (Figure 1.6) [141]. For example, the homeodomain transcription factors Nkx2.2 and Nkx6.1 are necessary for the development of β-cells with loss of either factor resulting in diminished β-cell genesis [142, 143]. Pax4 is also thought to play a role in the initial fate-choice between an α- or β/δ-cell lineage since Pax4 inhibition of Arx skews development towards a β-cell fate [144, 145].

As mentioned above the newly differentiated endocrine cells subsequently migrate out of the epithelium and aggregate into ribbon like chords in close association with the ducts [137]. This process is dependent of several signalling cascades including those regulated by Wnt5a, Egfr, Cdc42, Tle3, and Rac1; impairments in which inhibit normal endocrine cell delamination and migration, or the migration of islets away from ducts [12, 138, 146-148]. Islets then form from these ribbon like chords either by invagination of the α-cell mantle, pinching off small islets [149] or by growth of acinar tissue breaking the endocrine chords into segments [131]. Concomitant with the adoption of the typical islet architecture the cells continue to undergo a maturation process that culminates in stimulus-coupled release of hormones. This maturation process is dependent on the appropriate expression of key transcription factors such as Mafa, which is thought to play a key role in driving β-cell maturation through the regulation of *Pdx1, Neurod1, Glut2, Gck, Kir6.2* and *Sur1* expression [150, 151].

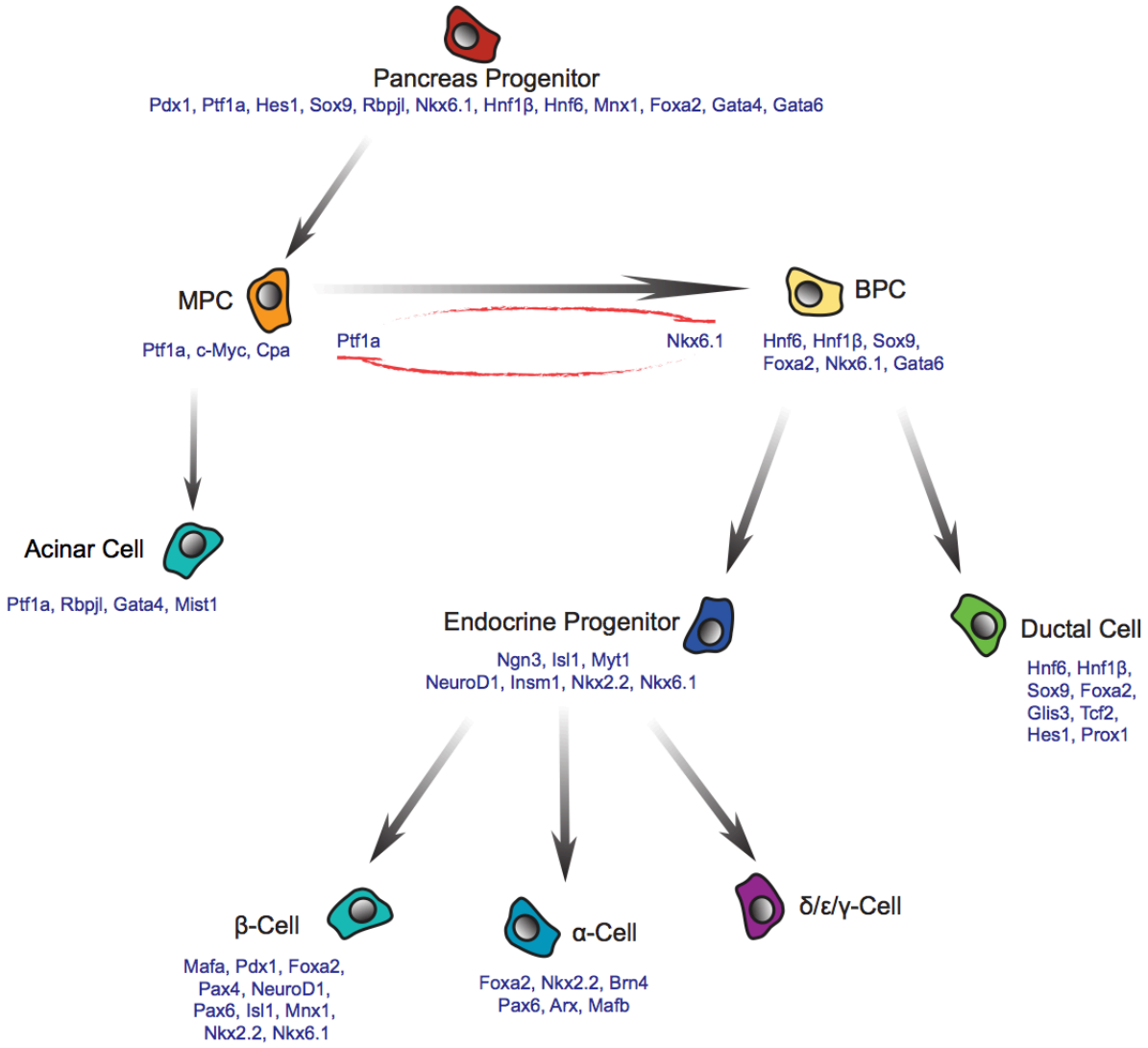

Figure 1.6: Transcriptional regulation of pancreas and endocrine cell development
As development progresses specific transcription factors are turned on or off to determine the specific nature of the differentiating cell.

1.6 Insulin secretion

The maturation into fully functional islets is characterized by the acquisition of stimulus-coupled hormone secretion. In the case of β-cells this functional maturity is exemplified by glucose-stimulated insulin secretion (Figure 1.7) [152-156], which must be precisely regulated to maintain circulating blood glucose concentrations within a very narrow range. This level of control is achieved via the coupling of small changes in glucose concentrations

to very rapid changes in cellular metabolism and signalling leading to insulin secretion [157]. Insulin secretion is initiated by uptake of glucose into β-cells by a high affinity facilitative transporter [158, 159] where it is metabolized in mitochondria via oxidative phosphorylation leading to an increase in the cellular ATP:ADP ratio [160].

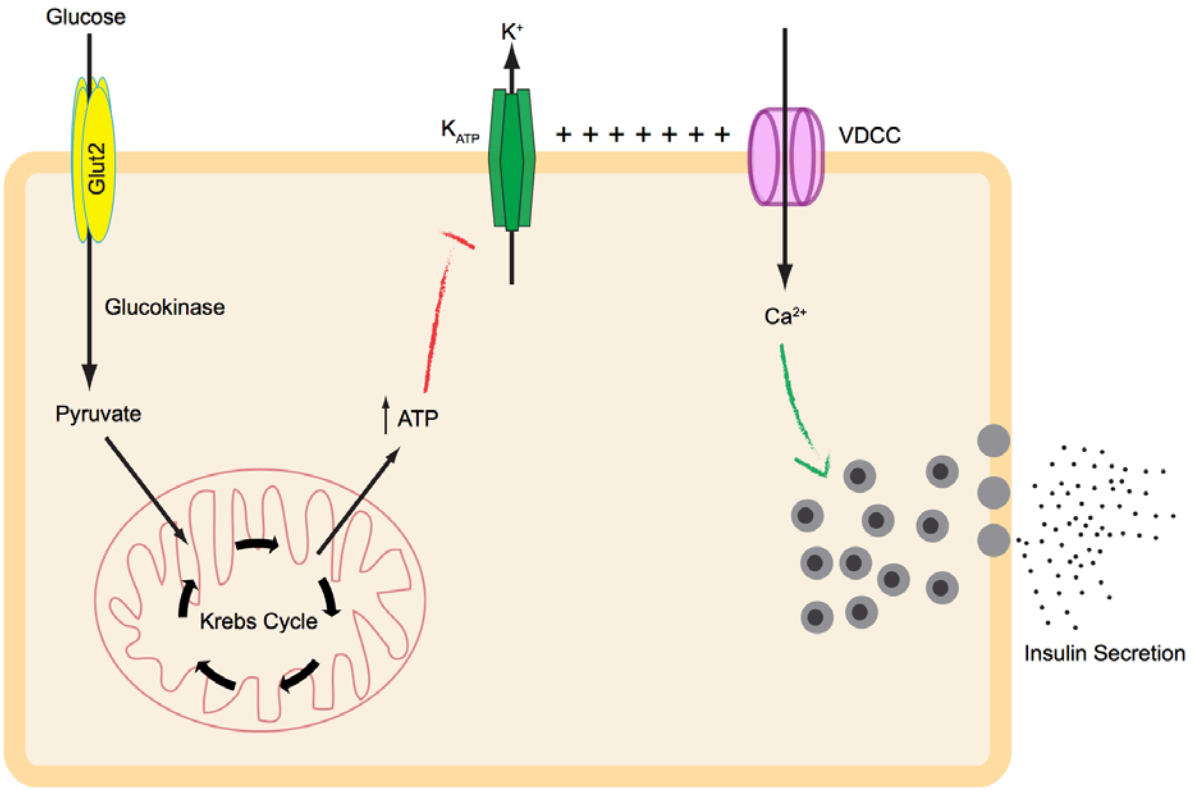

Figure 1.7: Insulin secretion in rodents
Insulin secretion is initiated by uptake of glucose via Glut2 in rodents and its processing by the mitochondria to produce ATP. ATP induces the closure of potassium channels leading to depolarization of the plasma membrane and opening of voltage-gated calcium channels. Elevated intracellular calcium promotes the release of insulin from dense core vesicles.

The increase in ATP induces the closure of ATP-dependent potassium channels leading to membrane depolarization and the opening of voltage-gated calcium channels and an increase in cytoplasmic calcium concentrations [161, 162]. Elevated intracellular calcium concentrations in turn induce the fusion of insulin granules, from the readily releasable pool,

to the plasma membrane and release of insulin. This pool of insulin granules is subsequently replaced by a reserve pool of insulin granules that are required for the maintenance of second phase insulin secretion and the replenishment of the readily releasable pool [163]. Subsequently, as blood glucose concentrations are reduced the production of ATP is blunted, the potassium channel opens, calcium influx is halted and insulin secretion returns to basal levels.

1.7 The MYT family

Myt3 is part of the C2HC-type zinc-finger, or MYT, family of transcription factors that in vertebrates is composed of three genes: *Myt1, Myt1l* and *Myt3* [164-167]. This family of transcription factors derives its name from its founding member *Myt1* which was isolated from a human foetal brain cDNA library [167]. The other members of the family, *Myt1l* and *Myt3*, were similarly isolated from a rodent brain cDNA library.

Both Myt1 and Myt1L were shown to contain a highly acidic N-terminal domain and a serine/threonine-rich motif, both of which function as trans-activation domains. Both factors also contain a central protein-protein interaction domain called the MYT domain which can interact with the co-repressor Sin3b, a scaffold protein known to recruit histone deacetylases [166, 168-170]. *Myt3* retains this MYT domain but does not contain the N-terminal acidic domain or the central serine/threonine-rich motif [165]. *Myt3* is otherwise most similar to *Myt1* containing six zinc-fingers arranged in two clusters of two and four. The highest degree of homology between the three family members is in the DNA-binding zinc-finger domains, with a lesser degree of conservation in the C-terminus (Figure 1.8).

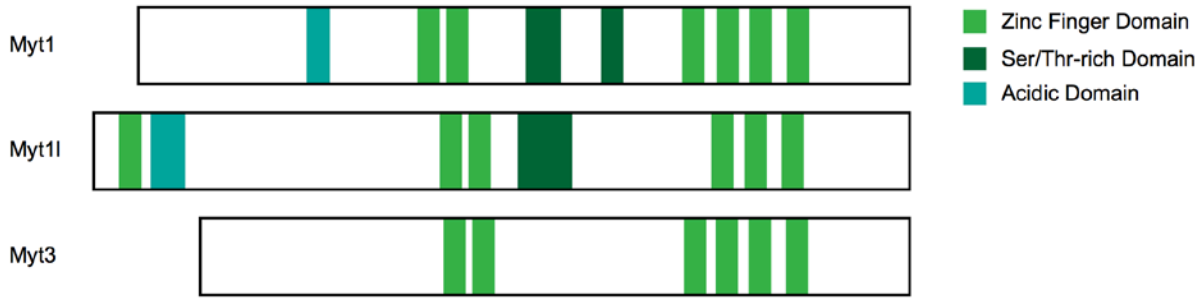

Figure 1.8: *Myt3* is a C2HC-type Zinc finger transcription factor of the MYT family
Shown is a schematic representation of the MYT family domain structure. All family members contain DNA-binding zinc-finger domains (lime green), while only Myt1 and Myt1l contain ser/thr-rich domains (dark green) and an acidic domain (teal).

1.8 Dissertation rationale

While an awareness of the global prevalence of diabetes, along with knowledge of the health, social and economic burdens associated with the disease, provides important context for research into diabetes it is not at the core of what we are trying to understand. At the center of diabetes is the pancreatic islet and we are striving to understand how this important micro-organ functions under physiological and pathophysiological conditions. Dr. Hoffman previously sought to identify pancreas enriched transcripts with the goal of identifying novel genes that would be important for the development and function of islets [8]. Of the genes identified in this screen the transcription factor *Myt3* was one of the few that had yet to be studied in the context of islet development and function making it a good candidate for further analysis.

Further insight into a potential regulatory role for *Myt3* in islet function was provided by Wang *et al.* who showed a compensatory increase in *Myt3* expression in *Myt1* knock-out mice. *Myt1* knock-out resulted in the formation of polyhormonal cells displaying aberrant Mafa and Mafb expression patterns consistent with an immature endocrine cell phenotype [11]. These mice also exhibited impaired glucose tolerance and reduced insulin secretion in

conjunction with reduced Glut2 production. Interestingly, during embryogenesis *Myt3* expression is up-regulated in endocrine cells lacking *Myt1* [11], suggesting *Myt3* may play a compensatory role. As discussed above cytokine exposure is a hallmark of T1D and this exposure is known to impair the expression of several genes that are key players in regulating islet function and survival [13, 171, 172]. Exposure of β-cells to pro-inflammatory cytokines impairs *Myt3* expression in an N*fκb* dependent manner [13] suggesting that it may act as a mediator of islet dysfunction and apoptosis in the context of diabetes.

These data suggested that *Myt3* may be a necessary component of the islet transcriptional machinery and this lead us to more closely examine the role of *Myt3* in islet function and survival. Specifically we **hypothesised** that *Myt3* helps to maintain β-cell functional maturity, while inhibiting pro-apoptotic and pro-inflammatory gene expression.

To test this hypothesis, we focused on the following objectives:

OBJECTIVE 1: To determine *Myt3's* role in regulating islet function and survival; and

OBJECTIVE 2: To evaluate the effects of *Myt3* suppression on islet graft function and survival.

Understanding the mechanisms and transcriptional networks that control β-cell function and survival, and how these are influenced by immune attack in T1D and T2D, is critical to developing novel approaches for treating diabetes. More specifically the data presented in this dissertation highlight an important role for *Myt3* in the regulation of islet-cell survival and migration and may implicate it as a novel therapeutic target or inform novel approaches to treat T1D and T2D.

Chapter 2: The transcription factor *Myt3* acts as a pro-survival factor in β-cells

2.1 Background

There is a growing body of evidence highlighting the importance of proper spatial and temporal regulation of gene expression for the development and function of the pancreas, endocrine cells and more specifically β-cells (Figure 1.6) [8, 173-175]. In the case of β-cells many of the same genes that are responsible for their specification also play key roles in maintaining them in a functionally mature state [151, 176-180]. For example, glucose regulated insulin (*Ins*) gene expression in mature β-cells is achieved by the synergistic activation of the insulin promoter by Pdx1, Mafa and Neurod1 [180]. Pdx1, Mafa and Neurod1 bind to the GG2, C1, and E1 regulatory elements within the *Ins* promoter to drive the synergistic activation of *Ins* gene expression [180].

In addition, *Pdx1* deficiency reduces the activity of key target genes, including *Mafa*, *Glut2* and *Ins1*, increases apoptosis in islets, and negatively affects β-cell regeneration [178, 181]. Further, the transcription factor Foxa2, which is important for *Pdx1* regulation in the developing pancreas [182], is essential for maintaining normal insulin and glucagon secretion from islets [176, 183]. Foxa2 knock-out mice exhibit hyperinsulinemic hypoglycaemia due to a reduction in the expression of the key components of the ATP-dependent potassium channel, impaired intracellular calcium oscillations and higher numbers of docked insulin granules in addition to reduced glucagon secretion [176, 183]. Meanwhile, in addition to its role in endocrine cell specification Neurod1 is essential for the regulation of insulin biosynthesis and secretion [140, 152, 180]. Disruption of *Neurod1* expression leads to almost complete ablation of *Ins1* gene expression and also leads to a profound defect in glucose-stimulated insulin secretion by shunting glucose into the glycolytic pathway, a phenotype

observed in immature β-cells [152]. Lastly, Mafa-deficient mice develop diabetes in an age dependent manner and display impaired glucose-stimulated insulin secretion both *in vivo* and in *ex vivo* islets. In addition to functional deficits in these mice, islet architecture is also disrupted with knock-out mice having altered α- to β-cell ratios compared to controls, and α-cells dispersed throughout the islet [151].

Despite this, our understanding of these processes is far from complete and we anticipate that the identification of novel transcriptional regulators expressed specifically in islets, examination of how they are regulated and the determination of their functional roles will help further elucidate these complex networks. To this end Hoffman *et al.* [8] undertook a comprehensive analysis of gene expression in the developing pancreas and mature islets. The authors generated ten serial analysis of gene expression (SAGE) libraries from pancreas tissues at various stages of development and compared them to 195 other mouse SAGE libraries. Comparative analysis of the libraries resulted in the identification of 2,536 genes with pancreas-enriched expression, including *Myt3* [8]. Examination of *Myt3* expression across the 205 libraries demonstrated that *Myt3* SAGE tags (representing *Myt3* expression) were present in neural tissue, as well as at low levels in pancreatic and endocrine precursor cells. However, maximal *Myt3* levels were found in pancreatic islets (Figure 2.1A).

In situ hybridization on mouse embryos at E9.5 and E14.5, as well as on adult islets (Figure 2.1B-D) was performed to validate the SAGE data. Whole mount *in situ* hybridization with E9.5 embryos showed strong *Myt3* staining in the telencephalon, the second and fourth rhombomeres, as well as in the ventral neural tube (Figure 2.1B). At E14.5 there was relatively strong *Myt3* staining in the anterior of the neocortex, with weaker staining in the thalamus and tectum (Figure 2.1C). In agreement with previous studies [11],

no staining was found in the pancreas at this time point. Despite this, strong *Myt3* staining was found in mature pancreatic islets, which co-localized with both insulin and glucagon (Figure 2.1D). These data demonstrate that although *Myt3* expression is minimal in the developing pancreas it is relatively abundant in mature islets.

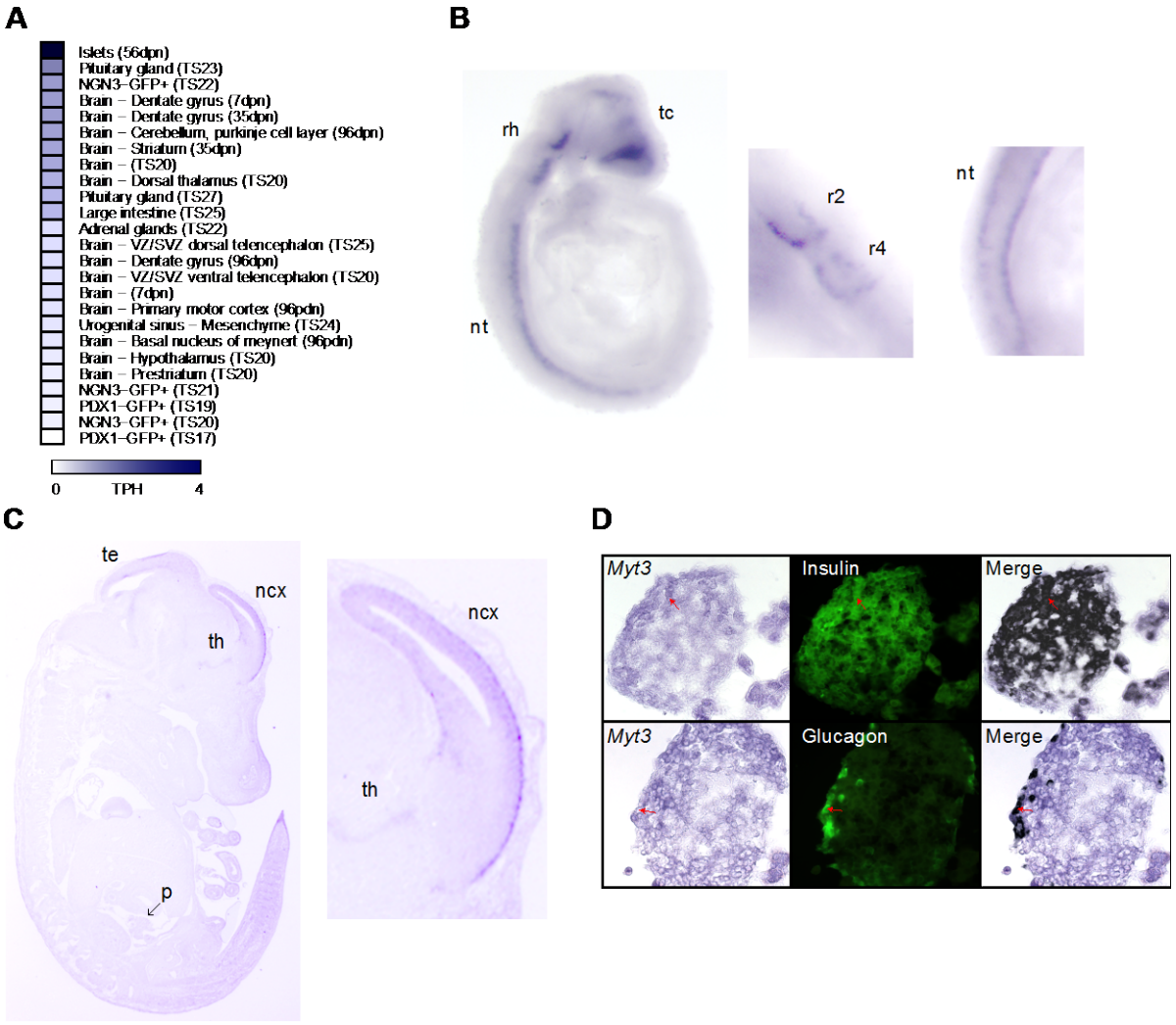

Figure 2.1: Developmental expression of *Myt3* is restricted to specific cell types
A) A heatmap showing the relative gene expression of *Myt3* in different tissues as determined by SAGE analysis of 205 Mouse Atlas of Gene Expression libraries. Tissues with no detected expression are not shown. *Myt3* expression was determined by in situ hybridisation of saggital sections of **B)** E9.5 and **C)** E14.5 mouse embryos. **B)** At E9.5 *Myt3* expression is restricted to the neural tube, second and fourth rhombomere and the telencephalon. **C)** *Myt3* expression is evident in the tectum, thalamus and neocortex in E14.5 embryos. *Myt3* is absent from the pancreas (arrow) at this time point. **D)** Combination of immunohistochemical analysis and in situ hybridisation demonstrates expression of *Myt3* in insulin and glucagon expressing cells. Co-expression in the merged image is indicated by black pseudo-colouring. Red arrow indicates single cell exhibiting co-expression of *Myt3* and insulin or glucagon.

The high degree of similarity between the MYT family members (78% similarity/53% identity between *Myt3* and *Myt1l*, 71% similarity/55% identity between *Myt3* and *Myt1*) [165], and their possible functional redundancy [165, 184], prompted the evaluation of which family member was most abundant in developing pancreas tissues and in adult islets. Analysis of the SAGE data showed that while *Myt1* is more highly expressed in *Ngn3* expressing endocrine precursor cells, *Myt3* is more abundant in mature islets (Figure 2.2A). *Myt1l* could not be assessed, as it does not produce any SAGE tags that uniquely map to it. In agreement, qPCR analysis of *Myt1*, *Myt1l* and *Myt3* in developing pancreas tissues and adult islets showed that *Myt1* was clearly more abundant than *Myt1l* or *Myt3* in the developing pancreas, particularly at E15.5 and E18.5 (Figure 2.2B-D). However, all three family members showed maximal expression in adult islets (Figure 2.2B-D), likely due to the higher proportion of cells expressing these factors in islets as compared to within the whole developing pancreas.

Total copy number of *Myt1*, *Myt1l*, and *Myt3* transcripts in islets, as well as in MIN6 (β-cell) and αTC1 (α-cell) cells was determined using absolute quantification qPCR to identify which MYT family member was most abundant in adult islets. *Myt3* was expressed at a 15-fold higher level in islets, a 4-fold higher level in MIN6 cells, and a 2.5-fold higher level in αTC1 cells than *Myt1*, and a 23-fold higher level in islets, a 3-fold higher level in MIN6 cells, and a 2.5-fold higher level in αTC1 cells than *Myt1l* (Figure 2.2E). Lastly, we found that although *Myt3* is expressed in human islets, *Myt3* expression is 4-fold higher in mouse islets (Figure 2.2F).

In addition to its enriched expression in islets, *Myt3* was hypothesised to compensate for a loss of *Myt1* based on the observation that it is upregulated in *Myt1* knock-out mice

exhibiting a milder phenotype than expected [11]. Along with its proposed compensation for the loss of *Myt1*, evidence demonstrating loss of *Myt3* following exposure of islets to cytokines [13] raises the possibility that *Myt3* may be an important mediator of islet function and survival. To test this hypothesis this Chapter assesses the expression of *Myt3* during pancreas development, its regulation by key transcription factors, and its role in islet function and survival.

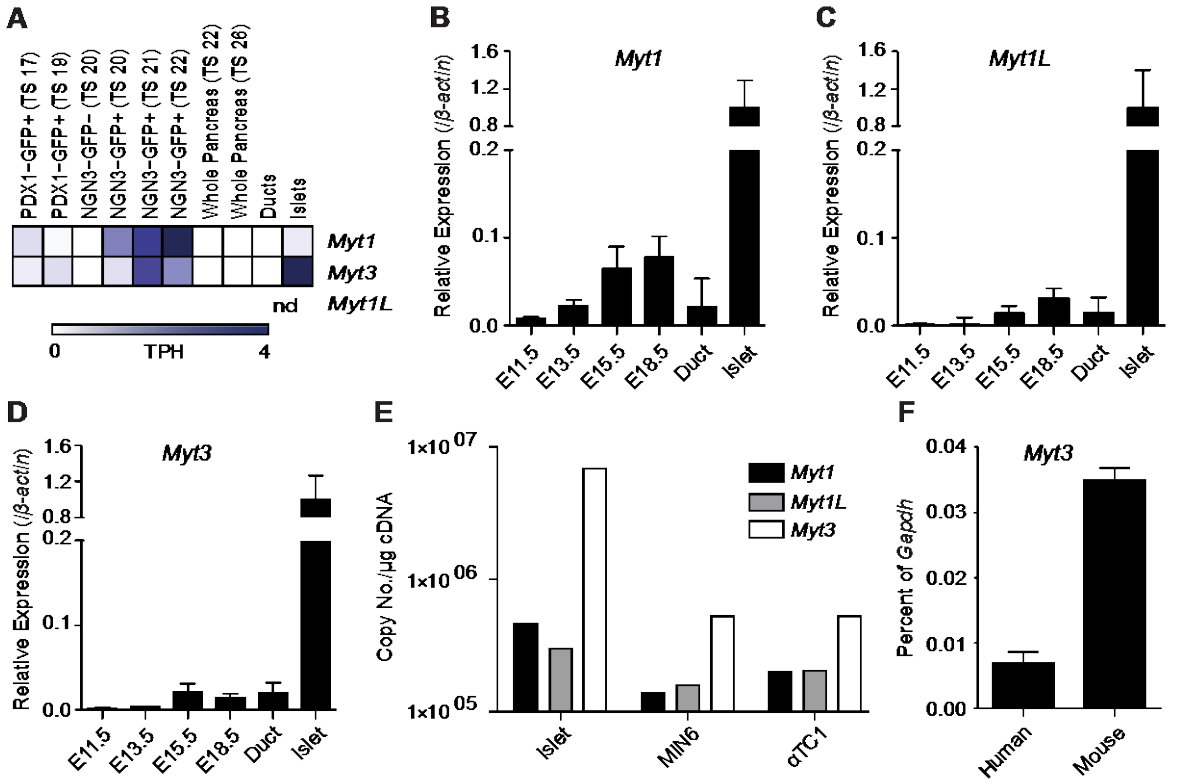

Figure 2.2: *Myt3* is the dominant MYT family member in adult islets
A) A heatmap showing the relative gene expression of *Myt1*, *Myt1l* and *Myt3* in pancreatic and endocrine precursor cells, whole pancreas, duct cells and mature islets as determined by analysis of 10 SAGE libraries (www.mouseatlas.org). nd = not detected. Expression levels for **B)** *Myt1*, **C)** *Myt1l* and D) *Myt3* in the pancreas as determined by qPCR at various stages of embryonic development as wells as in ductal cells and whole islets from adult mice (8-10 weeks of age). Expression is relative to β-actin and is normalised to expression levels in whole islets. **E)** Absolute level of *Myt1*, *Myt1l* and *Myt3* transcripts in islets, MIN6 cells (a β-cell line) and αTc1 cells (an α-cell line) as determined by qPCR. Absolute quantification expressed as number of copies per µg cDNA. **F)** Expression of *Myt3* in human and mouse islets as a percentage of *Gapdh* expression.

2.2 Methods and materials

Mouse maintenance and handling

Mice were maintained according to the guidelines of the Canadian Council on Animal Care using protocols approved by the UBC Animal Care Committee. Mice were housed in a group setting of up to five mice per cage with daily health checks and cage maintenance performed by animal facility staff members. In our colony, mice were maintained in a 12-hour light/dark cycle, fed a standard low fat diet (Labdiet 5053) *ad libitum* and their environment was enriched through administration of sunflower seeds and hiding places. Mice were housed in this setting until needed for experiments.

Mice used in non-survival procedures were anaesthetised using isofluorane inhalation followed by cervical dislocation. Toe pinch reflex was checked prior to cervical dislocation in order to ensure that the animals were at a surgical plane of anaesthesia.

ChIP-seq database analysis

Foxa2 and Pdx1 Chromatin Immunoprecipitation (ChIP) sequencing data were obtained from the Short Read Archive (SRX003306 and SRX003296) [185]. Mafa and Neurod1 ChIP sequencing data were obtained from the Gene Expression Omnibus (GSE30298). Data were analyzed as previously described [8, 185].

Islet isolations and cell culture

Pancreata from both male and female CD1 mice were perfused with 3ml 1000U/ml Collagenase XI (Sigma-Aldrich), surgically removed and placed in 50ml falcon tubes with an additional 2ml 1000U/ml Collagenase XI. Falcon tubes were incubated for 15 minutes in a

37°C water bath. Digested pancreata were manually disrupted by shaking the tubes for four minutes and passed through a 70μM filter (Corning) and islets were handpicked. Islets were cultured in RPMI 1640 (11mM glucose, RPMI Complete) supplemented with 10% FBS, 50U/ml penicillin/streptomycin and 2mM L-glutamine at 37° in a 5% CO_2 humidified incubator.

For experiments measuring *Myt3* expression in response to glucose or cytokines islets were cultured in 3mM, 7mM, 11mM, 16.7mM and 33mM glucose, or with various cytokine combinations (Ifnγ (1000U/ml), Il-1β (17.5ng/ml) and Tnfα (10ng/ml)) as appropriate. For cycloheximide (CHX) experiments, islets were pre-incubated in 3mM glucose for 6hrs and CHX (10μg/ml) or DMSO was added 1hr prior to transferring islets to fresh 3mM or 16.7mM glucose supplemented with CHX or DMSO.

MIN6 cells, a β-cell line derived from a mouse insulinoma [186], and mPAC cells, a mouse pancreatic adenocarcinoma cell line [187], were maintained in Dulbecco's Modified Eagle Medium (DMEM, 12.5mM glucose) supplemented with 10% FBS, 50U/ml penicillin/streptomycin and 2mM L-glutamine (DMEM Complete) at 37° in 5% CO_2 humidified incubator. For all experiments cells were cultured in 24-well tissue culture plates (Falcon) and plated at a density of 200,000 cells/well for MIN6 cells and 40,000 cells/well for mPAC cells. All media and supplements were purchased from Life Technologies.

Adenoviral mediated knockdown and over-expression

pLKO.1 vectors containing short hairpin constructs targeting *Myt3* under control of the hU6 promoter and a scramble shRNA construct were purchased from OpenBiosystems (Table 2.1). U6-shRNA expression cassettes were cloned into pAdTrack using InFusion cloning

(Clontech) and sequence verified. pAd-Track-hU6-shRNAs were linearized with PmeI and inserted into the pAd-Easy viral genome by homologous recombination to generate pAdV-sh*Myt3* ($5x10^3$ pfu/μl) and pAdV-sh*Scramble* ($9x10^4$ pfu/μl) [188]. Full length *Myt3* was cloned into pcDNA3.1-V5/His6 (Invitrogen) and pAdV-*Myt3* ($1x10^5$ pfu/μl) was generated as above. pAdV-*Ngn3* ($3.5x10^4$ pfu/μl) or pAdV-*βgal* ($1x10^5$ pfu/μl) were generated in a similar manner. Islets were transduced overnight with the sh*Myt3* or sh*Scramble* viruses at an MOI of 50, MIN6 cells were transduced with sh*Myt3* or sh*Scramble* viruses for 3 hours at an MOI of 0.1 to 9, and mPAC cells were transduced with *Ngn3* or *βgal* viruses for 3 hours at an MOI of 10.

Vector Name	**Target Sequence**
TRCN0000042478	AAGACTTCTGTGAGTGTTGCG
TRCN0000042479	TTAAAGACTGGATACTGCTGC
TRCN0000042480	TTACAGGGCATCTAAGTTCAG
TRCN0000042481	TATAGACTTGTCGTGGATTCG
TRCN0000042482	AAATTCTGCTCATTGATAGGC
RHS6848	Not available

Table 2.1: shRNA targeting sequences

Immunofluorescence and immunohistochemistry

Immunohistochemistry was performed on paraffin sections of E14.5 mouse embryos, as well as E16.5, E18.5 and adult ICR pancreata. Sections were washed for five minutes three times in xylene followed by two five minute washes in 100% ethanol, one five minute wash in 95% and 70% ethanol followed by a 10 minute wash in 1x PBS. Sections were incubated in a vegetable steamer for 10 minutes in 10mM sodium citrate pH6 supplemented with 0.05% tween-20. Slides were rinsed for five minutes in running tap water, five minutes in distilled water and five minutes in PBS. Sections were circumscribed with a pap pen (Liquid Blocker) and blocked for one hour at room temperature in 5% FBS in 1x PBS. Sections were co-

stained with rabbit anti-myt3 (1:250, OpenBiosystems) and guinea pig anti-insulin (1:1000; Linco), guinea pig anti-glucagon (1:1000; Linco), guinea pig anti-pancreatic polypeptide (1:100; Linco), goat anti-somatostatin (1:1000; Santa Cruz) or mouse anti-pdx1 (1:500; DSHB). Sections were washed three times in 1x PBS and primary antibodies were detected using donkey anti-rabbit Alexa 488, goat anti-guinea pig Alexa 546, goat anti-mouse Alexa 546 or donkey anti-goat Alexa 546 (1:2000; Invitrogen). The Myt3 antibody was generated by OpenBiosystems and was raised against the synthetic peptide RKGGIKMTPTKEEKEDSELR. The serum from the terminal bleed of two rabbits was affinity purified.

ChIP-qPCR

I dispersed handpicked islets by pipetting up and down in 0.01% trypsin (Gibco) in MEM (Global Cell Solutions). Cells were fixed in 1% formaldehyde and incubated at room temperature (RT) for 10 minutes, prior to the addition of 0.125M glycine followed by incubation at RT for five minutes. Cells were pelleted and resuspended in five volumes ChIP cell lysis buffer (10mM Tris-Cl, pH 8.0, 10mM NaCl, 3mM $MgCl_2$, 0.5% NP-40) containing protease inhibitor cocktail (Roche). Cells were then dounce homogenized, incubated on ice for five minutes and pelleted. The pellet was resuspended in 1.5 volumes ChIP nuclear lysis buffer (1% SDS, 5mM EDTA, 50mM Tris-Cl, pH 8.1) supplemented with protease inhibitor cocktail tablets (Roche). Cells were passed through a 26.5 gauge needle prior to sonication in a water-ice bath (Sonicator 3000, Misonix) for six cycles of 30 seconds on, 40 seconds off and chromatin was precleared with 250µl Protein G beads (Active Motif), Protein Inhibitor Cocktail (0.5µl, Active Motif) and supplemented with 7.5µl ChIP dilution buffer (0.1% SDS,

10% Triton X-100, 150mM NaCl, 16.7mM Tris-Cl, pH8.1). 3µg of anti-Foxa2 (Santa Cruz), anti-Pdx1 (Upstate), anti-Neurod1 (Cell Signaling) or normal rabbit IgG (Santa Cruz) was added to supernatants. Fresh Protein G beads were also blocked with 1mg/ml BSA and 0.1mg/ml salmon sperm DNA in ChIP dilution buffer. Following overnight incubation, rocking at 4°C, the samples were incubated with the blocked beads for four hours rocking at 4°C. The beads were then washed in low salt buffer (0.1% SDS, 1% Triton X-100, 2mM EDTA, 20mM Tris-Cl, pH8.1, 150mM NaCl), high salt buffer (low salt buffer with 500mM NaCl), Lithium Chloride buffer (0.25M LiCl, 1% NP-40, 1% deoxycholate, 1mM EDTA, 10mM Tris-Cl, pH8.1) and 2x TE buffer (10mM Trix-HCl pH8.0, 1mM EDTA). Beads were re-suspended in 125µl elution buffer (1% SDS, 0.1M $NHCO_3$) and rotated for one hour at RT. NaCl (0.192M) was added to reverse crosslink and samples were incubated overnight at 65°C. Samples were then incubated with Proteinase K (Invitrogen) and RNaseA (Sigma) for one hour at 50°C. DNA was purified by two rounds of phenol-chloroform extraction and ethanol precipitation and re-suspended in 50µl dH_2O. qPCR was performed on ChIP DNA with primers targeting Foxa2, Pdx1 and Neurod1 binding sites (Table 2.2).

To determine the chromatin state at the *Myt3* promoter, mPAC cells were transduced with pAdV-*Ngn3* or pAdV-*βgal*, and ChIP-qPCR was performed as described above, with 3µg anti-H3K4me1 (Abcam), anti-H3K4me3 (Abcam), anti-H3K27ac (Abcam), anti-H3K27me3 (Abcam) or rabbit IgG (Santa Cruz). qPCR was performed on ChIP DNA using primers targeting the *Myt3* promoter (Table 2.2). Fold enrichment was calculated relative to the IgG ChIP and percent recovery was calculated relative to sample input.

Primer Name	Forward Primer Sequence	Reverse Primer Sequence
Myt3 Promoter H3K4me1/H4K27ac	CTGGCAGTCTGTTAGTTGTTGC	GCTCTCTTTTCTCCCACAAGG
Myt3 Promoter H3K4me3/H3K27me3	TTTCAGCTACCCTCCTCCAG	AAACCACCTTCCTTCTTATAGGG
Foxa2 binding site in Nkx2.2	CCAGCTGAACAATCACTGGA	TTAGAGGGCCACTTGTCCTG
Pdx1binding site in Pdx1	CATCATCCTGACTGGGTCACT	GGTGGGAGGTAAATCGACAG
Neurod1binding site in Abcc8	GAGTGGTGGGAAATGCAGTC	CAGCCATCATCATTACCACCT
Foxa2 binding site in *Myt3*	CTAAGCTCCACCCCAAAGTG	TGGTAAACACAAGCCCCAAG
Neurod1 binding site in *Myt3*	TGTTATCATCCCTGGCCATC	TGCTGTGGCATATGTCCTTC
Pdx1 binding site in *Myt3*	CTAAGCTCCACCCCAAAGTG	TGGTAAACACAAGCCCCAAG
Negative Region	TTCCTTTCATAGCTTTCAGTACCA	GGAAGGACCATCAAGAAGAGTT

Table 2.2: PCR primers used for ChIP-qPCR

qPCR analysis

Cells were lysed in 500µl Trizol (Invitrogen) and vortexed for 10 seconds. Added 100µl chloroform to each sample and vortexted for 10 seconds. Samples were centrifuged for 10 minutes, 12000 rcf at 4°C. The aqueous layer was removed, mixed with an equal volume of 70% ethanol (EtOH) and processed using a PureLink RNA Mini kit (Ambion) according to manufacturers instructions. cDNA was generated from 1µg RNA using Superscript III according to the manufacturers instructions (Invitrogen). qPCR reactions were performed with 10ng cDNA using a Viia7 real-time PCR system and SYBR Green supermix or Universal PCR Master Mix (Applied Biosystems). Taqman probes were purchased from Applied Biosystems for *Pax6, β-actin, Myt3, Chop, Il-1 β, Il-1α, Il-6, Il-rn, iNOS* and *Tnfα.* All other primers were designed using Primer3plus (Table 2.3). *β-actin* or *Gapdh* were used as internal controls and the change in expression was calculated using $2^{-\Delta\Delta Ct}$.

Foxa2	CATCCGACTGGAGCAGCTA	TGTGTTCATGCCATTCATCC
Foxo1	AAGAGCGTGCCCTACTTCAA	TGCTGTGAAGGGACAGATTG
Hnf1a	CCGTGGTGGAGTCACTTCTT	GATGTTGTGCTGCTGCAAGT
Hnf1b	CTGCAATGGTGGTCACAGAT	ACCAGGCTTGCAGTGGAC
Hnf4a	GCCAAGATTGACAACCTGCT	CATCAGGTGAGGGTGCAG
Insm1	AGTGTGCGGGGAGACCTT	AGTACTTGCAGGGGAACACC
Mafa	AGTCGTGCCGCTTCAAG	CGCCAACTTCTCGTATTTCTCC
Myt1	ATGAGTGGGACCGTCCTCTA	AGCAAAAGAGTGTGCTGCTG
Myt1l	GCATCACCGCAGTCTGTCT	TGGAGTGGGACACTTGAGAA
Neurod1	AAGCCATGAATGCAGAGGAG	GTCTCTTGGGCTTTTGATCC
Ngn3	CAGCAAACAGCGAAGAAGCC	TCAGTGCCCAGATGTAGTTGTGG
Nkx6.1 exon 1-2	CCCGGAGTGATGCAGAGT	TCTCTCTGGTCCTGCCAAGT
Pdx1	GTACGGGTCCTCTTGTTTTCC	GATGAAATCCACCAAAGCTCAC
Rfx6	TCTGCACCCATTCTCAACTG	AGAAATCGGTGGTGTCATCAG
Sox4	CGCCTTGGTGATTTCTTGTT	TACAAAGAGGGGGTGGGTAG
Sox9	CTCCGGCATGAGTGAGGT	GTCGGTTTTGGGAGTGGTG
Abcc8	CAGGACCCTGTCCTCTTCAG	CCTCCCAGAGTGTGCTGTCT
G6pc2	AGCTGCCCTAAGCTACACCA	AACACTCCACAGAAAGGACCA
Gck	TGGTGGATGAGAGCTCAGTG	TGAGCAGCACAAGTCGTACC
Hadh	TTCCAGAGGCTGGACAAGTT	GGCATTGGCTATGTTTGTGA
Iapp	CAGCTGTCCTCCTCATCCTC	GCACTTCCGTTTGTCCATCT
Ins1	TCAGAGACCATCAGCAAGCA	CTCCCAGAGGGCAAGCAG
Ins2	GCTTCTTCTACACACCCATGT	ACGACTGATCTACAATGCCAC
Gcg	TGCAGTGGTTGATGAACACC	TGGTAAAGGTCCCTTCAGCATG
Sst	CCCAGACTCCGTCAGTTTCT	CAGCAGCTCTGCCAAGAAGT
Ppy exon 2-3	GAAACTCAGCTCCGCAGATAC	AGCAGGGAATCAAGCCAAC
Ghr	CAGTCACCAGCAGCACATTT	GGCTTGGATTGATTCTTTGC
Kcnj11	CAGGTCATCGACTCCAACAG	ACGCCTTCCAAGATGACAAT
Slc2a2	GCAACTGGGTCTGCAATTTT	CCAGCGAAGAGGAAGAACAC
Slc2a5	ATCACTGTCGGCATCCTTGT	CGGGGACTCCAGTTAGACC
Slc30a8	GGCTGACATTTGGGTGGTAT	TCACAGGCAAGGTACAGCAG
Myt3 exon 20-21	TGCCAGGATGCAATGGTC	CAATACCCCCAGTTGCTTTG
A20	AGGCTATGACAGCCAGCACT	AAACCTACCCCGGTCTCTGT
Bad	GGAGCAACATTCATCAGCAG	TCCTCCATCCCTTCATCCTC
Bak	AATGGCATCTGGACAAGGAC	TTCGAAAGACCTCCTCTGTG
Bax	GCTGGACACTGGACTTCCTC	AGCCACAAAGATGGTCACTG
Bcl-xl	GCATTGTTCCCGTAGAGATCC	ATGCAGGTATTGGTGAGTCG
Bcl2	AGAGCGTCAACAGGGAGATG	ATGCTGGGGCCATATAGTTC
Bid	CATCTTTGCTCCGTGATGTC	GTTCCTCTGGAGGCAGTGTC
Bim	GAGATACGGATTGCACAGGAG	ATTTGAGGGTGGTCTTCAGC
cIap1	TGAGAGAAGAGAAGAGGAGAAGG	CTGTTGAAAGAGGGCCATTC

cIap2	GAACATGCCAAGTGGTTTCC	GCGTCTGCATTCTCATCTTC
Igfr1	ACACGCGGTGATCTCAAAAG	ATGCCATCTGCAATCTCTCC
Noxa	GAGATGCCCGGGAGAAAG	CGATCTTCCTGAGTTGAGCTG
Puma	ACCTCAACGCGCAGTACG	TAGTTGGGCTCCATTTCTGG
Xiap	TTGGAAGCCAAGTGAAGACC	ATTCTTGCCCCTTCTCATCC
Bip	CAAGACATTTGCCCCAGAAG	GCATCTTTGGTTGCTTGTCG
Xbp1	TGAGCCCGGAGGAGAAAG	CTCTTCTTCCAAATCCACCAC
Fas	AAAAAGAGCCGAGGAGTGTG	TGATCACAAGGCCACCTTTC
Mcp1	AGGTCCCTGTCATGCTTCTG	GGATCATCTTGCTGGTGAATG
Gusb	TCAGAAGCCGATTATCCAGAGC	TGGTACTCCTCACTGAACATGC
Gapdh (HS/MS)	CTGCACCACCAACTGCTTAG	TGATGGCATGGACTGTGG

Table 2.3: qPCR primer sequences for β-cell function and survival genes

Insulin secretion assay

Fifty islets per well in a 24-well plate were transduced at an MOI of 50 and were subsequently washed and equilibrated in Kreb's Ringer Buffer (KRB) (115mM NaCl, 5mM KCl, 24mM NaHCO3, 2.5mM CaCl2, 1mM MgCl2, 10mM HEPES and 2% w/v BSA, pH7.4) with 2.8mM glucose for one hour before being transferred into 500µL KRB with either 2.8mM glucose, 16.7mM glucose, 30mM KCl or 10mM arginine for a further one hour. Supernatants were collected to measure insulin secretion and islets were lysed in 50µL RIPA buffer (ThermoFisher) for 10 minutes on ice with 1x Halt protease inhibitor cocktail (Pierce) to measure cellular insulin and total protein. All samples were analysed using the Insulin (Mouse) ELISA (Alpco) and plates were read using a Spectramax 190 plate reader (Molecular Devices).

Reporter constructs

A 1200bp region upstream of the *Myt3* transcriptional start site (TSS) was amplified from mouse genomic DNA and cloned into pGL3-Basic (Promega) to generate the *Myt3* reporter construct. The Foxa2, Pdx1 and Neurod1 binding site mutagenesis primers were designed

using the Agilent QuikChange Primer Design tool (Table 2.4). Site directed mutagenesis PCR was performed using Phusion Taq (Finnzymes).

Primer Name	Forward Primer Sequence	Reverse Primer Sequence
Myt3promPdx1mut	CACCCCAAAGTGTGGCTGCCTTTGTCATTTTACGGAGTCTGTGTTTGTGAAGT	ACTTCACAAACACAGACTCCGTAAAATGACAAAGGCAGCCACACTTTGGGGTG
Myt3promFoxa2Mut	GGCTGCCTTTGTCATTTTAATTGGTCTGGCGCCGTGAAGTGGGGCCTCTATTTACTTATA	TATAAGTAAATAGAGGCCCCACTTCACGGCGCCAGACCAATTAAAATGACAAAGGCAGCC
Myt3PromNeurodmut	AGCCATTGTTATCATCCCTGGCTCTCGTCTGCAGAGGAGTGATATTCCAT	ATGGAATATCACTCCTCTGCAGACGAGAGCCAGGGATGATAACAATGGCT

Table 2.4: *Myt3* promoter mutagenesis primer sequences

Luciferase assays

40,000 mPAC cells were transfected with 400ng of pGL3-*Myt3*-promoter reporter construct, pGL3-*Myt3*-promoter mutant constructs or a control pGL3-Basic vector, with or without 200ng of *Foxa2*, *Pdx1* or *Neurod1* and 2ng pRL-TK (renilla luciferase) using Lipofectamine 2000 (Invitrogen) according to manufacturers instructions. An *EGFP* vector was used to ensure equal amounts of DNA were transfected into each well. After 48hrs reporter activity was analyzed using the Promega Dual Luciferase kit as per manufacturer's instructions using a Spectramax L luminometer (Molecular Devices).

Western blot analysis

Cell lysates were prepared from islets by sonication in RIPA buffer (ThermoFisher). 25µg of total protein was loaded in each well of a 4-12% NuPAGE Bis-Tris gel (Invitrogen). Gels were transferred to 0.2um polyvinyl difluoride (PVDF) membranes (ThermoFisher) for one hour at 100V in an XCell SureLock Mini-Cell (Invitrogen) according to the manufacturers instructions. Membranes were probed with antibodies against: Myt3 (1:2000;

OpenBiosytems), Mafa (1:400; Abcam), and Pdx1 (1:500; Upstate) overnight at 4°C in 5% skim milk diluted in 1x TBS supplemented with 0.05% tween-20. Blots were subsequently stripped using the Abcam mild stripping protocol and re-probed with anti-β-actin (1:500; Santa Cruz). Donkey anti-Rabbit (Santa Cruz) and Rabbit anti-Goat (Santa Cruz) HRP-conjugated secondary antibodies were used at 1:10000 in 1xPBS for one hour at room temperature. Membranes were treated with ECL reagent (ThermoFisher) for one minute prior to developing films.

Statistical analysis

For ChIP-qPCR p-values for enrichment over a negative control region were calculated using a Kruskal-Wallis test with a Dunn's multiple comparison on $2^{-\Delta Ct}$ values, data are presented as fold-enrichment over a negative region +/- SD. For luciferase data relative luciferase activity values were compared using unpaired, two-tailed Student's t-tests combined with a Holm-Sidak correction for multiple comparisons, data are represented as mean +/- SD. For qPCR experiments paired, two-tailed Student's t-tests were used to compare ΔC_T. Data are presented as relative quantification values with upper and lower limits. P-values for western blot and apoptosis were determined using paired, two-tailed Student's t-tests and data are represented as mean +/- S.E.M. In all cases * indicates a statistically significant difference at $p \leq 0.05$, ** at $p \leq 0.01$, *** at $p \leq 0.001$.

2.3 Results

Myt3 is expressed in maturing and adult endocrine cells

To determine whether Myt3 protein levels match the observations made by Dr. Hoffman, and to identify the cell types that Myt3 is expressed in, we developed an antibody targeting the synthetic peptide RKGGIKMTPTKEEKEDSELR. Using this antibody we found no evidence of Myt3 protein in the developing pancreas at either E14.5 or E16.5 (Figure 2.3). At E18.5 however, Myt3 protein was found in both insulin (β-cells) and glucagon (α-cells) expressing cells (Figure 2.3). Similarly, Myt3 staining was evident throughout the islet in adult pancreas sections, while no Myt3 staining was evident in the surrounding tissue (Figure 2.4). Similar to *in situ* experiments with whole islets, co-staining of adult sections with endocrine cell markers showed that Myt3 co-localises in cells expressing insulin (β-cells), glucagon (α-cells), somatostatin (δ-cells) and pancreatic polypeptide (PP-cells) (Figure 2.4). Co-localisation of Myt3 with endocrine markers was confirmed at high magnification, and indicated that in mature endocrine cell types Myt3 is primarily cytoplasmic, with only a fraction of total protein localising to the nucleus (inset), similar to other β-cell transcription factors such as Pdx1 and Neurod1 [189, 190]. These data indicate that Myt3 is first evident at E18.5, and that it is expressed in mature α-, β-, δ-, and PP-cell types.

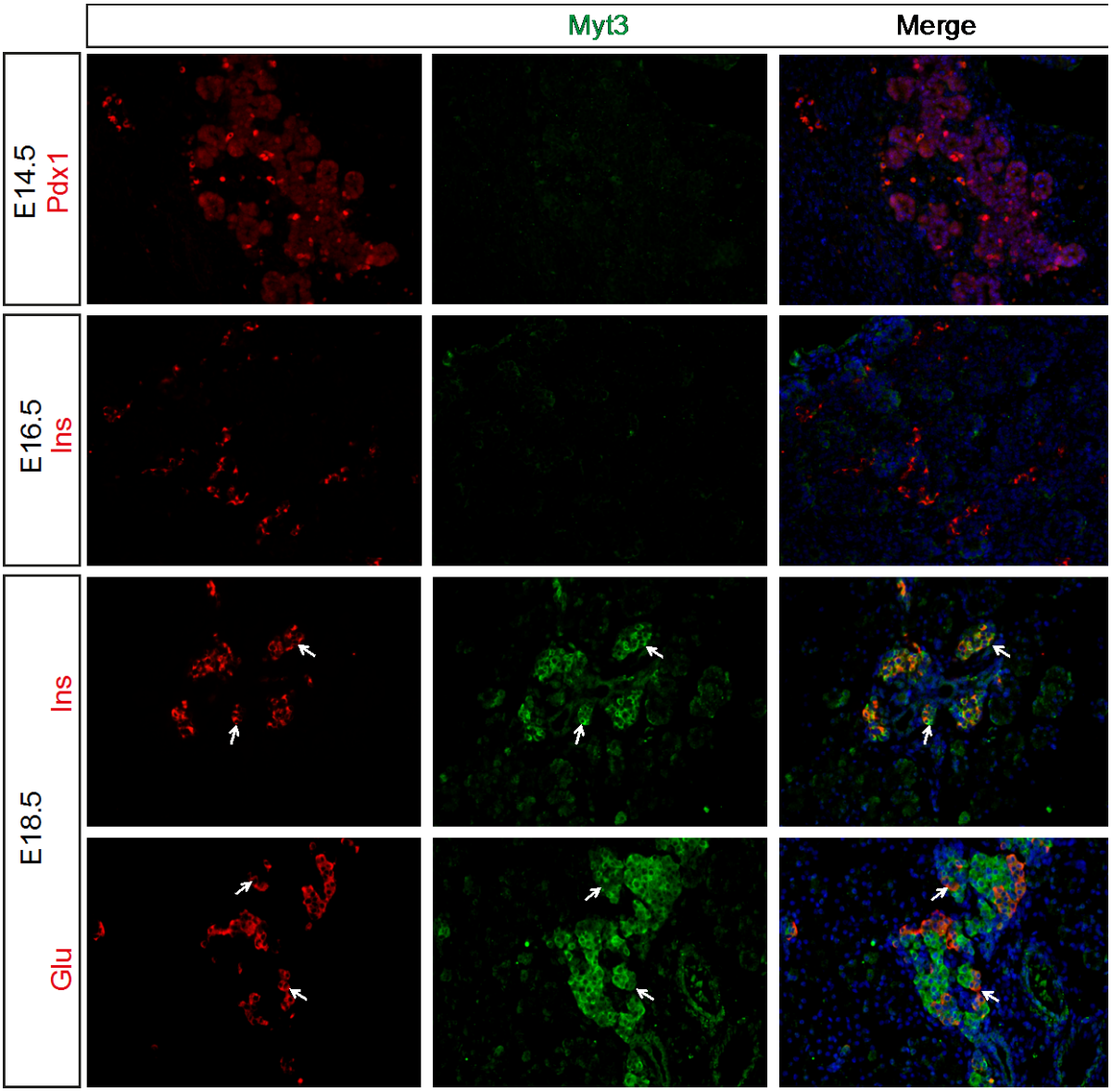

Figure 2.3: Myt3 protein is detected in endocrine cells from E18.5
Saggital sections of E14.5, E16.5 and E18.5 pancreata were analysed for expression of insulin, glucagon or Pdx1, as indicated (red), and Myt3 (green). Nuclei were stained with Hoechst (blue). Arrows indicate co-localisation of Myt3 with indicated endocrine markers.

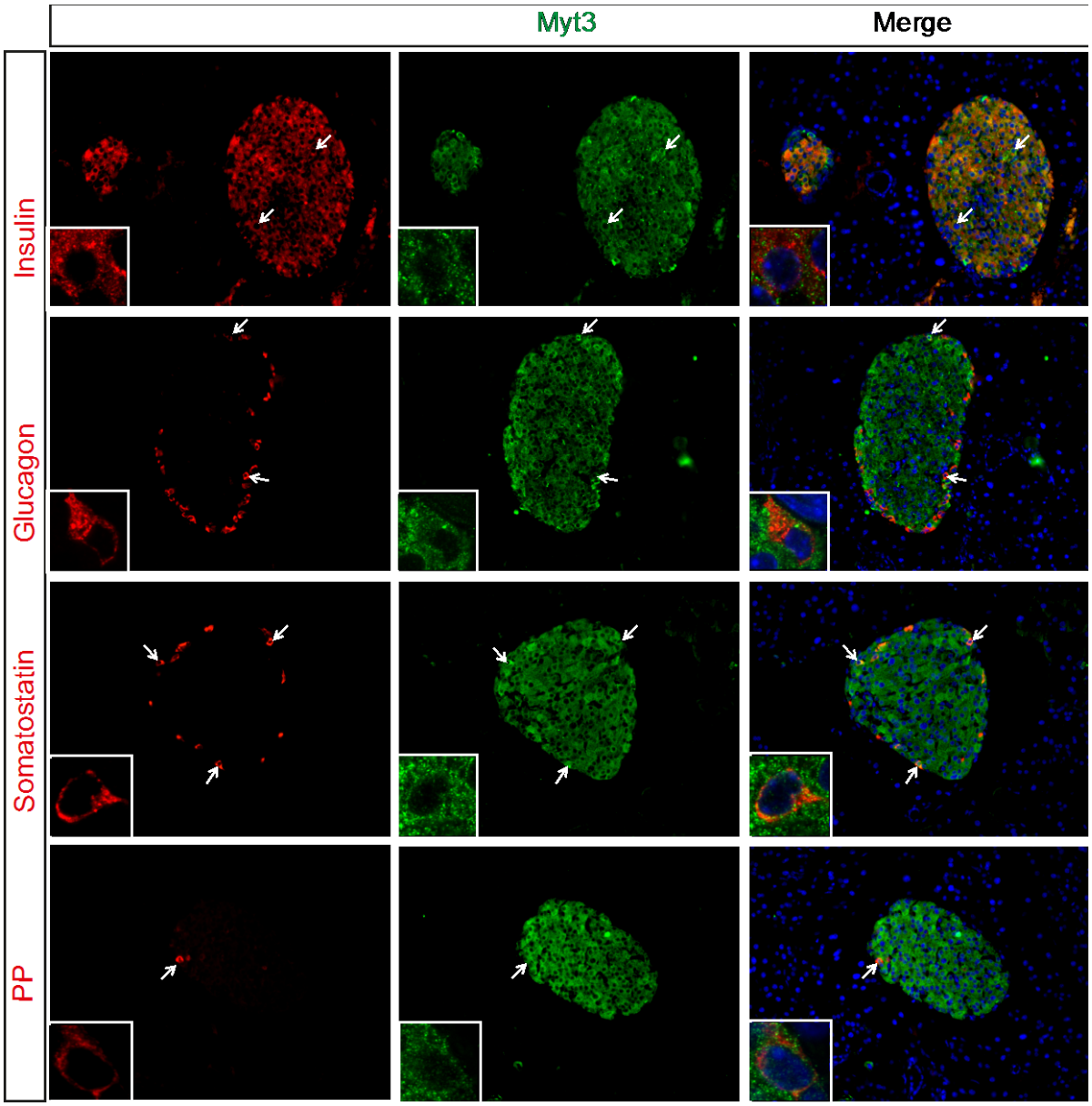

Figure 2.4: Myt3 co-localises with endocrine cell markers in adult islets
Sections of adult pancreata were analysed for expression of insulin, glucagon, somatostatin and pancreatic polypeptide, as indicated (red), and Myt3 (green). Nuclei were stained with Hoechst (blue). Arrows indicate co-localisation of Myt3 with indicated endocrine markers. High magnification confocal images of individual cells showing co-localization of Myt3 with insulin, glucagon, somatostatin and pancreatic polypeptide, representative cells are shown (inset), note that Myt3 staining is predominately cytoplasmic but can also be found within the nucleus.

Myt3 expression is regulated by Foxa2, Pdx1 and Neurod1

To characterise the factors responsible for regulating *Myt3* expression we assessed Foxa2, Pdx1, Neurod1 and Mafa ChIP-seq data generated from islets [185]. We identified Foxa2, Pdx1 and Neurod1 enrichment in the *Myt3* promoter region (Figure 2.5A) suggesting its expression is directly regulated by these factors. No enrichment of Mafa was noted. ChIP-qPCR using an antibody against Foxa2 resulted in a 250-fold ($p \leq 0.01$, n=3) enrichment of an *Nkx2.2* positive control region [8], and a 500-fold ($p \leq 0.01$, n=3) enrichment of the *Myt3* promoter (Figure 2.5B). Meanwhile, using an antibody against Pdx1 we obtained a 180-fold ($p \leq 0.01$, n=3) enrichment in a *Pdx1* positive control region [8], and a 90-fold ($p \leq 0.01$, n=3) enrichment of the *Myt3* promoter (Figure 2.5C); and using an antibody against Neurod1 we obtained a 21-fold ($p \leq 0.001$, n=3) enrichment of an *Abcc8* control region, and a 70-fold ($p \leq 0.001$, n=3) enrichment of the *Myt3* promoter (Figure 2.5D).

To further confirm the direct regulation of *Myt3* expression by these factors we generated a *Myt3*-promoter luciferase reporter. In co-transfections with this reporter, Foxa2 reduced *Myt3* promoter activity by 1.3-fold ($p \leq 0.001$, n=3), while Pdx1 and Neurod1 increased promoter activity by 1.3-fold ($p \leq 0.001$, n=3) and 9-fold ($p \leq 0.001$, n=3), respectively (Figure 2.6E-G). Mutation of the Foxa2 binding site reversed the suppressive effect of Foxa2 by 2-fold ($p \leq 0.001$, n=3), while mutation of the Pdx1 and Neurod1 binding sites reduced the relative luciferase activity by 3-fold ($p \leq 0.001$, n=3) and 3.4-fold ($p \leq 0.001$, n=3), respectively, over the non-mutated promoter (Figure 2.6E-G). Together, these data show that Foxa2, Pdx1 and Neurod1 directly regulate *Myt3* expression.

Genes regulated by Neurod1 in mature tissues are often initially induced during development by the related bHLH transcription factor Ngn3, which is critical to pancreas

endocrine cell specification [132], as both bind to E-box elements [191, 192]. Thus, to test whether *Ngn3* induces *Myt3*, we transduced mPAC cells with an *Ngn3* over-expressing adenovirus, or control *βgal* expressing virus at an MOI of 10. *Ngn3* over-expression resulted in a 963-fold ($p \leq 0.0001$, n=4) increase in *Myt3* expression relative to cells treated with the *βgal* virus (Figure 2.6H). We next evaluated the ability of *Ngn3* over-expression to alter the histone modification status of the *Myt3* promoter to establish the mechanism of *Myt3* induction. We performed ChIP-qPCR for mono-methylated Histone 3 Lysine 4 (H3K4me1) (Figure 2.6I), tri-methylated Histone 3 Lysine 4 (H3K4me3) (Figure 2.6J) and acetylated Histone 3 Lysine 27 (H3K27ac) (Figure 2.6K), which demarcate active cis-regulatory loci [193-196]; as well as, for tri-methylated Histone 3 Lysine 27 (H3K27me3) (Figure 2.6L), which is associated with repressed chromatin [41,42,43].

Our data demonstrate *Ngn3* over-expression in mPAC cells increased the levels of H3K4me1 and H3K27ac by 2-fold ($p \leq 0.0001$, n=3) and 3-fold ($p \leq 0.05$, n=3) respectively. Meanwhile levels of tri-methylated Histone 3 Lysine 27 (H3K27me3) were reduced 5-fold ($p \leq 0.01$, n=3) relative to *βgal* expressing cells. Levels of tri-methylated Histone 3 Lysine 4 (H3K4me3) were unchanged. These data suggest that *Ngn3* expression promotes changes in the epigenetic landscape around the *Myt3* promoter from an inactive, to an active chromatin state, thereby initiating its expression.

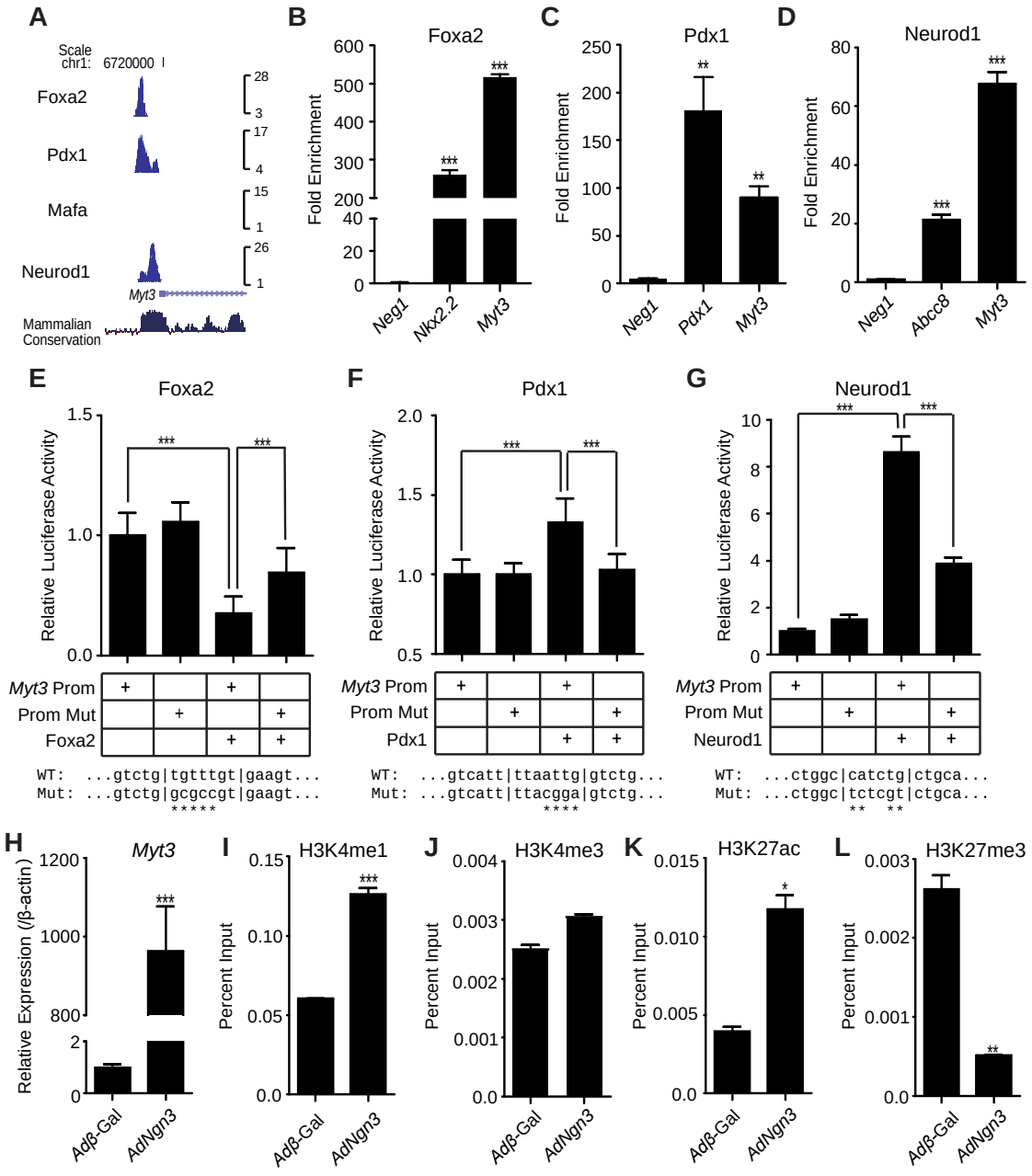

Figure 2.5: *Myt3* expression in islets is controlled by known regulators of β-cell function and survival
A) A screenshot of the *Myt3* promoter region in the UCSC genome browser showing Foxa2, Pdx1, Mafa and Neurod1 ChIP-seq data from islets. Peaks indicate binding sites. ChIP-qPCR was used to validate **B)** Foxa2, **C)** Pdx1 and **D)** Neurod1 binding within the *Myt3* promoter region. *Nkx2.2*, *Pdx1* and *Abcc8* are positive controls for Foxa2, Pdx1 and Neurod1 binding respectively. **E-G)** Relative luciferase activity of the indicated luciferase reporter vectors co-transfected with empty vector or with Foxa2, Pdx1 or Neurod1 expressing vectors. Mutant vectors had the indicated transcription factor binding sites altered by site-directed mutagenesis. Wild type and mutant binding site sequences are as indicated. **H)** *Myt3* expression relative to *β-actin* following treatment of mPAC cells with pAdV-*Ngn3*. ChIP-qPCR was used to determine **I)** H3K4me1, **J)** H3K4me3, **K)** H3K27ac and **L)** H3K27me3 histone modifications at the *Myt3* promoter. * indicates a statistically significant difference at $p \leq 0.05$, ** at $p \leq 0.01$, and *** at $p \leq 0.001$ based on student's t-test with a Holm-Sidak multiple comparison correction for luciferase data and a Kruskal-Wallis test with a Dunn's multiple comparison for ChIP-qPCR data.

Myt3 expression is regulated by glucose and cytokines

Under normal physiological conditions islets are exposed to fluctuating concentrations of glucose and many genes with critical roles in controlling islet function, such as *Ins*, *Iapp* and *Mafa*, are regulated by glucose [189, 197-199]. To determine whether *Myt3* is similarly regulated we assessed its expression in islets at various glucose concentrations 24 hours after transfer from 3mM glucose. Exposure of islets to 7mM, 11mM, 16.7mM and 33mM glucose increased *Myt3* expression by 1.78- ($p \leq 0.001$, n=4), 2.74- ($p \leq 0.001$, n=4), 2.71- ($p \leq 0.001$, n=4) and 2.86-fold ($p \leq 0.001$, n=4), respectively, over 3mM glucose (Figure 2.6A). We next sought to determine the timing of the increase in *Myt3* expression in response to glucose. Three hours after transfer to 16.7mM glucose there was no change in *Myt3* expression, and only a slight but significant (1.2-fold, $p \leq 0.05$, n=4) change by six hours; however, by 12 hours *Myt3* had reached maximal induction (1.84-fold, $p \leq 0.001$, n=4) and this was maintained at 24 hours (1.70-fold, $p \leq 0.001$, n=4) (Figure 2.6B).

The delay in glucose-induced *Myt3* expression suggests that it may be dependent on the synthesis of additional regulatory proteins in addition to the translocation of transcription factors to the nucleus. To test this we treated islets with cycloheximide (CHX, 10µg/ml) to inhibit protein synthesis. Interestingly, treatment with CHX increased basal *Myt3* expression by 4.2-fold ($p \leq 0.001$, n=3) relative to 3mM glucose with DMSO. Induction with 16.7mM glucose increased *Myt3* levels a further 3.6-fold ($p \leq 0.01$, n=3), similar to the level of *Myt3* induction by 16.7mM glucose in DMSO (3.2 fold, $p \leq 0.001$, n=3) (Figure 2.6C). These data indicate that *Myt3* expression is positively regulated by the glucose signals responsible for insulin secretion, and suggest that *Myt3* is repressed by some factor that requires continued protein synthesis.

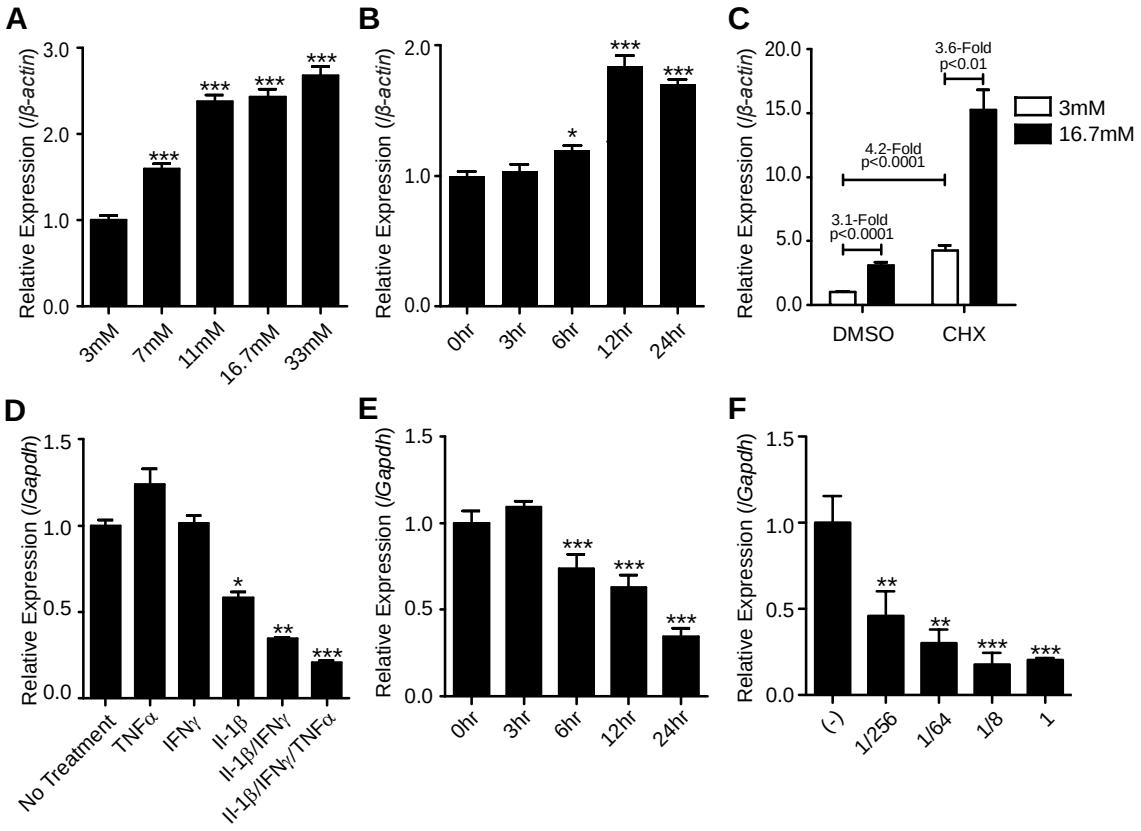

Figure 2.6: *Myt3* expression is sensitive to both glucose and cytokine exposure
A) Whole cultured islets were treated with the indicated glucose concentrations for 24hrs, after being pre-incubated for 24hr in 3mM glucose. Subsequently qPCR was used to determine the relative expression of *Myt3* as compared to *β-actin*. **B)** *Myt3* expression was determined at the indicated time points following transfer into 16.7mM glucose. **C)** *Myt3* expression was determined for islets incubated in low or high glucose following treatment with DMSO or cycloheximide (10µg/ml). Expression is expressed relative to *β-actin*. **D)** Whole cultured islets were treated with the indicated cytokine combinations, or **E)** with triple cytokine mix at the indicated time points. *Myt3* expression is expressed relative to *Gapdh*. **F)** Whole cultured islets were treated with the indicated cytokine doses (a dose of "1" equals 1000U/ml INFγ, 17.5ng/ml IL-1β and 10ng/ml of TNFα) for 24 hours. Subsequently qPCR was used to determine the relative expression of *Myt3*. Expression is expressed relative to *Gapdh*. * indicates a statistically significant difference at $p \leq 0.05$, ** at $p \leq 0.01$, and *** at $p \leq 0.001$, based on student's t-test.

In both type 1 and type 2 diabetes β-cell exposure to cytokines can induce dysfunction by altering the expression of genes responsible for regulating normal β-cell function [13, 200]. In fibroblasts *Myt3* was found to be up-regulated by exposure to TNFα [12], but to be down-regulated in a microarray study of genes affected by exposure to Il-1β and Ifnγ in rat islets [13]. To clarify this discrepancy, we examined the expression level of *Myt3* following

exposure of islets to different combinations of Il-1β, Ifnγ, and Tnfα. *Myt3* expression was reduced by exposure of islets to Il-1β (1.7 fold, $p \leq 0.05$, n=3) but not by Ifnγ or Tnfα, while a combination of Il-1β and Ifnγ reduced *Myt3* expression 3-fold ($p \leq 0.01$, n=3). Treatment of islets with Il-1β, Ifnγ and Tnfα together had the most significant effect, reducing *Myt3* expression 5-fold ($p \leq 0.001$, n=3) (Figure 2.6D). Cytokine-induced reduction of *Myt3* expression was also time dependent. At three hours post transfer into a full dose of cytokine mix *Myt3* expression was unchanged. By six hours post transfer *Myt3* expression was significantly reduced (1.35-fold, $p \leq 0.001$, n=3) with maximal suppression being reached by 24 hours (2.9-fold, $p \leq 0.001$, n=3) (Figure 2.6E). To determine how *Myt3* expression varied with cytokine dose we treated islets with varying concentrations of the triple cytokine mix. Our data demonstrate that maximal reduction in *Myt3* levels was evident at 1/8th the concentration of Il-1β, Ifnγ and Tnfα used above (i.e. 125 U/ml Ifnγ, 2.15ng/ml IL-1β and 1.25 ng/ml Tnfα) (Figure 2.6F).

As Il-1β, Ifnγ and Tnfα are important cytokine effectors of β-cell death in T1D [13, 200], we next sought to determine whether *Myt3* is reduced by immune-cell attack in non-obese diabetic (NOD) mice. We isolated RNA from whole pancreata from 4-week old pre-diabetic and 12-week old diabetic female NOD mice and analysed *Myt3* expression. Our data demonstrate that in pancreata from diabetic mice *Myt3* expression is reduced by 2.5-fold ($p \leq 0.05$, n=4) (Figure 2.7A). We also assessed Myt3 expression relative to the level of immune infiltration by immunofluorescence. For this, we independently scored insulitis levels and changes in Myt3 signal in pancreas sections from 12-week old female NOD mice (Figure 2.7B, C). From this analysis it was evident that as insulitis progresses there is a concomitant decrease in Myt3 expression. Together, these data suggest that cytokines that

cause β-cell dysfunction and apoptosis negatively regulate *Myt3* expression and that this may be relevant to the progression of diabetes in NOD mice.

Myt3 suppression reduces insulin content in β-cells

To determine whether *Myt3* plays a role in regulating insulin secretion we generated three adenoviruses expressing an shRNA sequence targeting *Myt3* (sh*Myt3*) (see methods) or a scramble sequence (sh*Scramble*). qPCR analysis of islets transduced with clone TRCN0000042479 showed the sh*Myt3* virus had no effect on *Gapdh*, but reduced *Myt3* levels by 5-fold ($p \leq 0.001$, n=10) as compared to islets treated with the sh*Scramble* virus (Figure 2.8A). Treatment of whole islets with the sh*Myt3* virus also significantly reduced Myt3 protein level by 2-fold ($p \leq 0.01$, n=3) (Figure 2.8B, C). *Myt3* suppression in islets modestly, but significantly (1.4-fold, $p \leq 0.05$, n=3) reduced cellular insulin levels (Figure 2.8D), but had no effect on their ability to secrete insulin following stimulation with glucose, KCl or arginine (Figure 2.8E-G). To determine how suppression of *Myt3* reduces cellular insulin levels we assessed the effect of *Myt3* suppression on the expression of selected transcriptional regulators important for pancreas development or function, or genes with well established roles in β-cell function. *Myt3* suppression in *ex vivo* islets had a significant effect on several transcription factors and cofactors known to regulate β-cell function, including *Hnf1α*, *Hnf1β*, *Hnf4α*, *Insm1*, *Sox9*, *Pdx1*, and *Mafa*, which were all reduced by at least 1.6-fold (Figure 2.9A). Of the genes involved in β-cell function, *Myt3* suppression reduced *Abcc8* and *Slc30a8* the most, by 1.54-fold and 1.67-fold respectively (Figure 2.9B). *Myt3* suppression also impaired *Ins1* and *Ins2* expression, while the expression levels of the other islet hormones were unaltered (Figure 2.9B).

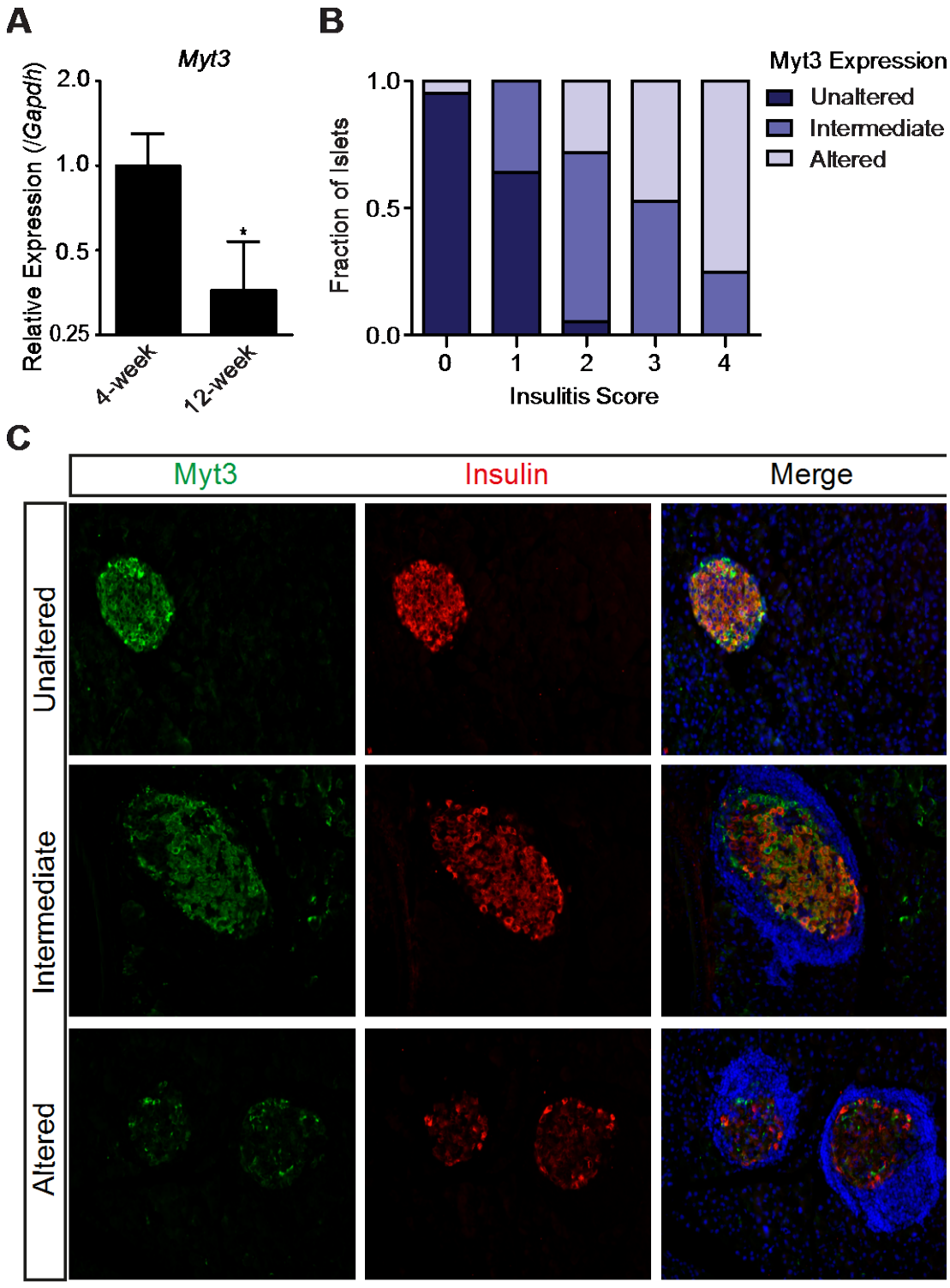

Figure 2.7: Exposure of islets to cytokines in a mouse model of T1D decreases Myt3
A) RNA was isolated from whole pancreas of female 4-week and 12-week old NOD mice and *Myt3* expression was determined relative to *Gapdh*. **B)** Insulitis levels, and Myt3 expression, were scored by analysing sections from 12-week old NOD mice. **C)** Representative images of NOD sections showing Myt3 (green) and Insulin (red) expression in islets that are unaltered, intermediately altered and altered. Nuclei were stained with Hoechst (blue). * indicates a statistically significant difference at $p \leq 0.05$ based on student's t-test.

Given this, and as Pdx1 and Mafa have well-established roles in β-cell function [151, 201], we attempted to validate their repression at the protein level. Western blot analysis showed Mafa protein levels were reduced by 1.67-fold ($p<0.001$, n=3) and Pdx1 levels by 1.48-fold ($p<0.001$, n=3) (Figure 2.9C, D), consistent with our qPCR data. These results suggest that *Myt3* affects cellular insulin content via the regulation of several genes including *Ins1, Ins2, Pdx1* and *Mafa.*

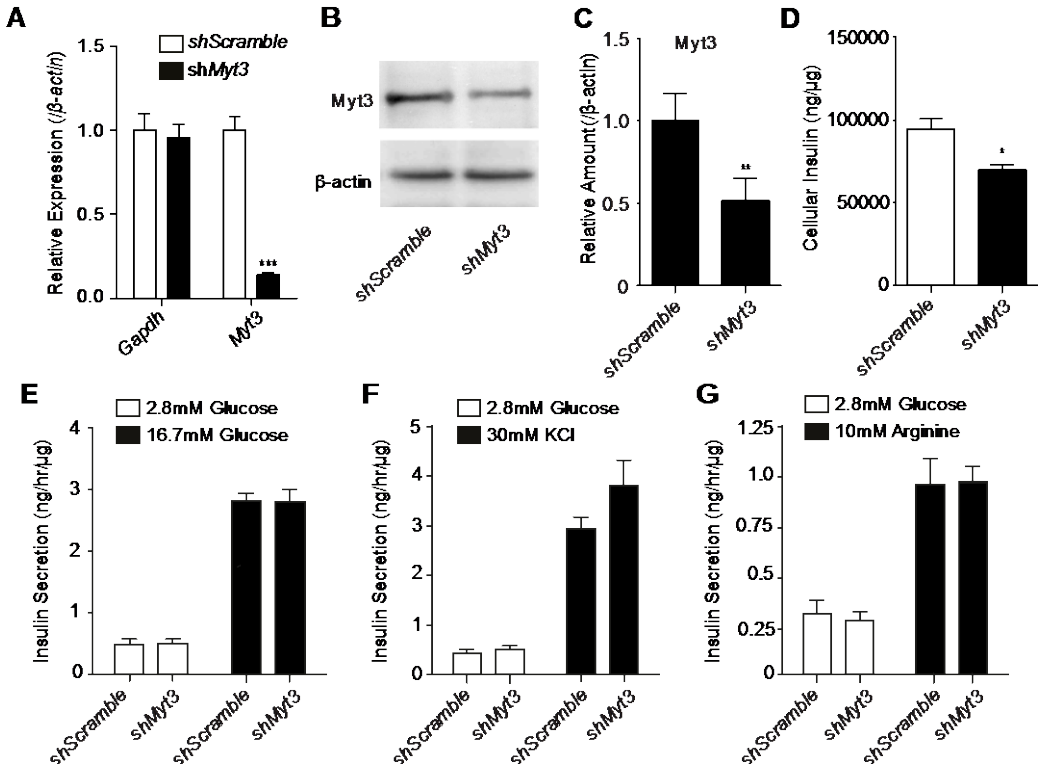

Figure 2.8: *Myt3* regulates insulin content but not insulin secretion
Islets were transduced with adenoviruses expressing shRNAs targeting *Myt3* or a scrambled sequence. **A)** *Myt3* expression relative to *β-actin. Gapdh* was used as a control for off target effects. **B)** Western blot analysis of Myt3 and β-actin protein levels in islets. **C)** Results of the densitometry of triplicate western blot analyses from B relative to β-actin. **D)** Cellular insulin content and insulin secretion induced with **E)** 16.7mM Glucose, F) 30mM KCl or **G)** 10mM Arginine. * indicates a statistically significant difference at $p\leq0.05$, ** at $p\leq0.01$, *** at $p\leq0.001$ based on students t-test.

Myt3 is required for β-cell survival

Exposure of islets to cytokines both *in vitro* and *in vivo* suppresses *Myt3* expression suggesting a potential role for *Myt3* in β-cell survival. To test this hypothesis we transduced MIN6 cells with our control or sh*Myt3* adenoviruses and incubated the cells with propidium iodide (PI). Increasing sh*Myt3* virus concentration significantly increased β-cell death over time ($p \leq 0.0001$, n=4) (Figure 2.10A). Similarly, *Myt3* suppression increased Annexin-V positive cells by 2-fold ($p \leq 0.001$, n=3) (Figure 2.10B), and the level of cleaved caspase 3 (Figure 2.10C). To validate these results we performed TUNEL analysis on dispersed islets treated with either the sh*Scramble* or sh*Myt3* virus.

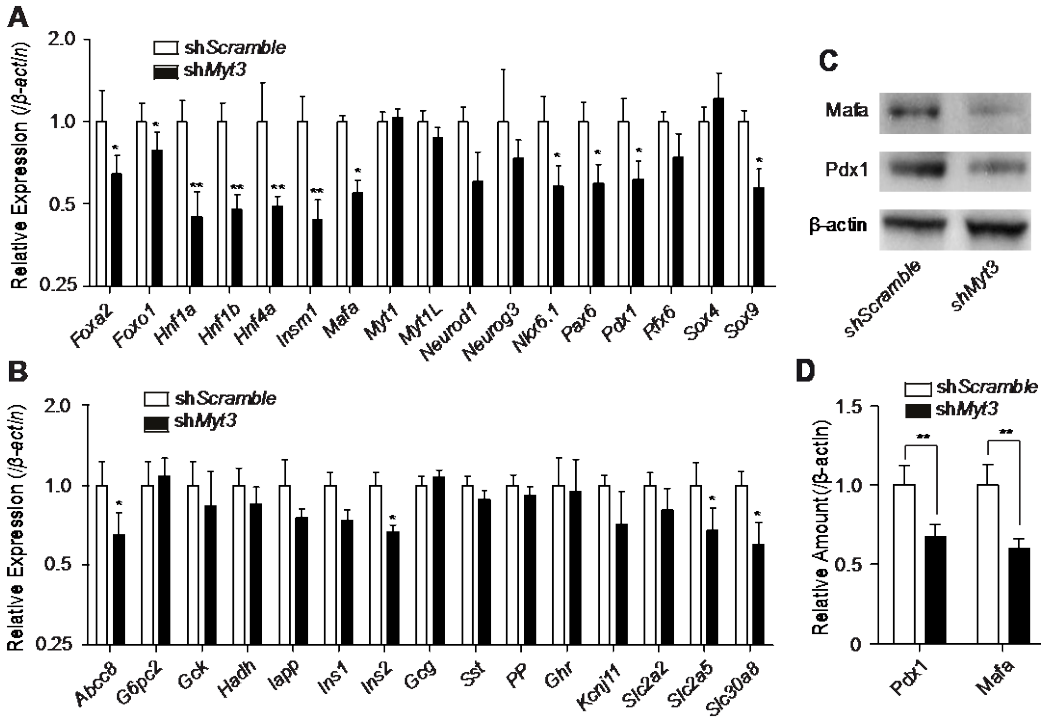

Figure 2.9: *Myt3* regulates gene expression in β-cells
Islets were transduced with adenoviruses expressing shRNA's targeting *Myt3* or a scrambled sequence. qPCR was used to determine the relative expression of **A)** transcription factors and cofactors and **B)** Genes involved in β-cell function/physiology as compared to *β-actin*. **C)** Western blot analysis of Mafa, Pdx1, and β-actin protein levels. **D)** Results of the densitometry of triplicate western blot analyses from C relative to β-actin. * indicates a statistically significant difference at $p \leq 0.05$, ** at $p \leq 0.01$ based on students t-test.

Our data show that apoptosis was increased by approximately 2-fold ($p \leq 0.01$, n=4) (Figure 2.10D), similar to our results in MIN6 cells. This was also confirmed in whole islets (Figure 2.10E). As cytokine exposure results in reduced *Myt3* expression, and adenoviral mediated suppression of *Myt3* increases apoptosis, we examined the ability of *Myt3* over-expression to protect islets from cytokine mediated cell death. Dispersed islets treated with an adenovirus over-expressing *Myt3* had a greater than 2-fold ($p \leq 0.01$, n=4) decrease in cytokine induced apoptosis, as compared to islets treated with a control adenovirus expressing eGFP, as revealed by TUNEL staining (Figure 2.10F).

To determine how *Myt3* regulates apoptosis in β-cells we examined the expression of a number of different anti-apoptotic and pro-apoptotic genes in sh*Myt3*- and sh*Scramble*-transduced islets. Our data demonstrate that *Myt3* suppression leads to a 1.25-fold ($p \leq 0.01$, n=3) reduction in *Bcl-xl*, a 1.54-fold ($p \leq 0.01$, n=3) reduction in *Igfr1* and a 1.4-fold ($p \leq 0.05$, n=3) reduction in *c-Iap2* (Figure 2.10G). To determine whether endoplasmic reticulum (ER) stress played a role in these changes we assessed the expression of genes characteristic of ER stress [202, 203]. We found that *Bip, Chop, Gadd34* and *iNos* were unchanged, however, *Xbp1* was reduced 2-fold ($p \leq 0.05$, n=3) (Figure 2.10H). Finally, as *Myt3* plays a role in pro-inflammatory gene expression in fibroblasts, we further assessed the expression of selected β-cell expressed cytokines. *Myt3* suppression caused a 2-fold ($p \leq 0.05$, n=3) reduction in *Il-6* expression but had no effect on the expression levels of *Il-1α, Il-1β, Il-1rn* or *Tnfα* (Figure 2.10I). Together, these results indicate that *Myt3* plays a significant role in regulating β-cell survival and pro-inflammatory gene expression in *ex vivo* islets.

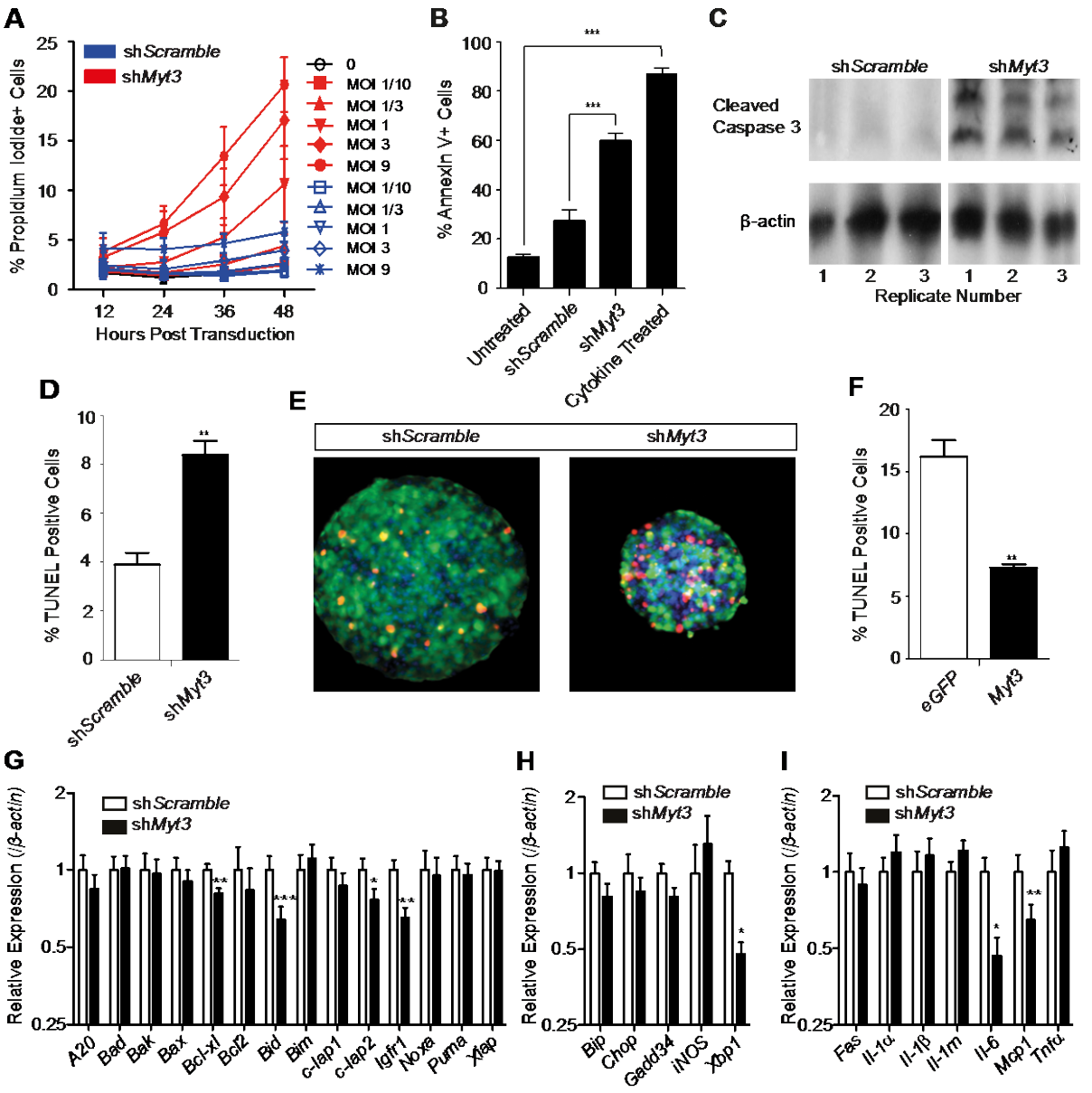

Figure 2.10: *Myt3* is critical for β-cell survival

A) The percent of MIN6 cells that were PI positive at the indicated time points after being transduced with varying amounts of adenoviruses expressing shRNA's targeting *Myt3* or a scrambled sequence. **B)** Quantification of Annexin-V APC positive cells in virus treated MIN6 cells. Untransfected cells were used as a negative control while cytokine treated cells acted as a positive control. **C)** Western blot analysis of cleaved Caspase 3 and β-actin levels in transduced MIN6 cells. Numbers indicate separate biological replicates. **D)** Quantification of TUNEL positive cells in dispersed islets treated with *shScramble* or *shMyt3* viruses. **E)** Representative images of TUNEL staining (red) of transduced islets. Transduced cells are stained in green and nuclei are labelled with Hoechst (blue). **F)** Quantification of TUNEL positive cells in cytokine treated, dispersed islets transduced with *eGFP* or *Myt3* over-expression viruses. **G-I)** Expression of pro- and anti-apoptotic genes relative to *β-actin*. * indicates a statistically significant difference at $p \leq 0.05$, ** at $p \leq 0.01$, *** at $p \leq 0.001$ based on students t-test.

2.4 Discussion

We anticipated that the identification of transcription factors specifically expressed in developing endocrine cells, or in adult pancreatic islets, would provide insight into the transcriptional networks that regulate β-cell genesis and function [8]. In trying to find such factors we identified *Myt3*. Previous reports indicated that the MYT family of transcription factors is highly expressed in neural tissue [166, 204], but that only *Myt1* is expressed in developing pancreas cells [205]. Our data agree with these reports and indicate that *Myt1l* and *Myt3* have little or no expression early in pancreas development [11]; however our SAGE, qPCR, and IHC data indicate that *Myt3* is relatively abundant in mature pancreatic islets. Furthermore, *Myt3* is expressed in human islets, albeit at a lower level than in mouse islets, suggesting that *Myt3* is important not only for islet function in rodents, but also in humans.

We demonstrated that Myt3 protein first appears in endocrine cells at ~E18.5 during the period of islet maturation and is maintained in mature α-, β-, δ-, and PP-cell types. The expression of Myt3 from E18.5 onwards suggested that it may play an important role in the regulation of this maturation step and in the maintenance of mature β-cell function. Our data clearly demonstrates however that *Myt3* is not necessary for these processes as islet function is unaltered in sh*Myt3*-transduced islets. Despite this the tightly controlled spatiotemporal expression of *Myt3* suggests precise, tissue specific transcriptional regulation. We show that the *Myt3* promoter is bound and directly regulated by Foxa2, Pdx1 and Neurod1. The regulation of *Myt3* expression by Foxa2, Pdx1 and Neurod1 nonetheless suggests that it may play an as yet unidentified role downstream of these transcription factors.

Genes that are maintained in the adult islet by Neurod1 are often induced by Ngn3 during development, as both bind similar E-box elements [191]. We show that ectopic expression of *Ngn3* induces a more open and active chromatin state around the *Myt3* promoter, through an increase in the enrichment of the activating H3K4me1 and H3K27ac marks, with a concomitant decrease in repressive H3K27me3 enrichment levels. These data suggest that Ngn3 mediated changes to the histone modification state around the *Myt3* promoter may allow it to become activated by other factors, and that once activated its expression is maintained in mature islets, at least in part, by Neurod1 and Pdx1.

Pancreatic islets are required to respond to changing glucose levels under physiological conditions and are exposed to cytokines during disease progression. Gene expression changes are some of the earliest events that occur in islets following exposure to either glucose or cytokines [206]. These functional responses are mediated, in part, through altered translocation of Pdx1 and Neurod1 to the nucleus where they can affect gene expression changes [190, 207]. As we determined both of these factors are direct regulators of *Myt3* expression we evaluated the role of glucose and cytokines in the regulation of *Myt3* expression. Exposure of islets to glucose resulted in increased *Myt3* expression while cytokine exposure inhibited it. These responses were both time and dose dependent and in the case of glucose exposure is likely dependent on a need to recruit additional transcription factors, or the adoption of a more active chromatin state. Furthermore, in a mouse model of T1D, immune infiltration into the islet results in a concomitant reduction in *Myt3* expression likely due to exposure of the islets to pro-inflammatory cytokine secretion from the infiltrating immune cells confirming the *in vivo* relevance of our cytokine results. These data

indicate that *Myt3* expression is dependent on external stimuli under both physiological and pathophysiological conditions.

Prolonged exposure to cytokines, which occurs in type 1 and type 2 diabetes, results in β-cell dysfunction and apoptosis [1, 208]. We have clearly demonstrated that suppression of *Myt3* does not affect islet function but interestingly, our data clearly show that *Myt3* suppression leads to increased apoptosis in islets and MIN6 cells, suggesting that Il-1β, Tnfα and Ifnγ-induced *Myt3* repression may be a significant factor in cytokine-induced β-cell apoptosis. A pro-survival role for *Myt3* is further supported by the fact that adenoviral-mediated *Myt3* over-expression largely prevents cytokine-induced apoptosis in islets.

In contrast to these results Henry *et al.* have recently demonstrated that treatment of late-passage MIN6 cells with cytotoxic levels of fatty acids (FA) and cytokines leads to an increase in *Myt3* expression levels and that suppression of *Myt3* protects against FA- and cytokine-induced cell death [209]. We suggest this is due in part to the loss of a true "β-cell" state and the adoption of a more fibroblast-like phenotype. This is an important distinction as in fibroblasts *Myt3* is a pro-apoptotic factor [12]. Furthermore, they show that transfection of MIN6 cells with a *Myt3* over-expression construct leads to a significant increase in apoptosis. Work performed in our lab with transfection and late passage MIN6 cells supports the findings of Henry *et al.*, however we propose the increase in cell death in this model is the result of increased endocytosis induced by transfection of the *Myt3* over-expression construct since we do not observe this phenotype with viral transduction. The increased endocytosis is likely causing the observed increase in cell death due to the uptake of the transfection reagent, which is toxic to the cells.

In agreement with a pro-survival role for *Myt3*, its suppression resulted in a significant reduction in the expression of *Bcl-xl*, which prevents cytochrome c release, and subsequently apoptosis, via inhibition of Bax and Bak activity [115], and *c-Iap2* that regulates cell survival via inhibition of effector caspase activity [210]. Also, *Il-6* and *Igfr1* expression were significantly reduced by *Myt3* suppression. *Il-6* induces α-cells to secrete the incretin hormone Glp-1 [211]. Glp-1 stimulates β-cell *Igfr1* expression, which regulates β-cell survival via Akt signalling [212, 213]. This suggests that *Myt3* may indirectly affect β-cell survival by reducing levels of Il-6 induced Glp-1 secretion from α-cells, thereby reducing *Igfr1* and thus increasing β-cell apoptosis; although, further work is required to validate this model. Further, *Il-6* has been shown to protect islets from pro-inflammatory cytokine exposure both *in vitro* and *in vivo* [214]. Similar to our findings, increased β-cell apoptosis in *Pdx1* heterozygous mice is due to reduced expression of the pro-survival factors *Bcl2* and *Bcl-xl* [178]. In further agreement, insulin secretion is similarly unimpaired in these mice [178]. Thus, the *Myt3* suppression-induced reductions in *Pdx1* levels that we note, and the phenotype we see, are consistent with the phenotype of *Pdx1* heterozygous mice that have similar levels of *Pdx1* in their islets. Together, these data clearly demonstrate that changes in *Myt3* expression levels are sufficient to alter apoptosis in islets, likely through the regulation of pro-survival genes such as *Pdx1*, *Il-6*, *Bcl-xl*, *c-Iap2*, and *Igfr1*.

In summary, this work identifies *Myt3* as the predominant MYT family member in mature islets, and shows that it is present in all major endocrine cell types. We show that *Myt3* expression is regulated by the transcription factors Foxa2, Pdx1 and Neurod1 and that its expression is responsive to both glucose and cytokines. We demonstrate that *Myt3* suppression reduces cellular insulin levels, and significantly increases the rate of β-cell

apoptosis. Importantly, over-expression of *Myt3* is able to protect cells from cytokine-induced apoptosis. The data presented in this chapter are an important step in clarifying the regulatory networks responsible for β-cell function and survival, and suggest that *Myt3* may be an interesting therapeutic target for improving β-cell survival in diabetic patients and islet graft recipients.

Chapter 3: *Myt3* mediates laminin-V/integrin-β1 induced islet-cell migration via *Tgfbi*

3.1 Background

As discussed in Chapter 1 pancreatic islet formation is dependent on the migration of individual endocrine cells to form islet-like clusters. Distinct islets are subsequently formed either by fission of the clusters or outgrowth of acinar cells through islet-like clusters [124, 125, 131, 149]. The newly formed islets then undergo further migration to reach their final positions within the developed pancreas [148, 215]. Although *Myt3* has not been implicated in mediating islet-cell migration to date, in Chapter 2 we noted that its expression in pancreas endocrine cell types during development is initiated at a time in which islet-cell migration and morphogenesis is occurring [125, 216]. Thus, in this chapter we sought to confirm whether *Myt3* is present in migrating islet-cells, and subsequently to determine what role it plays in this process.

Cell migration is a complex process critical to a wide array of cellular programs including embryonic development, immune functions, and disease progression [217-220]. The underlying mechanisms responsible for controlling the directed migration of cells, both independently and in concert with their neighbours, have been well characterized and are typically well conserved [217-225].

The cyclical nature of cell migration progresses from the sensing of external stimuli that polarizes the cell and results in the extension of either broad lamellipodia or spike-like filopodia, to the stabilization of membrane protrusions and finally to the disassembly of trailing edge adhesions and retraction of the cell body [221, 223, 226]. Polarization towards an external stimulus is generated by a positive feedback loop involving phosphatidylinositol 3,4,5-trisphosphate (Pip3), phosphatidylinositol kinase 3 (Pik3), Rac1 and Cdc42 [218].

Ligand binding to cell surface receptors induces the localized activation of Pik3 leading to the production of the second messenger Pip3, which in turn activates Rac through the recruitment of Rac guanine nucleotide exchange factors. Rac activation enhances Pip3 accumulation amplifying the signalling cascade, while active Cdc42 restricts the signalling zone promoting the formation, and subsequent stabilization, of a single pseudopod [218, 219]. Active Rac1 also regulates the accumulation of actin monomers at the leading edge of the newly formed lamellipodium [218]. This accumulation of actin monomers itself is not sufficient to actually extend membrane protrusions; for this the dynamic addition of actin monomers to the barbed end of growing actin filaments is required. This is accomplished via active Cdc42 and Rac1 which recruit, and subsequently activate, the nucleation promoting factors, N-Wasp and Wave, via conformational changes that expose the active site of the proteins [227-229] . The conformational changes associated with N-Wasp/Wave activation promotes the binding and activation of the actin-related proteins 2 and 3 (Arp2/3) complex, and also recruits actin monomers for incorporation into the growing actin filaments [230].

Tractional forces are also required for lamellipodia and filopodia to facilitate cell migration. This is accomplished via the formation of cellular adhesions by integrins which not only provide traction sites but also serve as sensory and signalling hubs for the cell [223, 225]. Integrins interact with extracellular matrix (ECM) proteins via the extracellular domains of both the α- and β-subunits and link the ECM to the actin cytoskeleton through binding to talin, vinculin and α-actinin [231]. The tractional forces that are necessary for migration are dependent on several factors including ECM and receptor density, receptor affinity, force transmission and adhesion turnover. Force is generated by the interaction of the motor protein myosin II with actin filaments that is controlled by myosin phosphorylation, while

adhesion turnover is regulated by activation of Fak and Src which in turn activate Rac and Erk [223]. In addition to Erk signalling, integrin-mediated adhesions are also important for Mapk, Jnk and lipid metabolism pathways [231].

Recently, the involvement of cell migration and adhesion in endocrine cell specification and in β-cell maturation and function has gained increasing interest [146, 215, 232, 233]. During pancreas development endocrine α-, β-, δ-, ε-, and PP-cell precursors migrate away from the Sox9 positive ductal epithelium, in which they are initially specified [125, 137]. This process is initiated by Ngn3-induced delamination of the endocrine precursors from the progenitor layer [137]. Subsequently, the cells migrate together to form interconnected islet-like structures. During neonatal development, islets composed of the different pancreas endocrine cell types split off from these structures and migrate apart [138, 146-149]. Thus, cell migration is critical for both islet formation, and the migration of the islets themselves away from the ducts. Despite this, the mechanisms regulating these processes are unclear; although, impairments in Wnt5a, Egfr, Cdc42, Tle3, and Rac1 signalling inhibit normal endocrine cell delamination and migration, or the migration of islets away from ducts [12, 138, 146-148].

3.2 Methods and materials

Mouse maintenance and islet isolations

Mice were maintained and islets were isolated as described in Chapter 2. Isolated islets were incubated for 4-6 hours prior to use in experiments. 8-12 week old C57/B6 mice, mice expressing GFP under the control of the mouse insulin promoter (MIP-GFP) [234] and *Bak*$^{-/-}$*:Bax*$^{fl/fl}$:Pdx1-CreER mice were used in these studies. Islet-specific ablation of *Bax* was

achieved by injecting 0.075mg/g of tamoxifen (Sigma-Aldrich) into the intraperitoneal space of 8-12 wk old *Bak*$^{-/-}$:*Bax*$^{fl/fl}$:Pdx1-CreER mice on five consecutive days [235]. Tamoxifen was prepared by vortexing for two minutes in corn oil.

Immunofluorescence and immunohistochemistry

Immunostaining was performed on whole and dispersed paraformaldehyde (PFA)-fixed islets and paraffin-embedded E18.5 and P1 pancreas tissues as previously described in Chapter 2. Primary antibodies included rabbit anti-Myt3 (1:1000; as described in Chapter 2), mouse anti-E-cadherin (1:250; Cell Signalling Technology), guinea pig anti-insulin (1:1000; Abcam), guinea pig anti-glucagon (1:1000; Linco). Fluorescently conjugated secondary antibodies included donkey anti-rabbit Alexa 488, goat anti-guinea pig Alexa 594, donkey anti-mouse Alexa 546, donkey anti-guinea pig Alexa 633 (1:2000; Life Technologies). To detect F-actin, islets were labelled with Alexa 647 conjugated Phalloidin (1:10; Life Technologies). Sections were imaged with an SP8 confocal microscope (Leica). Fluorescence intensity for E-cadherin and F-actin was determined using a line segment analysis within the Leica LAS AF confocal software.

Islet plating and transduction

We prepared 804G, a complete extracellular-matrix (ECM) produced by a rat bladder carcinoma cell line [236], by culturing the 804G cells in serum-free DMEM Complete media for 48 hours. The supernatant was collected and filtered through a 0.2µm bottle top filter and stored at -20°C. We treated tissue culture dishes with 300µl of 804G supernatant overnight, rinsed the wells with water and allowed them to dry. We plated 50 handpicked islets per well

of a 24-well 804G-treated plate in 500µl RPMI Complete media. Islets were incubated with control, sh*Myt3* and *Myt3* over-expression adenoviruses generated in Chapter 2 at an MOI of 50 overnight. The media was changed and spreading islets were imaged on day one, three and seven, and area was measured using ImageJ (NIH). To visualise F-actin, 50 islets were transduced with $5x10^6$ pfu LifeAct TagRFP (ibidi). For cytokine and Tgfbi experiments, islets were incubated with 0.4ng/ml Ifnγ, 0.07ng/ml Il-1β and 0.04ng/ml Tnfα (eBioscience) or 50µg/ml mouse recombinant Tgfbi (R&D Systems). Images of plated islets were taken at 20x on an Olympus CKX41 microscope using a Canon EOS60D DSLR camera. Islet area was measured using ImageJ (NIH).

Islet-cell migration

To image islet-cell migration in our whole islet model we plated islets as above and transduced with an EGFP expressing virus at an MOI $5x10^{-3}$. Islets were imaged every six hours for seven days using an SP8 confocal microscope (Leica) with an attached GM-8000 gas mixing stage top incubator (Tokai Hit). For single cell migration analysis islets were dispersed and plated on 804G-treated plates at 200 islets per well and transduced as above at an MOI of 5. Cells were imaged every three hours for seven days. Cell migration traces were determined using the chemotaxis and migration tool (ibidi).

Quantification of apoptosis and proliferation

Islets were plated on 804G-treated coverslips and transduced or treated with cytokine as above. Islets were cultured for three days in the presence of 1µM propidium iodide (Sigma-Aldrich) or 10µM EdU (Life Technologies) to label dead or proliferating cells respectively.

Islets were stained as per manufacturer's instructions. All islets were incubated with Topro3 (1:5000, Life Technologies) for 30 minutes before mounting. Cells were imaged with an SP8 confocal microscope (Leica) and quantification was performed with CellProfiler image analysis software (Broad Institute).

Cell adhesion and spreading

For adhesion assays, islets were transduced overnight with the adenoviruses as above and cultured for 48 hours. Islets were then dispersed and plated at 5000 GFP positive cells per well. Cells were allowed to adhere for two hours, washed and fresh media added. Wells were imaged at 4x on an Olympus CKX41 microscope using a Canon EOS60D DSLR camera. Total GFP positive cells were quantified using CellProfiler (Broad Institute). Cell spreading was measured using dispersed islet cells treated as above and then plated in 804G-treated 24-well tissue culture plates. The cells were imaged every hour using an IncuCyte ZOOM (Essen Bioscience) live cell imaging system. Transduced cell area was quantified using the IncuCyte software. For cell morphology whole islets were transduced as above and cultured for 72 hours. Islets were then dispersed and plated on 804G-treated coverslips and cultured for a further seven days. Cells were stained for F-actin as described above and imaged with an SP8 confocal microscope (Leica). For whole islet spreading islets were plated on 804G-treated plates and transduced as described in Chapter 2. Islets were imaged at 20x on an Olympus CKX41 microscope using a Canon EOS60D DSLR camera on day one, three, and seven, post plating. Islet area was measured by circumscribing the islets using ImageJ (NIH).

Islet functional assays

Calcium imaging was performed on transduced, dispersed islets as previously described [235, 237]. In short, islet cells were loaded with 5μM Fura-2AM (Life Technologies) for 30 minutes at 37°C in a 5% CO_2 humidified incubator in 3mM glucose Ringer's solution (5.5mM KCl, 2mM $CaCl_2$, 1mM $MgCl_2$, 20mM HEPES, 144mM NaCl; pH 7.4). Prior to imaging, coverslips were transferred to a 2ml-imaging chamber and cells were perifused with 3mM glucose Ringer's solution at a flow rate of 2.5ml/min. Baseline intensity was measured for 10 minutes immediately after the wash. Next cells were stimulated by glucose and KCl, as indicated in the figures. Cytosolic calcium changes are represented as the ratio of Fura-2AM emission intensity following excitation at 340nm and 380nm. For glucose induced F-actin remodelling cells were incubated in KRBH buffer (115mM NaCl, 5mM KCl, 24mM $NaHCO_3$, 2.5mM $CaCl_2$, 1mM $MgCl_2$, 10mM HEPES and 2% w/v BSA, pH7.4) supplemented with 3mM glucose for two hours prior to treatment with KRBH supplemented with either 3mM or 16.7mM glucose for five minutes. Cells were fixed in 2% PFA for 10 minutes and mounted. Glucose-stimulated insulin secretion assays were performed, as described in Chapter 2, on transduced and untransduced islets with and without culture on 804G.

RNA-seq and qPCR

For RNA-seq islets were transduced as above and cultured for seven days. Transduced cells were FACs sorted and cells were pooled from a minimum of three independent experiments. Cells were lysed in 500μl Trizol (Invitrogen) and vortexed for 10 seconds. Added 100μl chloroform to each sample and vortexted for 10 seconds. Samples were centrifuged for 10

minutes, 12000 rcf at 4°C. The aqueous layer was removed, and incubated for 30 minutes at -20°C with 1:10 volume of 3M sodium acetate and 3 volumes 100% EtOH. The samples were spun at maximum speed in a tabletop centrifuge (Eppendorf) and pellets were rinsed with 70% EtOH. The supernatant was discarded and pellets were re-suspended in 20µl distilled water. Library construction was performed using the TruSeq Sample Prep Kit (Illumina) according to manufacturer's protocol and 100bp paired-end sequencing was performed at the Canada's Michael Smith Genome Sciences Centre. TopHat and Cufflinks were used to map the reads to the UCSC mm9 reference genome and to identify differentially expressed genes [238]. The data was deposited in the Gene Expression Omnibus (GEO) database under accession number GSE70699.

qPCR was performed as described in Chapter 2. Taqman probes were used to quantify *β-actin*, and *Myt3*, all other primers were designed using Primer3plus (Table 3.1).

Itga1	CAGCCCTTGGAATAGACACAG	TGCGATTCTCCATCAGTCAC
Wasf1	AATCAGTGACGCAAGGAGTG	CTCGTGTTTTGCTTCCTGTTC
Wasf2	TCAAGACACGCAAGGAAGAG	CCGCATCCACATTTTCAAC
Wasl	GAAATTACTGTGGGAACAAGAGC	CTTCATTGGCAAAATTAAGAGC
Cdc42	TGTTGGTGATGGTGCTGTTG	TGGCTCTCCACCAATCATAAC
Itga3	CAATGTGACCGTGAAAGCAC	TGTTGATGGTAGGGATGCTG
Pak1	AGATGCTTTGACCCGGAAC	CTGAAGCACCTTGTCCAATC
Ptk2	TTTCGACGTTTTACCTCAGC	CTCCTTGAAAAGGCTTCACG
Pxn	ACATTTCAGCCCTCAACACC	CAAAGAAGCTGCCGTTGAC
RhoA	TGGTTGGGAACAAGAAGGAC	TGGTCTTTGCTGAACACTCC
Rock1	GAGGGCATGATTCTGAGATG	GCCTCTTTTCTTTCTCCTTCC
Cdh1	TGACCAGCAGTTCGTTGTTG	TCAAAGGGTTCCTCGTTCTC
Ctnnb1	TCTTCAGGACAGAGCCAATG	CCACCAGAGTGAAAAGAACG
Rac1	AGATGCAGGCCATCAAGTG	GGATGTACTCTCCAGGAAATGC
Tgfbi	GGCTGTCATCTCCAACAAAG	ATGTCAATGGCAGTGGAGAC

Table 3.1: qPCR primer sequences for cell adhesion and migration related genes

Statistical analysis

Statistical analysis was performed using the paired, two-tailed student's *t*-test. Data from at least three independent experiments are represented as mean +/- S.E.M. Statistical significance was accepted at *P* values ≤ 0.05.

3.3 Results

Myt3 is expressed in developing endocrine cells undergoing migration

Endocrine precursors undergo an Ngn3 dependent delamination from the pancreas progenitor layer [125, 137]. As ectopic over-expression of *Ngn3* also induces *Myt3* expression [216] we wanted to determine whether *Myt3* is expressed in cells undergoing Ngn3-induced delamination. However, at E14.5 and E16.5, time points at which *Ngn3* is expressed, we did not observe any Myt3 positive cells within the developing pancreas indicating that Myt3 is not expressed in delaminating endocrine precursors. However, at E18.5 and post-natal day 1 (P1), when the islet-like clusters that have formed begin to split and migrate apart, Myt3 positive cells were identified within clusters of insulin or glucagon positive cells (Figure 3.1A) in the pancreas. Within these islet-cell clusters the Myt3 positive cells typically showed E-cadherin both localized at the plasma membrane and redistributed into the cytoplasm, while Myt3 negative E-cadherin positive cells showed E-cadherin staining localized to the plasma membrane (Figure 3.1B). Given that E-cadherin redistribution is characteristic of migrating cells these data suggest that at E18.5 and during the early post-natal period Myt3 is expressed in endocrine cells within clusters that are actively migrating away from the pancreatic ducts.

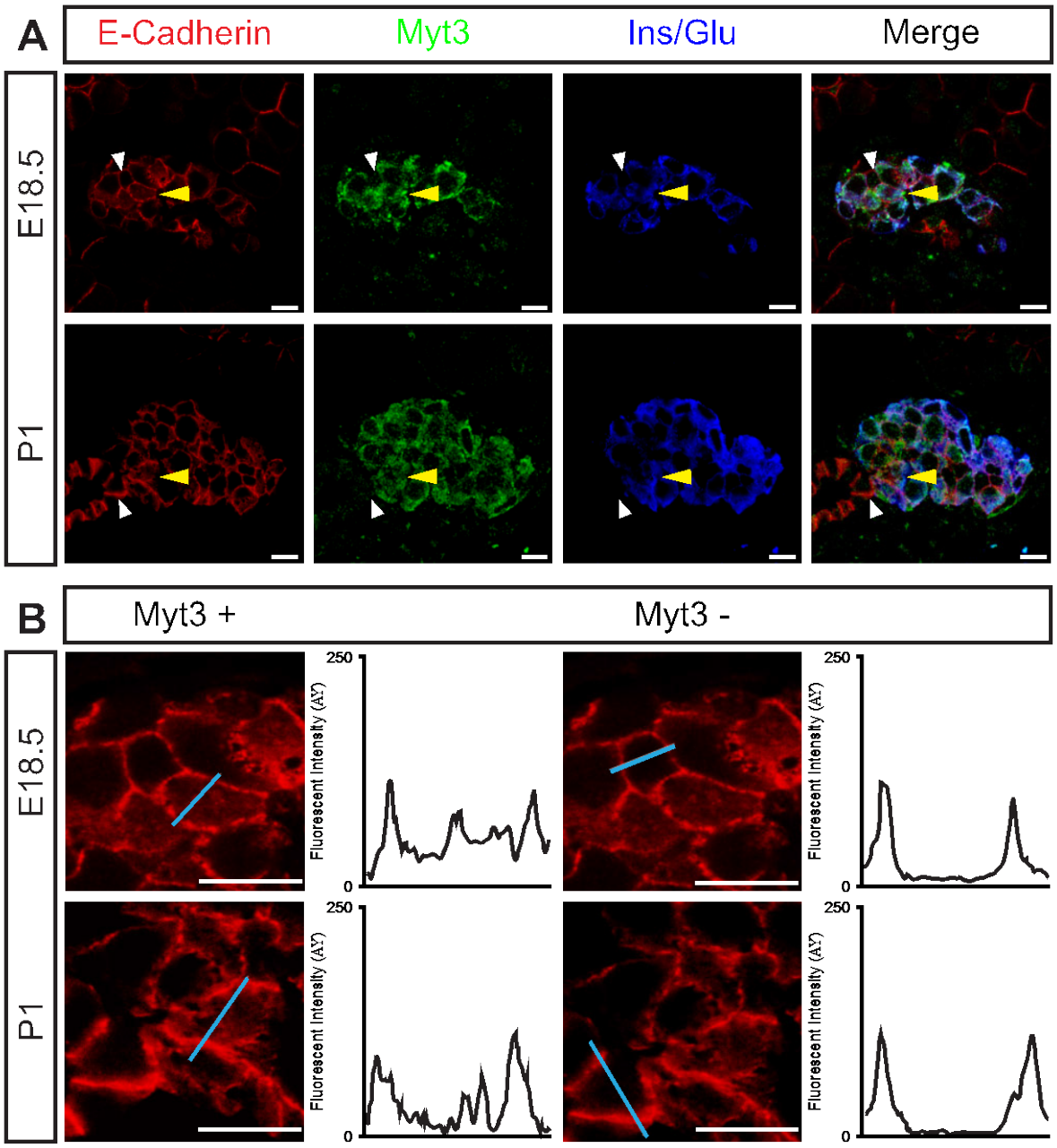

Figure 3.1: Myt3 is expressed in migrating islet-cells
A) E18.5 and P1 pancreata were analyzed for expression of Myt3 (green), E-Cadherin (red) and Insulin/Glucagon (blue). Yellow arrowheads indicate Myt3 positive cells with redistributed E-cadherin. White arrowheads mark Myt3 negative cells with E-cadherin distributed at their plasma membrane. **B)** Cells marked by arrowheads are shown at higher magnification and signal intensity was measured along the blue line and is shown in the histograms beside each image. Scale bars = 10 µm (white bar).

Myt3 suppression inhibits islet-cell migration

To begin to assess the role of *Myt3* in endocrine cell migration we used an *ex vivo* model of islet-cell migration [148]. For this, *ex vivo* pancreatic islets were plated on 804G, a matrix produced by a rat bladder carcinoma cell line that improves islet survival and function in culture [232, 239], and cultured for seven days. Tracking individual GFP positive cells within islets in real time clearly shows the migration of the islet-cells onto the 804G over the seven-day culture period (Figure 3.2A). To confirm the cells migrating onto the 804G included α- and β-cells we initially used islets from mice that express GFP under the control of the mouse insulin promoter (MIP-GFP) [234]. After three and seven days GFP positive cells were found at the periphery of the spreading islets, indicating β-cells had migrated onto the 804G (Figure 3.2B). In addition, whole mount staining showed clear insulin and glucagon positive cells at the periphery of the spreading islets after seven days (Figure 3.2C), further confirming the migration of α- and β-cells in this model. Next, to confirm the cells at the periphery of the spreading islets are actively migrating we assessed the cellular distribution of E-cadherin and F-actin. One day after plating on 804G the cells at the periphery of the islets displayed plasma membrane localised E-cadherin and F-actin. However, on day three and seven post plating, cells at the periphery largely showed redistributed E-cadherin and F-actin staining, indicating that these cells were in fact migrating (Figure 3.2D). Assessment of Myt3 expression by immunofluorescence (IF) and qPCR demonstrated that *Myt3* expression was unaltered by culture on 804G (Figure 3.3A, B). Further, glucose-stimulated insulin secretion assays indicated that culture time did not significantly impair insulin secretion (Figure 3.3C). Together, these data indicate this is a viable model with which to study the potential regulatory role of *Myt3* in pancreas endocrine cell migration.

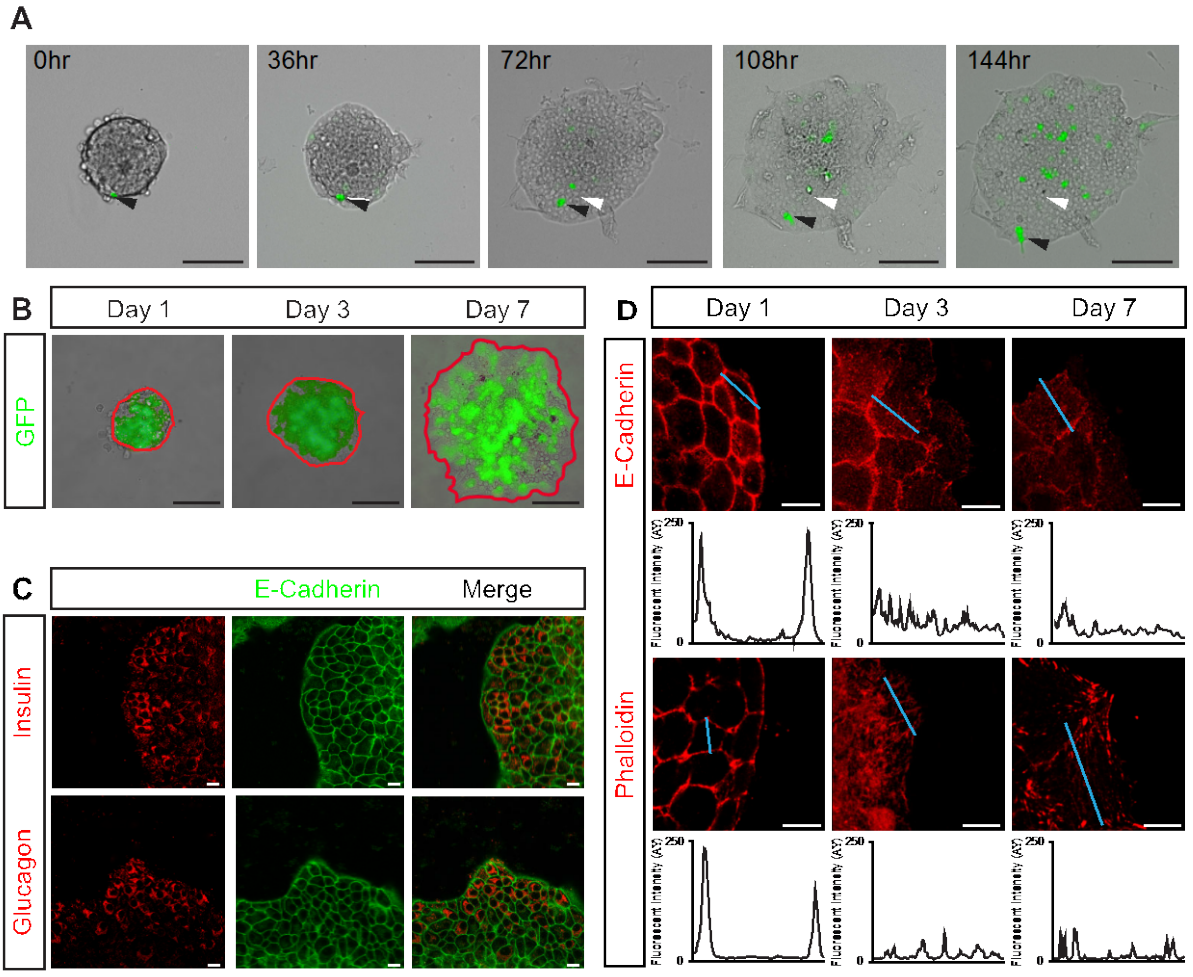

Figure 3.2: Extra-cellular matrix induces islet-cell migration *ex vivo*
A) Time lapse images of wild type islets cultured for 7 days on 804G. Transduced cells are marked by GFP expression (green). White arrowheads mark the start position and black arrowheads mark the current position of the indicated cell. **B)** Representative images of MIP-GFP islets plated on 804G after 1, 3 and 7 days. The red line indicates the islet boundary; GFP positive cells are marked in green. The GFP positive cells at the islet edge indicate insulin-producing β-cells have migrated to the islet periphery. **C)** Cultured islets were stained for E-cadherin (green) to mark cell-cell boundaries and either insulin or glucagon (red) to identify α- and β-cells. **D)** E-cadherin (red) and F-actin (red) staining after 1, 3 and 7 days on 804G. Signal intensity was measured along the blue line and is shown in the histograms below each panel. Scale bars: white bar = 10 µm, black bar = 100µm.

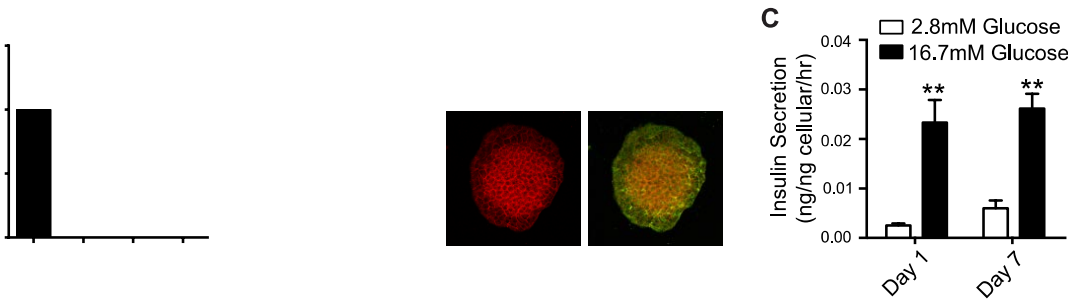

Figure 3.3: Prolonged culture on 804G does not affect Myt3 expression or function
A) qPCR analysis of *Myt3* expression in islets plated on 804G. **B)** Islets cultured for one, three and seven days on 804G were stained with Myt3 (green) and E-cadherin (red). **C)** Glucose-stimulated insulin secretion assays on wild-type islets on day one and seven post plating on 804G.

To determine whether *Myt3* is involved in regulating islet-cell migration we transduced the plated islets with adenoviruses expressing a scramble shRNA (control), an shRNA targeting *Myt3* (sh*Myt3*), or full-length *Myt3* (*Myt3*). After one day of culture control-, sh*Myt3*-, and *Myt3*-transduced islet area was equivalent (Figure 3.4A, B). However, three days after transduction, sh*Myt3*-transduced islets were significantly smaller than control- and *Myt3*-transduced islets (1.3 and 1.4-fold, $p<0.001$), and by seven days post-transduction sh*Myt3*-transduced islets had a 3-fold smaller area ($p<0.001$) (Figure 3.4A, B). In fact, while by seven days post plating control- and *Myt3*-transduced islets had increased approximately 6-fold, sh*Myt3*-transduced islets barely reached a 2-fold increase in islet area (Figure 3.4A, B).

In addition, cells at the periphery of control- and *Myt3*-transduced islets showed clear signs of E-cadherin and F-actin redistribution, indicating they are in fact migrating, while sh*Myt3*-transduced islets had E-cadherin and F-actin staining only at the plasma membrane,

reminiscent of islets that have yet to spread (Figure 3.4C, D). These data suggest that in this model *Myt3* suppression significantly inhibits islet-cell migration onto 804G.

Myt3 expression partially rescues cytokine-induced loss of islet-cell migration

Pro-inflammatory cytokines, such as Ifnγ, Tnfα, and Il-1β, are major contributors to the pathogenesis of type 1 diabetes [77, 114, 240] and we previously found that exposure of islets to a combination of these cytokines significantly repressed *Myt3* expression [216]. Thus, we wanted to determine whether exposure of islets to these cytokines impaired islet-cell migration via their suppression of *Myt3*. For this we exposed islets cultured on 804G to 0.4ng/ml Ifnγ, 0.07ng/ml IL-1β and 0.04ng/ml Tnfα, a dose that is extremely low (roughly 1/256) compared to what is often used to induce β-cell dysfunction and apoptosis [13, 241], yet sufficient to effectively suppress *Myt3* expression [216]. Exposure of islets to even this low dose of Ifnγ, Tnfα, and Il-1β significantly inhibited islet-cell migration onto 804G (2.6-fold, $p<0.001$) (Figure 3.5A, B), and prevented the redistribution of E-cadherin and F-actin (Figure 3.5C). To determine whether this effect was a result of cytokine-induced *Myt3* suppression we transduced cytokine-treated islets with our control or *Myt3* over-expressing adenovirus. *Myt3*-transduced islets exposed to cytokine had significantly improved (1.7-fold, $p<0.05$) ability to spread on 804G as compared to control-transduced islets (Figure 3.5D, E). These data suggest that pro-inflammatory cytokines inhibit islet-cell migration and that this inhibition is likely mediated through *Myt3* suppression.

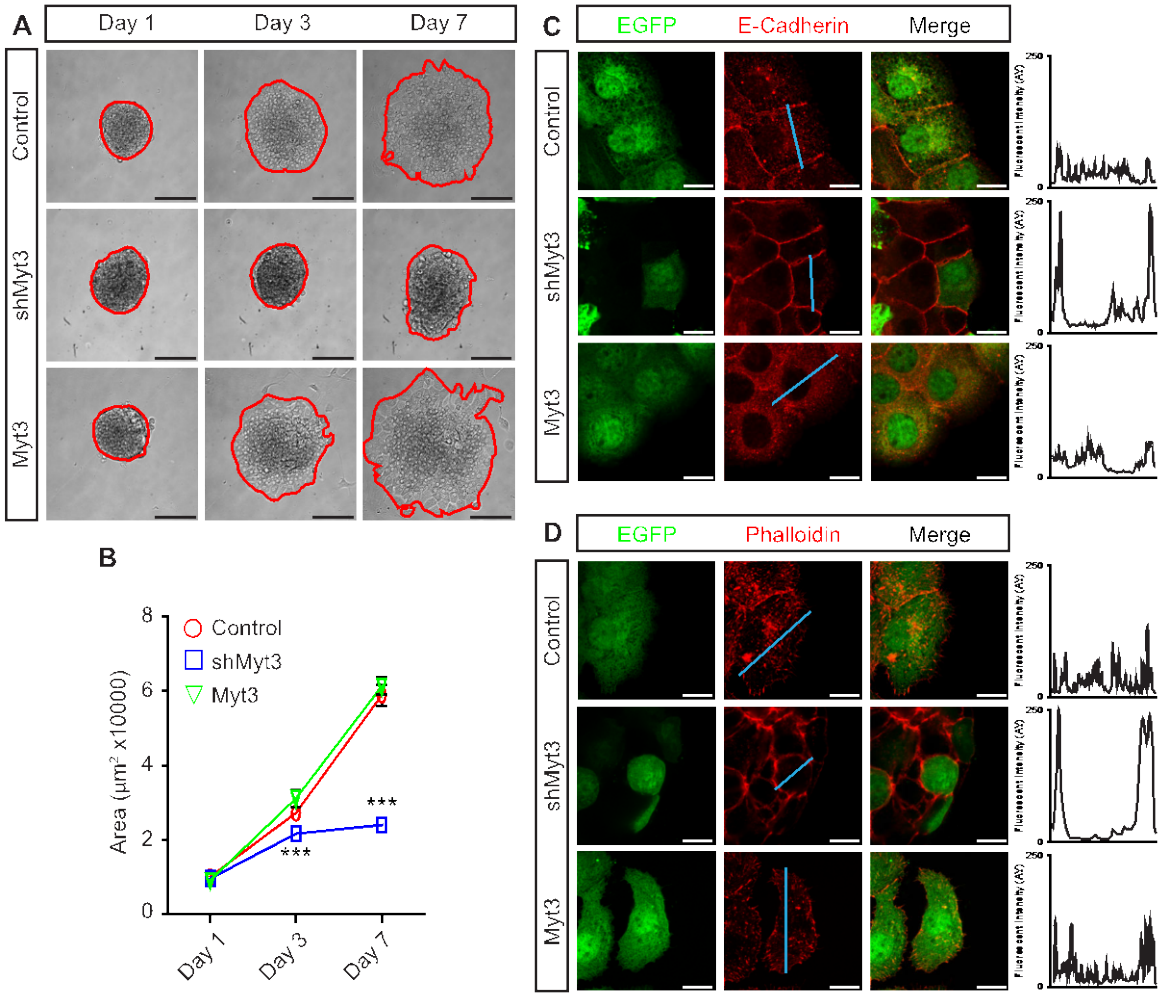

Figure 3.4: *Myt3* suppression inhibits islet-cell migration
A) Representative images of transduced islets cultured for 1, 3 and 7 days on 804G. The red line indicates the islet boundary. **B)** Quantification of islet area for islets in A. The data represents mean values from at least 3 experiments with 10 islets per experiment. Islets transduced as above were stained after 7 days in culture for **C)** E-cadherin (red) or **D)** phalloidin (red) to mark F-actin. GFP positive cells indicate transduced cells (green). Histograms show signal intensity along a line segment (blue line) drawn through the cell. *** indicates a statistically significant difference at $p \leq 0.001$. Scale bars: white bar = 10 µm, black bar = 100µm.

Myt3 regulates islet-cell migration independent of cell death and proliferation

As noted above, *Myt3* suppression and Ifnγ, Tnfα, and Il-1β exposure induce islet-cell death [100, 114, 216, 240, 242]. To determine what level of contribution this effect might be having on the failure of sh*Myt3*-transduced and Ifnγ, Tnfα, and Il-1β-treated islets to spread onto

804G we assessed the level of cell death in these cultures after three days. No significant differences were found in the levels of cell death in Ifnγ, Tnfα, and Il-1β-treated (Figure 3.6A, B), or sh*Myt3*-transduced (Figure 3.6C, D) islets as compared to controls. Thus differences in cell death do not account for the differences in islet area seen. To further confirm this, we performed islet-cell migration assays using islets from *Bak*$^{-/-}$:*Bax*$^{fl/fl}$:Pdx1-CreER double knock-out mice that are highly resistant to undergoing apoptosis [243, 244]. Both sh*Myt3*-transduced and Ifnγ, Tnfα, and Il-1β-treated *Bak*$^{-/-}$:*Bax*$^{fl/fl}$:Pdx1-CreER double knock-out mouse islets showed impaired islet-cell migration, similar to our results using islets from wild-type mice (Figure 3.7A-D), indicating that the observed phenotype is independent of any effects on apoptosis. Next, to ensure differences in islet area were not a result of changes in cellular proliferation we performed EdU incorporation assays in control-, sh*Myt3*-, and *Myt3*-transduced islets. No significant differences in EdU incorporation were found in control-, sh*Myt3*-, and *Myt3*-transduced islets with roughly ten EdU positive cells found per islet in each (Figure 3.6E, F). This level of islet-cell proliferation is clearly insufficient to account for the expansion in islet size seen during our seven-day culture on 804G. Together these data rule out increased cell death or impaired proliferation contributing to the impaired islet-cell migration seen in sh*Myt3*-transduced, or Ifnγ, Tnfα, and Il-1β-treated islets, supporting the assertion that these differences are due to an impairment in sh*Myt3*-transduced islet-cell migratory ability.

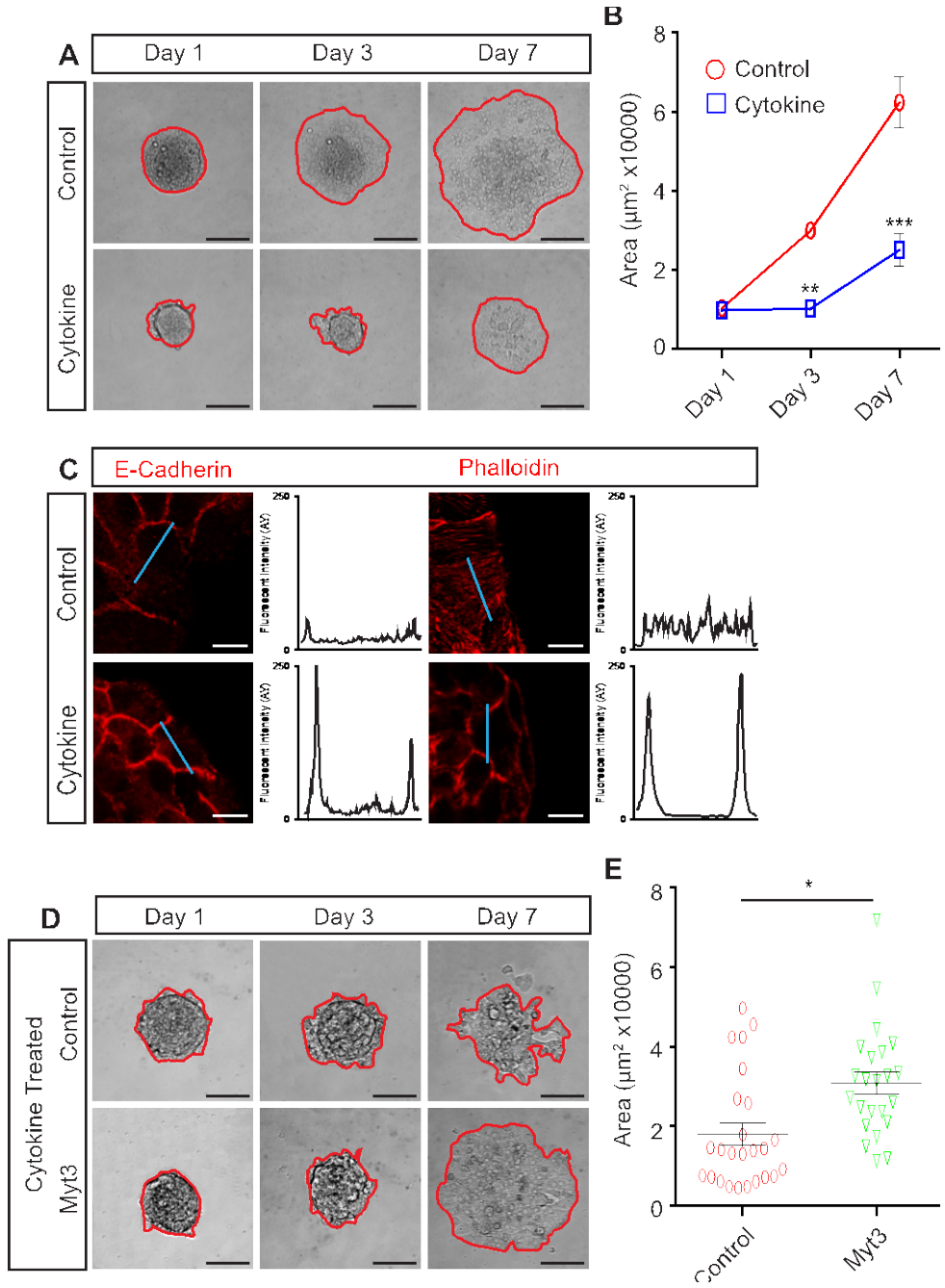

Figure 3.5: Cytokine exposure inhibits islet-cell migration
A) Representative images of control or cytokine treated islets cultured for one, three and seven days on 804G. The red line indicates the islet boundary. **B)** Quantification of islet area for islets in A. The data represents mean values from at least three experiments with 10 islets per experiment. **C)** Control and cytokine-treated islets were stained for E-cadherin (red) and phalloidin (red) to mark F-actin after three days in culture. Histograms show signal intensity along a line segment (blue line) drawn through the cell. **D)** Representative images of cytokine-treated, control- or *Myt3*-transduced islets cultured for one, three and seven days on 804G. The red line indicates the islet boundary. **E)** Scatter plot of islet area for individual islets from E. Data from three independent experiments is represented. Sample means +/- S.E.M. are indicated by the black lines. * indicates a statistically significant difference at $p \leq 0.05$, ** at $p \leq 0.01$ and *** at $p \leq 0.001$. Scale bars: white bar = 10 µm, black bar = 100µm.

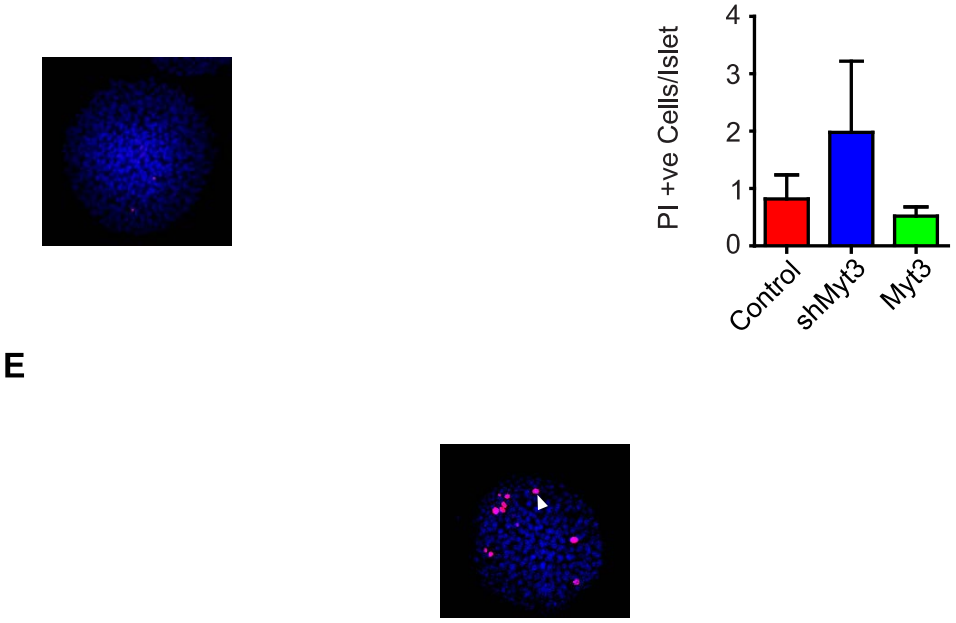

Figure 3.6: Islet-cell migration is independent of islet-cell apoptosis and proliferation
A) Representative images of wild-type islets cultured on 804G and exposed to Ifnγ, Tnfα, and Il-1β (cytokine) or not (control) for three days. Nuclei are stained with Hoescht (blue) and apoptotic cells are stained with propidium iodide (red). **B)** Quantification of propidium iodide positive cells in A. The data represents mean values from at least three experiments with 50 islets per experiment. **C)** Representative images of islets transduced with adenoviruses producing a scramble shRNA sequence (control), an shRNA targeting *Myt3* (sh*Myt3*), or full-length *Myt3* (*Myt3*) cultured for three days on 804G. Nuclei are stained with Hoescht (blue) and apoptotic cells are stained with propidium iodide (red). **D)** Quantification of propidium iodide positive cells in C. The data represents mean values from at least three experiments with 50 islets per experiment. **E)** Representative images of islets transduced with adenoviruses producing a scramble shRNA sequence (control), an shRNA targeting *Myt3* (sh*Myt3*), or full-length *Myt3* (*Myt3*) cultured for three days on 804G. Nuclei are stained with Hoescht (blue) and proliferating cells are stained with EdU (red). **F)** Quantification of EdU positive cells in E. The data represents mean values from at least three experiments with 50 islets per experiment.

Myt3 regulates integrin mediated cell spreading and migration

One of the triggering events for the initiation of cell migration is ECM-induced integrin signalling [146, 224, 225, 227]. Downstream of this initiating signal is the dynamic regulation of cell adhesion to the matrix, of cell-cell contacts, and of the actin cytoskeleton [221, 223]. To determine whether *Myt3* mediates any of these aspects of cell migration we examined these different processes in whole and dispersed islet cells. First, we compared the ability of transduced islet-cells to migrate onto 804G, or the individual matrix components collagen-IV, fibronectin, and laminin-I. As expected, islet-cells were able to migrate onto 804G and this was inhibited by suppression of *Myt3*, however the islet-cells did not migrate to nearly the same extant onto collagen-IV, fibronectin, or laminin-I as they did on 804G (Figure 3.8A). Laminin-V is the principal component in 804G [245], and laminin-V and its binding partner, integrin-α6β1, are essential for β-cell spreading on 804G, and for the beneficial effects of 804G on β-cell function and survival [232, 245-247]. Thus, to determine whether laminin-V is the matrix component in 804G that is responsible for inducing islet-cell migration in our model we cultured islets in the presence or absence of an anti-integrin-β1 antibody. In fact, anti-integrin-β1 treatment significantly impaired the ability of control and *Myt3* expressing islet-cells to migrate onto 804G (2.5-fold, $p<0.001$) relative to control IgG-treated islet-cells (Figure 3.8B) indicating that laminin-V is in fact the matrix component in 804G that largely mediates islet-cell migration in our model. Thus, these data suggest that *Myt3* suppression impairs islet-cell migration through effects on laminin-V/integrin-β1-induced signalling.

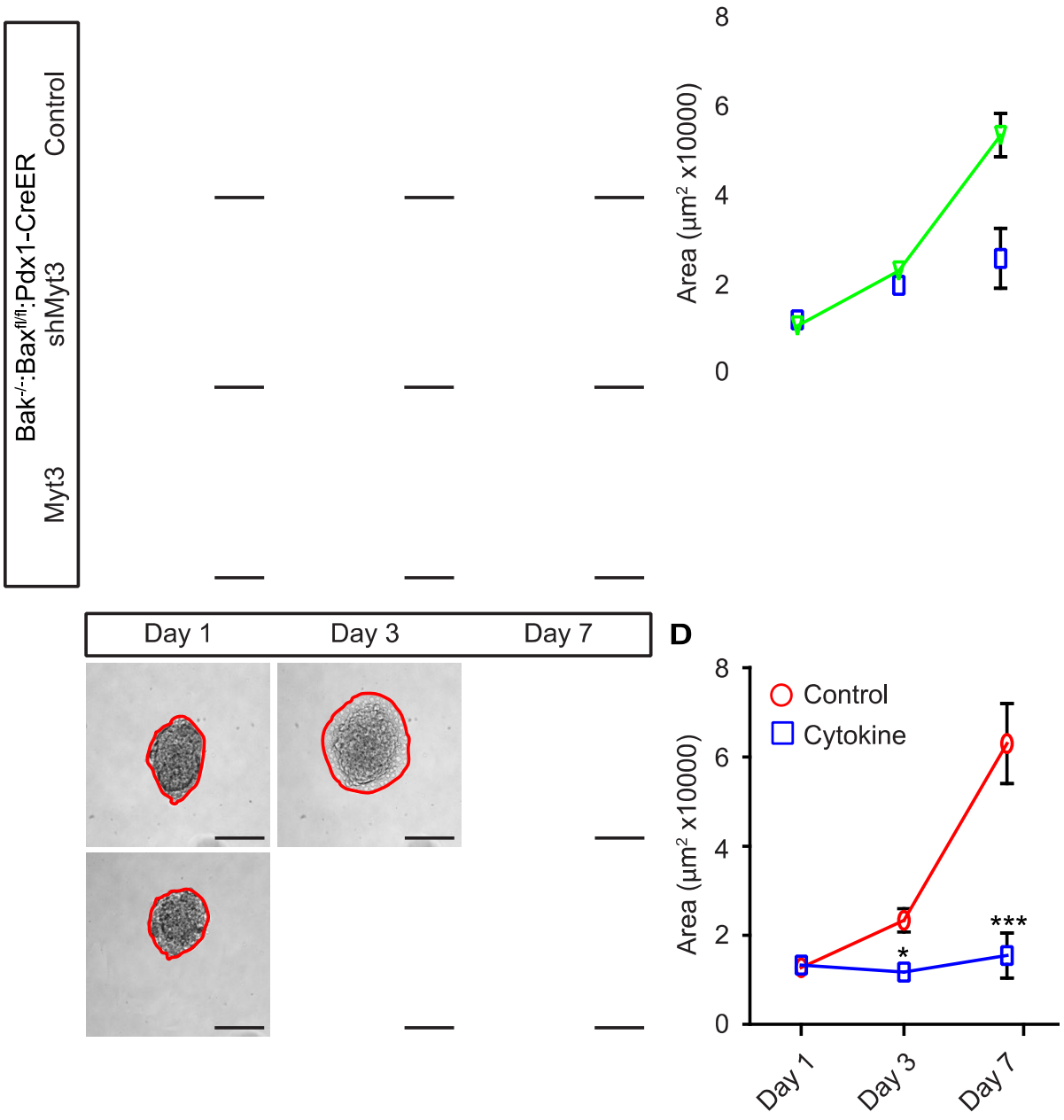

Figure 3.7: Islet-cell migration in apoptosis deficient *Bak*$^{-/-}$:*Bax*$^{fl/fl}$:Pdx1-CreER DKO mouse islets
A) Representative images of *Bak*$^{-/-}$:*Bax*$^{fl/fl}$:Pdx1-CreER DKO mouse islets transduced as above and cultured for one, three and seven days on 804G. Red line indicates islet boundary. **B)** Quantification of islet area for islets in A. The data represents mean values from at least three experiments with 10 islets per experiment. **C)** Representative images of cytokine-treated *Bak*$^{-/-}$:*Bax*$^{fl/fl}$:Pdx1-CreER DKO mouse islets cultured for one, three and seven days on 804G. Red line indicates islet boundary. **D)** Quantification of islet area in C. The data represents mean values from at least three experiments with 10 islets per experiment. * indicates a statistically significant difference at $p<0.05$ and *** at $p<0.001$. Scale bars: black bar = 100µm.

Next, to specifically confirm that 804G induces islet-cell migration we performed time-lapse imaging of control-, sh*Myt3*-, and *Myt3*-transduced dispersed islets. While, control- and *Myt3*-transduced cells migrated on the 804G on average 145μm and 134μm, respectively, sh*Myt3*-transduced cells migrated on average only 80μm ($p<0.001$) (Figure 3.8C, D). This confirms that *Myt3* suppression impairs islet-cell migratory ability on 804G. We noted during these single cell migration experiments that the control- and *Myt3*-transduced cells showed characteristic elongated or cuboidal morphologies with clear F-actin striations through the cells (Figure 3.8E), while sh*Myt3*-transduced cells remained round in morphology and had F-actin localized at the plasma membrane (Figure 3.8E). This suggests that sh*Myt3*-transduced cells may also have a reduced ability to adhere or spread on the 804G, since the machinery responsible for cell migration is also required for adhesion and spreading. We thus sought to more carefully analyze the adhesion and spreading of these cells. Although there were clear differences in the ability of the islet-cells to adhere to 804G, collagen-IV, fibronectin, or laminin-I, sh*Myt3*-transduced cells appeared to adhere equally well as control- or *Myt3*-transduced cells, although *Myt3*-transduced cells had a slight increase (1.4-fold, $p<0.05$) in their ability to adhere to 804G (Figure 3.8F). We next assessed the ability of the control-, sh*Myt3*-, and *Myt3*-transduced islet-cells to spread on 804G over 12 hours. After only two hours post plating *Myt3*-transduced cells were significantly larger (~250μm^2, $p<0.05$) relative to controls (~235μm^2), although control and *Myt3*-transduced cells were similar in size after 12 hours (~290μm^2). sh*Myt3*-transduced cells, on the other hand, had significantly impaired spreading, with cell area only reaching ~220μm^2 two hours post plating ($p<0.05$). By 12 hours the average cell size was still significantly lower in sh*Myt3*-transduced cells (~250μm^2) relative to control- and *Myt3*-transduced cells ($p<0.01$) (Figure 3.8G). These results make it

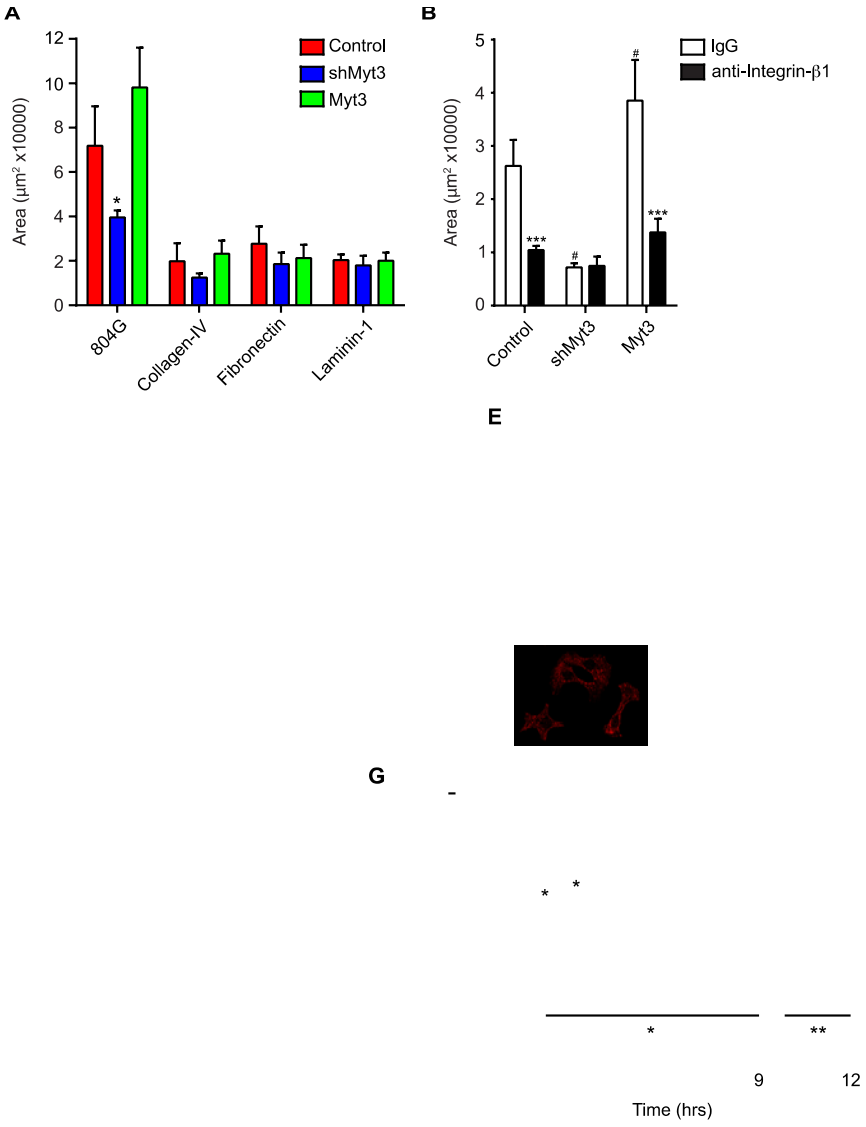

Figure 3.8: *Myt3* mediated islet-cell migration and spreading are dependent on laminin-V and integrin-β1 **A)** Islet area was quantified for control-, sh*Myt3*-, or *Myt3*-transduced islets cultured for seven days on the indicated ECMs. The data represents mean values from at least three experiments with 10 islets per experiment. **B)** Islet area was quantified for transduced islets treated with control IgG or anti-integrin-β1 blocking antibody for seven days. The data represents mean values from at least three experiments with 10 islets per experiment. **C)** Representative traces of cell migration paths for transduced, dispersed islets cultured on 804G for seven days. **D)** Box-whisker plots representing cumulative migration distance for transduced, dispersed islets cultured on 804G for seven days. **E)** Representative images of phalloidin (red) stained transduced, dispersed islets cultured on 804G for seven days. GFP (green) indicates transduced cells. Histograms show signal intensity along a line segment (blue line) drawn through the cell. **F)** Quantification of the number of transduced, dispersed islet cells remaining on the indicated ECM following a two-hour incubation and subsequent wash. The data represents mean values from five independent experiments and presented as a percentage of starting cells. **G)** Average cell size over time for transduced, dispersed islet cells plated on 804G. * indicates a statistically significant difference at $p \leq 0.05$, ** at $p \leq 0.01$ and *** at $p \leq 0.001$. # indicates a statistically significant difference at $p \leq 0.01$ relative to control-transduced IgG-treated. Scale bars: white bar = 10 µm.

clear that sh*Myt3*-transduced cells are unable to spread and migrate in response to signals from the ECM despite being able to adhere to the ECM as well as control- and *Myt3*-transduced cells.

Myt3 suppression does not affect glucose-induced F-actin remodeling

The ability of β-cells to secrete insulin in response to elevated glucose levels is, in part, dependent on their ability to redistribute F-actin to facilitate insulin vesicle trafficking to the membrane [248-250]. As *Myt3* suppression affected the ability of the cells to redistribute their F-actin in response to 804G, we next wanted to determine whether *Myt3* suppression would also prevent glucose induced F-actin redistribution and thereby impair glucose-stimulated insulin secretion. First, we confirmed that altered *Myt3* expression does not influence signalling upstream of F-actin redistribution by performing calcium imaging on transduced, dispersed islets. Our data show that neither suppression nor over-expression of *Myt3* affects the ability of cells to stimulate calcium influx in response to glucose or KCl (Figure 3.9A). Exposure to high glucose for five minutes similarly had no effect on the rapid mobilization of F-actin away from the plasma membrane (Figure 3.9B). Further, glucose-stimulated insulin secretion assays on transduced islets showed that altered *Myt3* expression had no effect on the ability of cells to secrete insulin in response to elevated glucose levels (Figure 3.9C). These results suggest that loss of *Myt3* has no effect on the ability of cells to mobilize F-actin and secrete insulin in response to glucose.

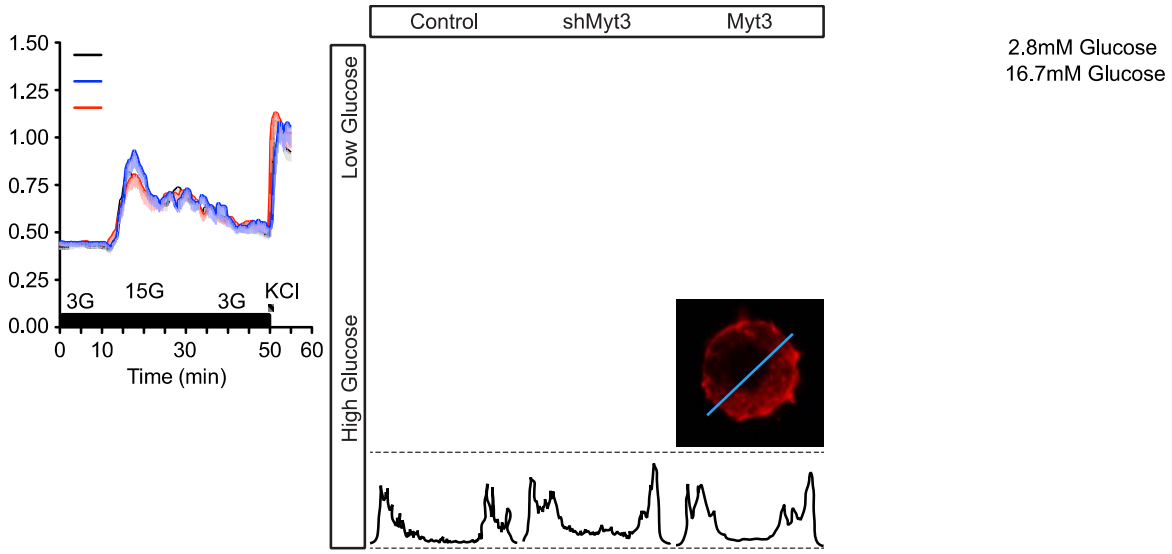

Figure 3.9: Alterations in *Myt3* level do not affect β-cell function
A) Stimulus-coupled calcium influx in control-, sh*Myt3*-, or *Myt3*-transduced, dispersed islets. **B)** Glucose-induced F-actin (red) redistribution in control-, sh*Myt3*-, or *Myt3*-transduced, dispersed islets. Histograms represent signal intensity along a line segment (blue line) drawn through the cell. **C)** Glucose-stimulated insulin secretion in control-, sh*Myt3*-, or *Myt3*-transduced whole islets cultured for one and seven days. ** indicates a statistically significant difference at $p \leq 0.01$.

Myt3 regulates islet-cell migration through *Tgfbi*

To determine the mechanism by which *Myt3* might affect islet-cell migration we performed RNA-seq on control-, sh*Myt3*-, and *Myt3*-transduced islets. To ensure only transduced cells were used in the analysis we FACs sorted islets for GFP positive cells, which accounted for 40-50% of total cells (Figure 3.10A). Comparison of gene expression levels between control-transduced islets and either sh*Myt3*- or *Myt3*-transduced islets resulted in the identification of 51 and 89 significantly altered genes respectively, including *Myt3* in both cases (Figure 3.10B). Further analysis of 166 genes with known roles in adhesion, migration and ECM-induced signalling demonstrated that suppression of *Myt3* resulted in only minor changes in these genes (Figure 3.11A, B), except for *Tgfbi*, a known diabetogenic gene that is involved in regulating cellular adhesion [251-254], which showed a significant increase in expression in sh*Myt3*-transduced islets relative to controls (Figure 3.10C and 3.11A, B).

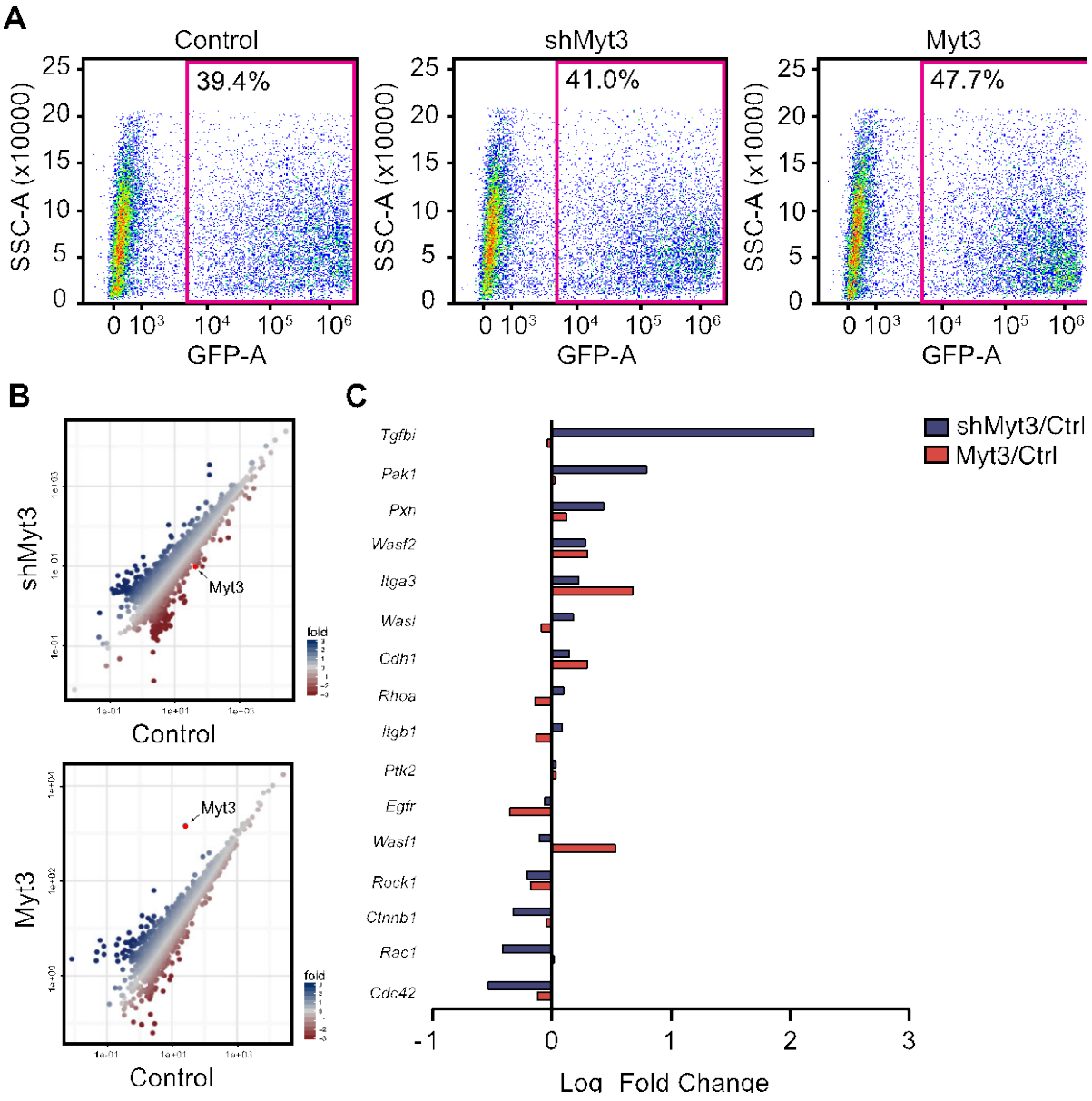

Figure 3.10: *Myt3* suppression alters the expression of multiple genes including *Tgfbi*
A) FACs plots of control-, sh*Myt3*- or *Myt3*-transduced islet cells sorted on the GFP+ population. **B)** Scatter plots showing gene expression changes for sh*Myt3* and *Myt3* samples relative to control as determined by RNA-seq. **C)** Bar graph of the fold changes relative to control-transduced islets for adhesion and migration genes.

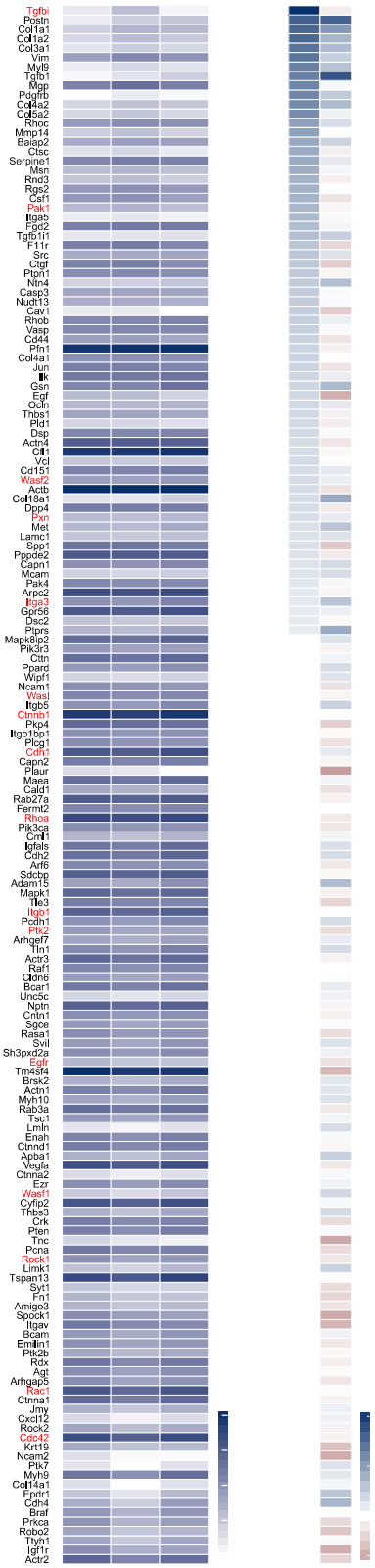

Figure 3.11: *Myt3* suppression alters expression of genes involved in migration and adhesion

A) Heat map representing FPKM values for all genes associated with migration or adhesion for control-, sh*Myt3*- and *Myt3*-transduced islets. Genes highlighted in red were validated by qPCR. **B)** Heat map of fold changes relative to control. * indicates a statistically significant difference at $p<0.05$.

Examination of read density at the *Tgfbi* locus confirmed that suppression of *Myt3* increases its expression relative to control- and *Myt3*-transduced islets and that there is only a single splice variant of *Tgfbi* present in these cells (Figure 3.12A). qPCR validation of the RNA-seq data showed modest decreases in the expression of *Rac1*, *Cdc42*, *Wasf1* and *Egfr* ($p<0.05$), but a significant increase in the expression of *Tgfbi* (5.8-fold, $p<0.01$) (Figure 3.12B, C). These results suggest that *Myt3* likely acts to inhibit *Tgfbi* expression in islet-cells, and that *Myt3* suppression results in the up-regulation of this gene.

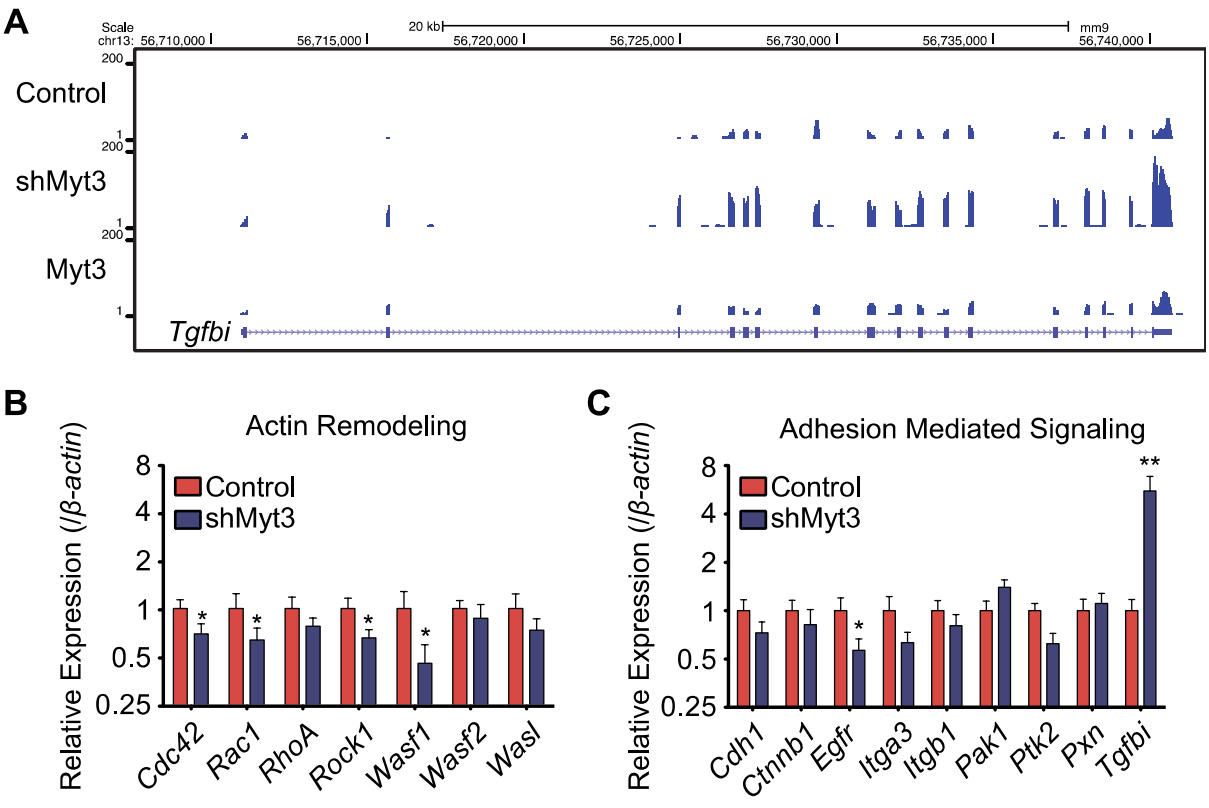

Figure 3.12: *Myt3* suppression induces *Tgfbi* expression in islets
A) Screenshot of UCSC genome browser RNA-seq bigWig tracks for control-, sh*Myt3*- or *Myt3*-transduced islet cells at the *Tgfbi* locus. **B)** qPCR analysis of genes involved in actin remodeling. **C)** qPCR analysis of genes involved in adhesion mediated signalling. * indicates a statistically significant difference at $p\leq0.05$ and ** at $p\leq0.01$.

To establish whether *Tgfbi* up-regulation may be responsible for the effects of *Myt3* suppression on islet-cell migration, we first correlated *Myt3* and *Tgfbi* expression with the appearance of the islet-cell migratory defects. qPCR analysis of sh*Myt3*-transduced islets showed that by three days *Myt3* is significantly down-regulated (2.3-fold, $p<0.05$) while *Tgfbi* is significantly up-regulated (2-fold, $p<0.01$), while on day seven these effects are even more pronounced (4-fold, $p<0.01$ and 6.3-fold, $p<0.01$, respectively) (Figure 3.13A). A similar result was obtained with cytokine exposure, at three days *Myt3* was significantly repressed (2-fold, $p<0.01$) with a concomitant increase in *Tgfbi* (4.6-fold, $p<0.001$) (Figure 3.13B), while at seven days *Myt3* was suppressed 2-fold ($p<0.01$) and *Tgfbi* was up-regulated 6-fold ($p<0.001$). Finally, we cultured wild-type islets for seven days on 804G in the presence of 50μg/ml Tgfbi. Exogenous Tgfbi inhibited islet-cell migration (2-fold, $p<0.05$) (Figure 3.14A, B), and prevented E-cadherin and F-actin redistribution, similar to sh*Myt3*-transduced islets (Figure 3.14C). Taken together these results suggest that Tgfbi production may mediate the effects of *Myt3* suppression on islet-cell migration in response to signals from the ECM.

3.4 Discussion

After delaminating from the ductal epithelium, pancreatic endocrine cells cluster together into islet-like structures adjacent to the pancreatic ducts [125]. Subsequently, the fission of these elongated islet-like clusters is initiated and the newly formed islets migrate away from the ducts [149]. We find that Myt3 is expressed widely in these islet-like clusters, and is found in all insulin and glucagon positive cells, with the few Myt3 positive cells that were negative for these hormones likely representing δ-, ε-, or PP-cells [216]. Although many of

these Myt3 positive cells showed signs of E-cadherin redistribution, Myt3 positive cells with E-cadherin largely at the plasma membrane were also frequently found within larger clusters of insulin or glucagon positive cells, particularly at P1. Taken together, we believe these data suggest that Myt3 is present in pancreas endocrine cells only after they have begun to cluster together into islet-like structures, within islets that are actively migrating away from the pancreatic ducts, and is maintained in mature endocrine cells.

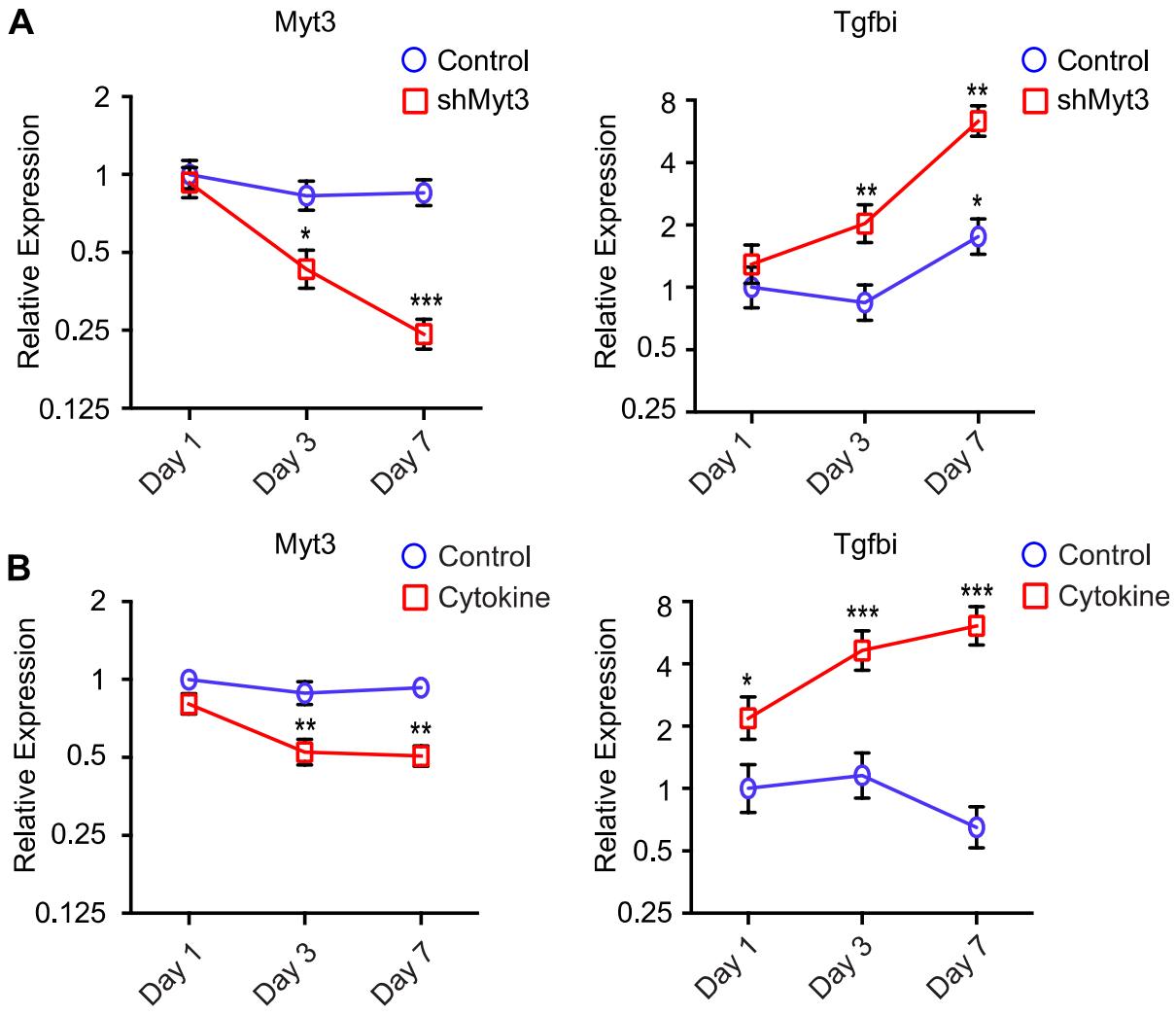

Figure 3.13: *Myt3* suppression impairs islet-cell migration via up-regulation of *Tgfbi*
A) Time course of *Myt3* and *Tgfbi* expression in control- and sh*Myt3*-transduced islets plated on 804G. **B)** Time course of *Myt3* and *Tgfbi* expression in cytokine-treated islets plated on 804G. * indicates a statistically significant difference at $p \leq 0.05$, ** at $p \leq 0.01$ and *** at $p \leq 0.001$.

As a model of islet-cell migration we cultured whole isolated islets for seven days on 804G, a matrix produced by a rat bladder carcinoma cell line that improves β-cell spreading, function, and survival [232, 245-247]. During this time frame islet area expanded substantially and we show that this is largely due to the migration of endocrine cell types (i.e. α- and β-cells) onto the 804G, and is not a consequence of islet-cell proliferation or the migration of contaminating endothelial or fibroblast cells. Laminin-V/integrin-β1 interactions are essential for the effects of 804G on β-cell adhesion, spreading and function [232, 245-247]. Likewise, blocking the interaction between laminin-V and integrin-β1 in our model inhibits the ability of islet-cells to migrate onto 804G, indicating that islet-cell migration onto 804G is dependent on laminin-V/integrin-β1-induced signalling.

Using this model we find that *Myt3* suppression dramatically reduces the increase in islet area and our data strongly support that this is largely due to the inability of these cells to migrate onto the 804G. First, we show that altered islet-cell numbers, either via proliferation or apoptosis, caused by *Myt3* suppression are not sufficient to account for the differences in islet size seen. Second, we show that *Myt3* in fact impairs the ability of dispersed islet-cells to migrate on 804G using live-cell imaging. Together these data strongly suggest that Myt3 suppression in whole islets directly affects the ability of islet-cells to migrate onto 804G. It is however still possible that Myt3 also prevents islet-cells from breaking down cell-cell junctions, which could also lead to impaired islet spreading.

Interestingly, we saw no impairment in the ability of sh*Myt3*-transduced cells to secrete insulin in response to glucose, which is dependent upon the ability of cells to redistribute their F-actin network at the plasma membrane in order to facilitate access to the membrane for insulin secretory granules [232, 255]. This suggests the cells are capable of F-actin, and

likely E-cadherin, redistribution, but that they fail to do so specifically in response to laminin-V-induced signalling.

Intriguingly, we find that comparatively low levels of Ifnγ, Tnfα, and Il-1β cause a similar impairment in islet-cell migration as *Myt3* suppression. We have previously shown that exposure of islets to these cytokines significantly inhibits *Myt3* gene expression [216] (Figure 9B), and we show here that over-expressing *Myt3* in cytokine-treated islets partially rescues their migratory ability. These data suggest that even low levels of pro-inflammatory cytokines, as may be found early in T1D pathogenesis or in T2D, may impair islet migratory ability via suppression of *Myt3*.

Myt3 suppression resulted in a significant increase in the expression of *Tgfbi*, although whether Myt3 directly binds and represses *Tgfbi* gene regulatory regions, or whether this effect is indirect remains to be determined. Tgfbi is a secreted extracellular matrix component that has been reported to have diverse effects on cell adhesion and migration in various cancers [256-258], and was previously shown to prevent islet-cell migration, in the absence of any ECM, via dis-regulation of FAK signalling [251]. In our model, we show that exogenous Tgfbi inhibited islet-cell migration onto 804G and also resulted in impaired redistribution of E-cadherin and F-actin similar to our results from sh*Myt3*-transduced islets. This result helps explain why in sh*Myt3*-transduced islets both transduced and neighbouring untransduced cells seem to be equally affected, as Tgfbi secreted from transduced cells likely inhibits migration of adjacent cells through paracrine mechanisms.

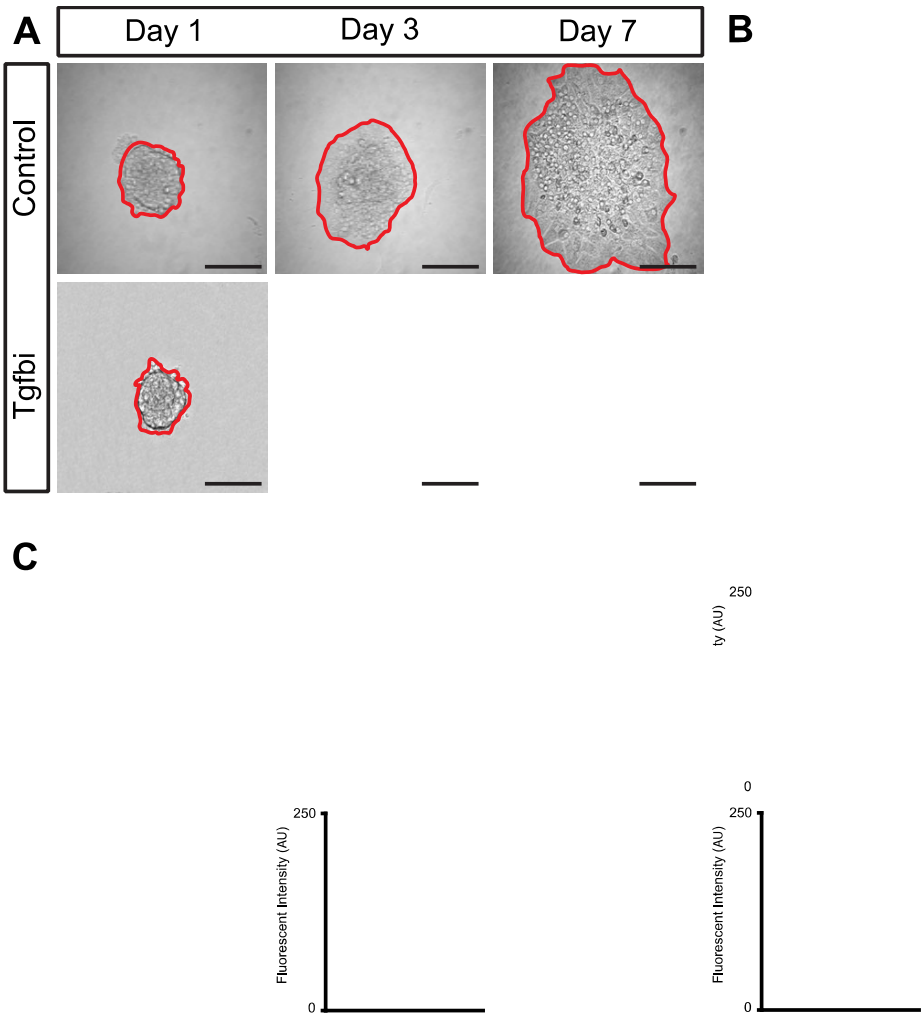

Figure 3.14: *Myt3* suppression impairs islet-cell migration via up-regulation of *Tgfbi*
A) Representative images of untreated (control) or Tgfbi-treated (Tgfbi) islets cultured for one, three and seven days on 804G. The red line indicates the islet boundary. **B)** Quantification of islet area from A. The data represents mean values from at least three experiments with 10 islets per experiment. **C)** Islets were stained for E-cadherin and phalloidin (red) after seven days in culture. Histograms show signal intensity along a line segment (blue line) drawn through the cell. * indicates a statistically significant difference at $p \leq 0.05$. Scale bars: black bar = 100µm.

Taken together the data in this chapter argue that when whole islets are plated onto 804G, laminin-V/integrin-β1-induced signalling induces islet-cell migration out onto the 804G, and that suppression of *Myt3* specifically impairs this migration by relieving the repression of the secreted factor Tgfbi. We believe this may be relevant not only to adult islet-cells, but also to the migration of islets during pancreas development given the expression of Myt3 in E18.5 islet-clusters as shown in Chapter 2. Further, our data implies that exposure to pro-inflammatory cytokines in the early stages of T1D and in T2D may inhibit islet migratory ability via suppression of *Myt3* and subsequent up-regulation of *Tgfbi*, although the relevance of this to the pathogenesis of these diseases needs to be confirmed. In sum, the work presented in this chapter contributes to our understanding of the role of *Myt3* in islets and to the mechanisms regulating islet-cell migratory ability.

Chapter 4: *Myt3* suppression induces cell death in syngeneic islet transplants

4.1 Background

In the classical model of T1D, patients with an underlying genetic predisposition are exposed to an environmental insult that drives auto-immunity and gradually leads to a loss of β-cells and hyperglycaemia. In this model it is thought that a diagnosis of T1D is not made until 80-90% of β-cells have been lost, although there is some evidence to suggest that hyperglycaemia is evident with a loss of as little as 40-50% of β-cells [19]. In either case it is clear that in order to cure diabetes it is imperative that we develop strategies to identify T1D patients before they become symptomatic.

Once we are able to reliably diagnose T1D patients before they have lost the majority of their functional β-cell mass it will then be essential to halt the immune assault on the remaining islets, prevent cytokine-induced apoptosis and replace the cells that have already been lost. Several strategies are currently being employed to address short-comings in the aforementioned areas of diabetes treatment including: utilizing antigen-specific approaches to inhibit only those immune responses targeting T1D auto-antigens [259], focusing on immune cell reprogramming and blockade of pro-inflammatory cytokine signalling [38], and transplanting cadaveric islets or embryonic stem cells differentiated into β-cells *in vitro.*

Despite advances in immune modulation and transplantation treatments for diabetes there are still significant shortfalls that need to be addressed. For example, although we know that the immune assault during the initial phases of diabetes onset and following islet transplantation results in a loss of β-cell functional maturity, the induction of pro-inflammatory gene expression in β-cells, and eventually in β-cell death, we are still far from understanding how these events occur. An understanding of these events is critical to develop

novel therapeutic approaches to block the detrimental effects of immune assault during diabetes progression and islet transplantation.

In Chapter 2 we show that the transcription factor *Myt3* is down regulated by exposure to immune cell secreted pro-inflammatory cytokines *in vitro*. We subsequently showed that suppression of *Myt3* increases apoptosis in islets grown *in vitro* [216], suggesting that, in the context of diabetes and also during transplantation, cytokine-induced loss of *Myt3* may promote cell death exacerbating disease progression. Despite these findings, the work presented in Chapter 2 focused on the acute effects of *Myt3* suppression on islet survival and did not address the long-term consequences of Myt3 suppression *in vivo.* Therefore, the work in this chapter aims to determine what effect suppressing *Myt3* will have on islet graft function and survival in syngeneic islet transplants.

4.2 Methods and materials

Islet isolations and culture

Islets from female C57/B6 mice were isolated and transduced as described in Chapter 2 and cultured for 48 hours prior to transplantation.

Islet transplantation

Eight to 12-week old, female C57/B6 mice were rendered diabetic by injection of streptozotocin (STZ, 230mg/kg) into the intraperitoneal space. We monitored these animals on a daily basis for signs of illness and measured blood glucose, via needle poke of the tail, using a One Touch Ultra glucose test meter. Three days post STZ administration, mice with at least two blood glucose readings above 20mM were weight matched and transplanted with

300 donor islets that had been isolated and transduced as described above. One hour before surgery, mice received subcutaneous injection of a combination of meloxicam (1mg/kg) and buprenorphine (0.1mg/kg). The mice were anaesthetized for surgery with isofluorane (2% in 2L/min oxygen flow), and a surgical plane of anaesthesia was assessed by toe pinch reflex. A small nick was made in the kidney capsule and a small pouch under the kidney capsule was created. A piece of disposable PE50 tubing with one end attached to a syringe and the other containing a pellet of islets was introduced into the sub-capsular space. The islets were then slowly injected into the space. The incisions were sutured closed and the mice were placed on warming pads to recover before being placed into fresh cages with the other transplanted mice with a maximum of four mice per cage. Mice were monitored on a daily basis for overall health and blood glucose and body weight measurements were taken twice per week for five weeks.

Glucose tolerance Tests

In vivo islet function was assessed by intraperitoneal glucose tolerance test. Mice were fasted for six hours and injected with 2g/kg D-glucose (Sigma-Aldrich), and saphenous blood glucose was measured at 0, 15, 30, 60, and 120 minutes. Blood was also collected at these time points and centrifuged at 10000 rcf for 10 minutes at 4˚C. The plasma was collected into new tubes and stored at -20˚C until being run on Mouse Insulin ELISA kits (Alpco).

Immunofluorescence and immunohistochemistry

Immunohistochemistry was performed on paraffin sections of islets embedded under the kidney capsule. Sections were stained with goat anti-glucagon (1:500, Santa Cruz), guinea pig anti-insulin (1:500; Linco), rabbit pig anti-GFP (1:1000; MBL), rat anti-CD45 (1:25; Life Technologies), and rabbit anti-PCNA (1:250; Santa Cruz). Primary antibodies were detected using donkey anti-rabbit Alexa 488 (1:1000, Molecular Probes), goat anti-guinea pig Alexa 546 (1:500, Molecular Probes), goat anti-mouse Alexa 546 (1:500, Molecular Probes), goat anti-rat 594 (1:100, Molecular Probes) or donkey anti-goat Alexa 488 (1:1000; Molecular Probes).

RNA-seq and qPCR

RNA-seq and qPCR were performed as described in Chapter 3. Primers for chemokine genes were designed using Primer3plus (Table 4.1).

Ccl2	AGGTCCCTGTCATGCTTCTG	CTTGCTGGTGAATGAGTAGCAG
Cxcl2	GGCGGTCAAAAAGTTTGC	CTTTGGTTCTTCCGTTGAGG
Cxcl10	CGTCATTTTCTGCCTCATCC	TATGGCCCTCATTCTCACTG
Ccl20	TGAAAAGGGCTGTGAACCTC	CCAGCTGTGATCATTTCCTC

Table 4.1: qPCR primer sequences for chemokine genes

Statistical analysis

Statistical analysis was performed using the paired, two-tailed student's *t*-test. Data from at least three independent experiments are represented as mean +/- S.E.M. Statistical significance was accepted at *P* values ≤ 0.05.

4.3 Results

Myt3 suppression does not affect blood glucose or body weight

In Chapter 2 we established that exposure of islets to a cytokine cocktail suppresses the expression of *Myt3* in a dose and time dependent manner. We further demonstrated that suppression of *Myt3* in *ex vivo* islets, for as little as 48 hours, results in an increase in cell death [216]. These data suggested that *Myt3* may participate in the development of diabetes downstream of immune assault, but provided no evidence for the long-term consequences of *Myt3* suppression *in vivo*. To determine the effect of *Myt3* suppression on islet function and survival *in vivo* we performed optimal syngeneic transplants on C57/B6 mice. This model was chosen to specifically assess the affects of *Myt3* suppression on transplant survival and function, in the absence of immune assault or β-cell stress, associated with allogeneic and suboptimal transplants respectively, which have multiple effects on the transplanted cells and given that *Myt3* is suppressed by cytokine exposure would likely have induced *Myt3* suppression even in the controls. We hypothesized that in this model suppression of *Myt3* would induce islet-cell apoptosis potentially resulting in a reduced capacity to maintain normoglycaemia following transplant of islets under the renal kidney capsule.

We rendered female C57/B6 mice diabetic via treatment with streptozotocin (STZ) and subsequently transplanted them with 300 control- or sh*Myt3*-transduced islets that had transduction efficiencies of 39.4% and 41 % respectively (Figure 3.10A). Monitoring of random-fed blood glucose levels showed that both control and sh*Myt3*-transduced islets were equally capable of normalizing blood glucose (Figure 4.1A, B). We also measured body weight to ensure that *Myt3* suppression was not having any effects on the general health of the mice. Our data show that body weight dropped after STZ treatment as expected and then

slowly recovered, and that there was no difference between control and sh*Myt3* mice (Figure 4.1C). These results were not unexpected given that only 40-50% of the islet cells are transduced by our adenoviruses. Thus, even if all the transduced cells became apoptotic and were cleared from the graft there may still be sufficient β-cell mass remaining to maintain normoglycaemia.

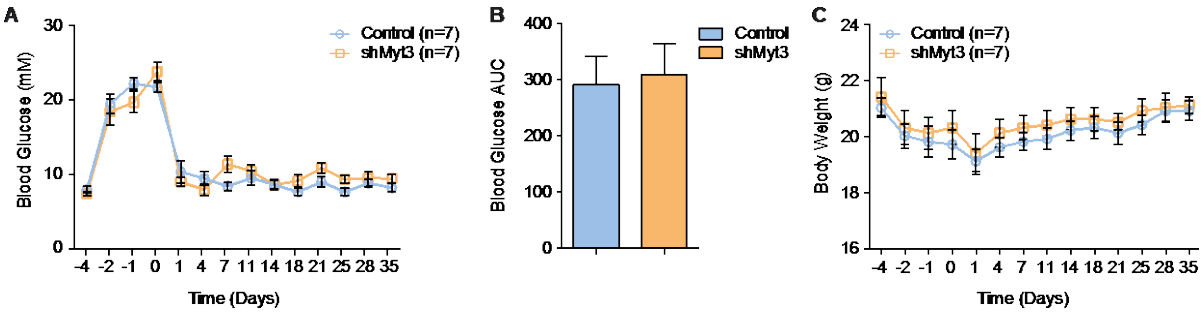

Figure 4.1: *Myt3* suppression does not affect islet graft function
A) Random-fed blood glucose measurements for mice transplanted with control- and sh*Myt3*-transduced islets. **B)** Area under the curve for blood glucose measurements from day 1 to 35 post-transplant. **C)** Body weight measurements for transplanted mice. All data represented as mean ± S.E.M.

To determine whether sufficient β-cell mass was remaining to respond to an acute glucose load we performed an intraperitoneal glucose tolerance test (IPGTT) on weight matched (Figure 4.2A) mice five weeks post-transplant. Both control and sh*Myt3* mice responded equally well to the glucose challenge and were able to clear the glucose bolus by two hours post injection (Figure 4.2B, C). Intriguingly, five days post-transplant weight matched (Figure 4.2D) control and sh*Myt3* mice exhibited an impaired ability to clear the glucose bolus (Figure 4.2E, F). Since both groups displayed a similar inability to secrete insulin in response to glucose it is likely that the defect is a result of the transplant process itself and is independent of any effects of *Myt3* suppression. These data suggest in these optimal syngeneic transplants sufficient β-cell mass remains even in the sh*Myt3*-transduced islets to respond to a glucose challenge.

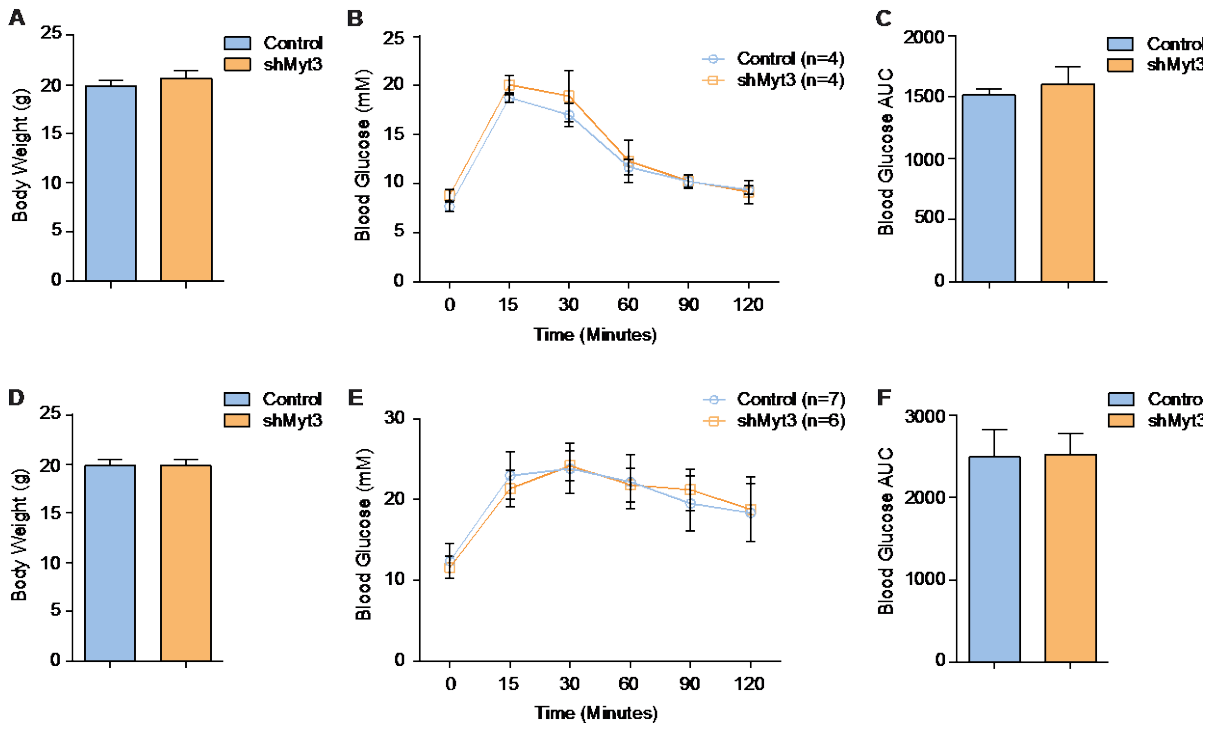

Figure 4.2: Time but not *Myt3* suppression affects glucose tolerance
A) Body weight was determined for mice following a six-hour fast and mice were weight matched prior to IPGTT. **B)** IPGTT on control and sh*Myt3* mice five weeks post-transplant. **C)** Area under the curve for blood glucose measurements from B. **D)** Body weight was determined for mice following a six-hour fast and mice were weight matched prior to IPGTT. **E)** IPGTT on control and sh*Myt3* mice five days post-transplant. **F)** Area under the curve for blood glucose measurements from E. All data represented as mean ± S.E.M.

Myt3 suppression increases cell death in syngeneic islet transplants

Work presented in Chapter 2 suggested that sh*Myt3*-transduced islets should exhibit higher levels of islet-cell death than control-transduced islets. As we performed optimal syngeneic transplants, significant cell loss may have occurred without significantly impairing islet-graft function. Thus, to determine if suppression of *Myt3* was inducing an increase in cell death in the islet grafts we performed IHC on isolated grafts. Transduced cells express GFP and quantification of GFP area in the grafts five weeks post-transplant showed that sh*Myt3* grafts were composed of only 2-3% GFP positive cells, roughly 1/5th ($p \leq 0.001$) the number found

in control grafts (13%) (Figure 4.3A, B). Given that ~40% of the cells were transduced prior to transplantation, the reduced number of GFP+ cells indicates that sh*Myt3*-transduced cells are likely undergoing cell death. The loss of GFP+ cells in the control-transduced islets may be due to cell death induced by the virus itself or it could be due to the suppression of GFP expression over time.

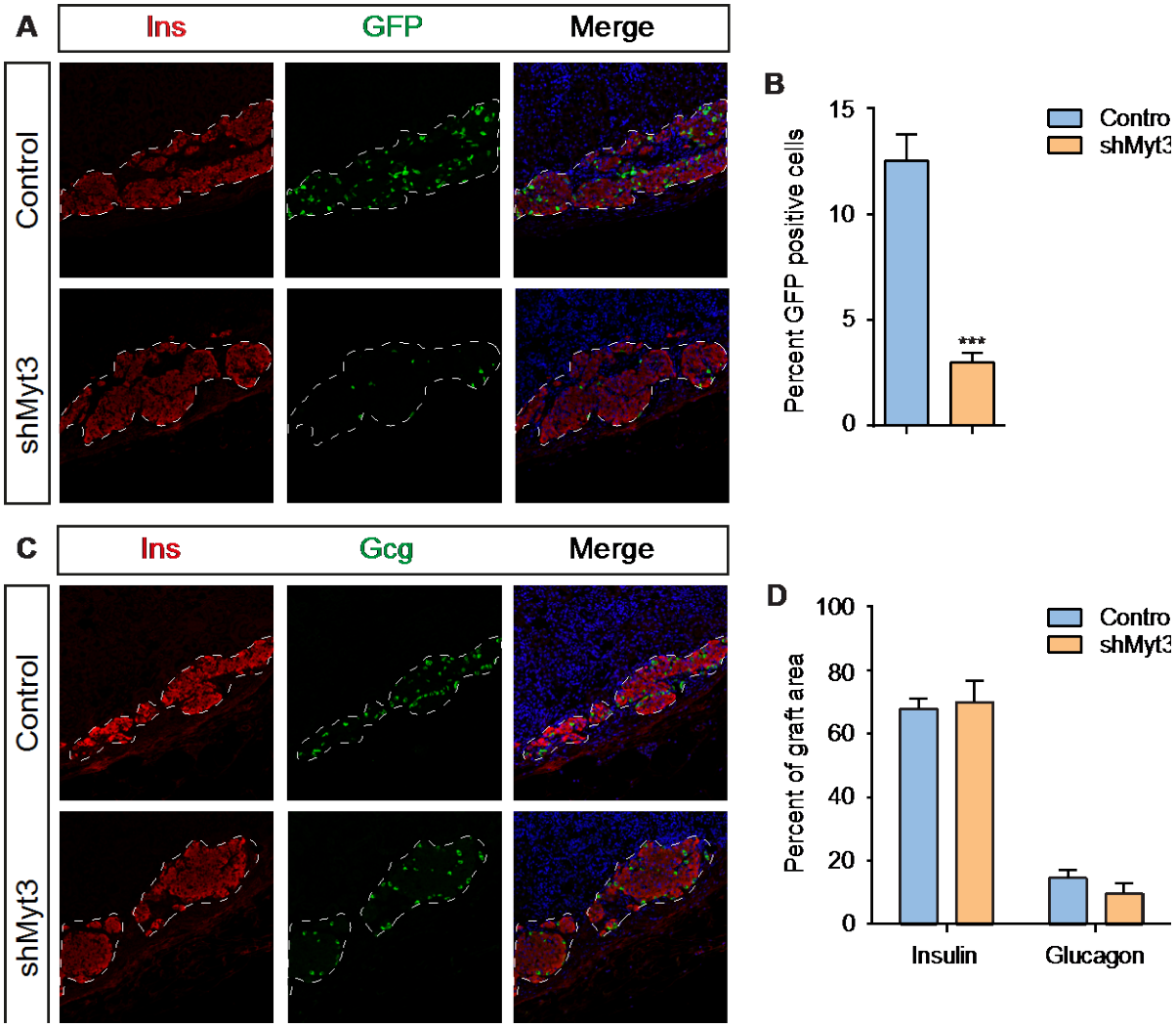

Figure 4.3: sh*Myt3*-transduced cells are lost from grafts without altering graft morphology
A) Control- and sh*Myt3*-transduced islet grafts were stained for insulin (red) and GFP (green) to mark transduced cells. **B)** Quantification of GFP area in A. **C)** Grafts were stained with insulin (red) and glucagon (green). **D)** Quantification of insulin and glucagon area in C. Nuclei are labeled with Topro3 (blue). White dashed lines represent the graft boundaries. All data represented as mean ± S.E.M. *** represents a significant difference of $p \leq 0.001$.

Quantification of the relative number of α- and β-cells in grafts shows that control- and sh*Myt3*-transduced islets have a roughly equal ratio of remaining of α- and β-cells, and shows that indeed adequate numbers of α- and β-cells to maintain normoglycaemia appear to still remain even in the sh*Myt3*-transduced islet grafts (Figure 4.3C, D).

Analysis of grafts five days post-transplant showed that while control-transduced islets contained approximately 40% transduced cells, sh*Myt3*-trasnduced islets only contained around 25% transduced cells (Figure 4.4A, B) suggesting that *Myt3* suppression is beginning to induce cell death within days of the islets being transplanted. Assessment of α- and β-cell numbers and distribution within the grafts (Figure 4.4C, D) showed that, similar to the grafts harvested at five weeks, there are no differences between control and sh*Myt3* grafts.

Myt3 suppression increases chemokine expression but not immune infiltration

Prior to inducing β-cell apoptosis immune-cell produced cytokines induce the expression of pro-inflammatory chemokines and cytokines in β-cells that act to recruit immune cells which induce further β-cell dysfunction and apoptosis [1, 13, 24, 76-78, 80, 81, 87, 113, 114, 200]. In Chapter 2 we showed that cytokine exposure causes the down-regulation of *Myt3* expression [216] and therefore sought to determine whether *Myt3* suppression similarly induces pro-inflammatory chemokines and cytokines in β-cells. Analysis of our RNA-seq data showed that *Myt3* suppression is sufficient to induce the expression of several chemokines including *Ccl2, Cxcl2, Cxcl10* and *Ccl20* (Figure 4.5A). qPCR validation demonstrated that a 2.4-fold ($p \leq 0.001$) reduction in *Myt3* expression resulted in a significant increase in the expression of *Ccl2* (3.7-fold, $p \leq 0.05$), *Cxcl10* (7.7-fold, $p \leq 0.05$) and *Ccl20* (8.3-fold, $p \leq 0.05$) (Figure 4.5B).

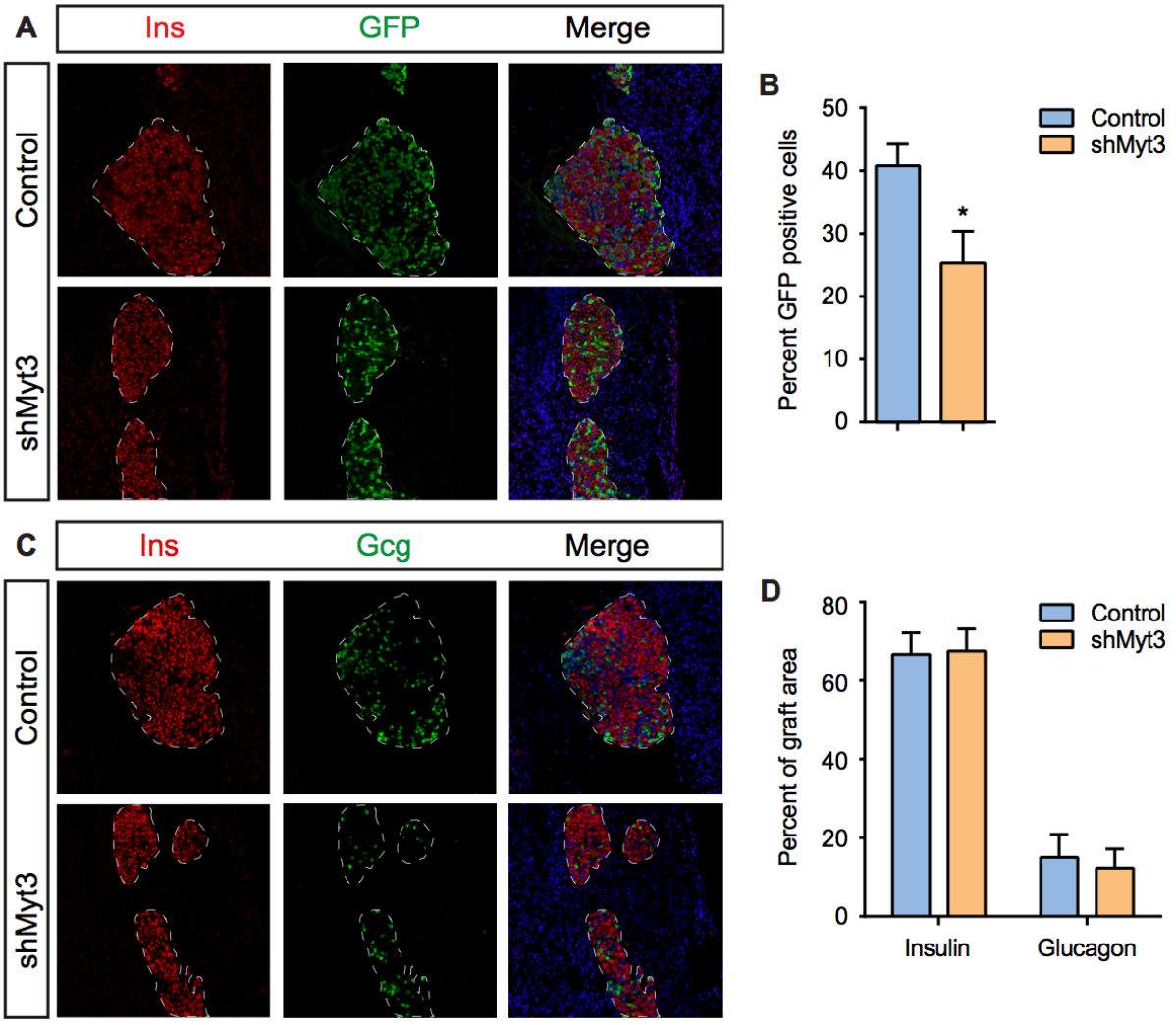

Figure 4.4: Loss of sh*Myt3*-transduced cells occurs within five days of transplantation
A) Control- and sh*Myt3*-transduced islet grafts were stained for insulin (red) and GFP (green) to mark transduced cells. **B)** Quantification of GFP area in A. **C)** Grafts were stained with insulin (red) and glucagon (green). **D)** Quantification of insulin and glucagon area in C. Nuclei are labeled with Topro3 (blue). White dashed line represents the graft boundary. All data represented as mean ± S.E.M. * represents a significant difference of $p \leq 0.05$.

To determine if *shMyt3*-induced pro-inflammatory chemokine expression is sufficient to drive recruitment of immune cells to the grafts we performed IHC on grafts at both five days (Figure 4.6A) and five weeks (Figure 4.6C) post-transplant with the pan-immune cell marker CD45. Quantification of immune cell infiltration into the grafts showed that infiltration was negligible and equivalent between control and sh*Myt3*-transduced islets (Figure 4.6B, D). These data suggest that the level of chemokine production induced by *Myt3* suppression was insufficient to drive the recruitment of immune cells to the graft.

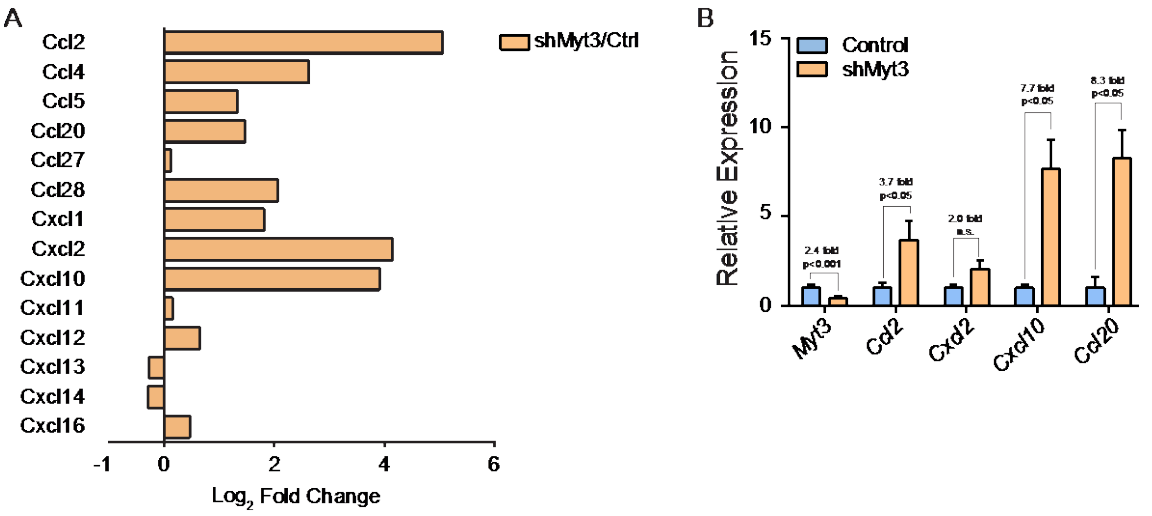

Figure 4.5: *Myt3* suppression induces the expression of chemokine genes
A) Bar graph of the $\log_2$-fold changes for chemokine genes in sh*Myt3*-transduced islets relative to control-transduced islets. **B)** qPCR validation of select chemokine genes.

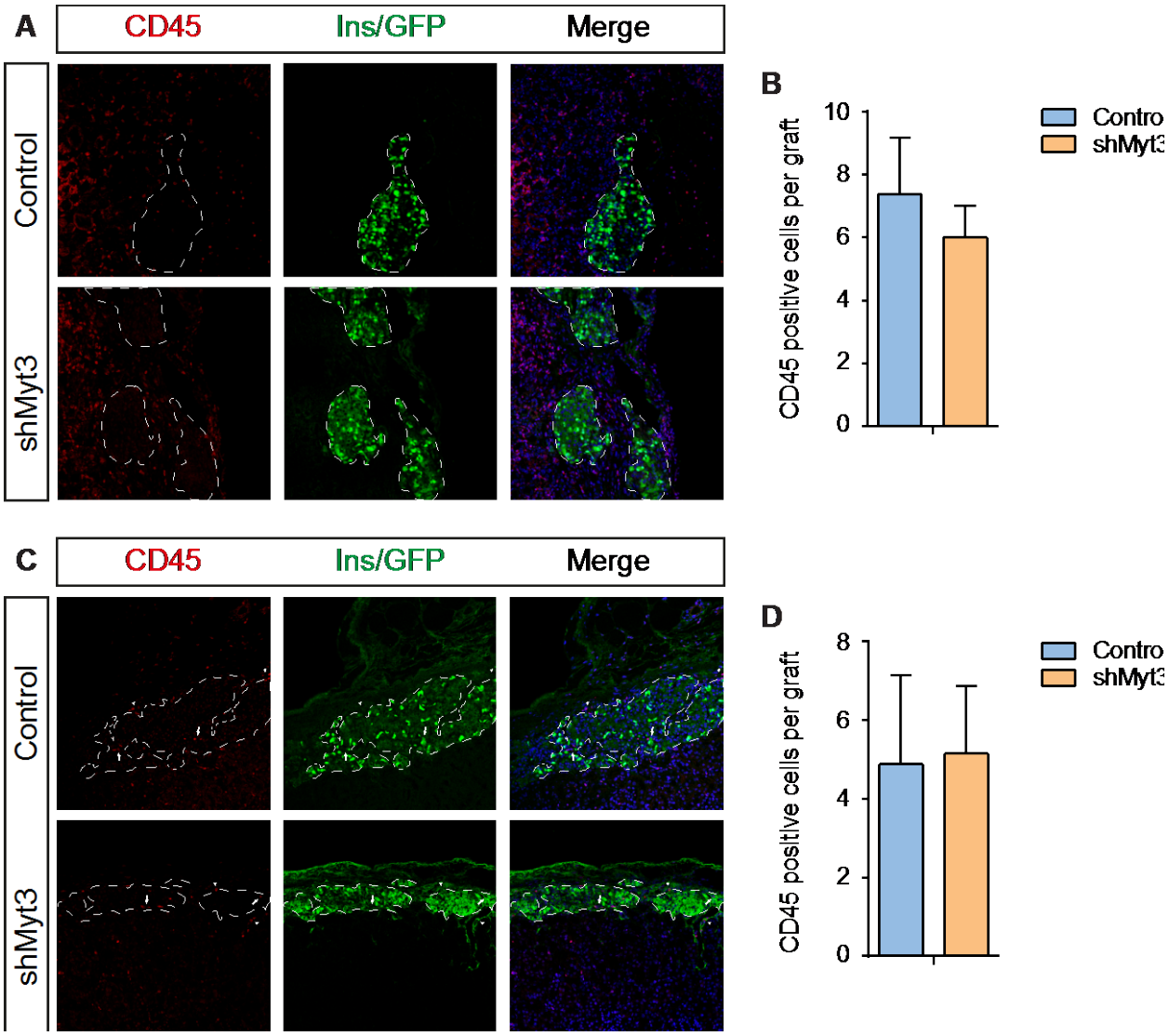

Figure 4.6: sh*Myt3*-induced chemokine expression does not induce immune cell recruitment
A) Control- and sh*Myt3*-transduced islet grafts were stained for CD45 (red) to mark immune cells and Insulin/GFP (green) to mark the graft boundaries five days post transplant. **B)** Quantification of CD45 positive cells within the graft area in A. **C)** Control- and sh*Myt3*-transduced islet grafts were stained for CD45 (red) to mark immune cells and insulin/GFP (green) to mark the graft boundaries five weeks post transplant. **D)** Quantification of CD45 positive cells within the graft area in C. Nuclei are labeled with Topro3 (blue). White dashed lines represent the graft boundaries. All data represented as mean ± S.E.M.

4.4 Discussion

Exposure of β-cells to cytokines, produced by infiltrating immune cells in diabetes, activates pro-inflammatory signalling cascades that ultimately lead to amplification of inflammatory signals and initiation of apoptosis [1, 13, 24, 76-78, 80, 81, 87, 113, 114]. In Chapter 2 we demonstrated that expression of the transcription factor *Myt3* is inhibited by exposure to Il-1β, Tnfα, and Ifnγ in β-cells and its suppression is sufficient to induce apoptosis in cultured islets [216]. Our initial analysis of the role of *Myt3* in regulating islet-cell death was conducted over a very short period (~48 hours) and didn't provide any insight into the long-term effects of *Myt3* suppression on islet function and survival *in vivo*. In the current chapter we sought to address this question using a syngeneic islet transplant model to examine the effects of *Myt3* suppression on graft function and survival.

We demonstrate that over five weeks of monitoring neither body weight nor blood glucose homeostasis were affected in mice transplanted with sh*Myt3*-transduced islets relative to controls. Also, administration of a glucose bolus into the intraperitoneal cavity five weeks post-transplant was unable to uncover an insulin secretion deficit in mice receiving sh*Myt3*-transduced islets relative to mice receiving control-transduced islets. Despite this we find that by five weeks only 2-3% of the sh*Myt3*-transduced islet grafts were composed of transduced cells, which is significantly lower than the 13% remaining in control-transduced grafts indicating that increased cell death is likely a contributing factor to this reduction. These results suggest that although many of the sh*Myt3*-transduced islet cells had undergone cell death, sufficient β-cell mass remained to maintain normal islet graft function. This is likely due to the fact that transplants were performed with 300 islets and only 40-50% of cells within each islet being transduced prior to transplantation.

Interrogation of graft function five days post-transplant, a time when we predicted islet-cell death was likely beginning to occur and dysfunction was potentially greatest, demonstrated that there is some graft dysfunction, independent of *Myt3* suppression, at this time likely due to the graft still recovering from the transplantation procedure or due to delayed vascularization of the graft. Despite this, our data show that as early as five days post-transplant there is a reduction in the number of transduced cells in the sh*Myt3* grafts relative to control grafts and this difference is even more prevalent five weeks post-transplant. While this is only a surrogate measure of cell death it seems to indicate that the suppression of *Myt3* increases cell death and that, under the right conditions, could have important implications for the progression of diabetes.

We further show that suppression of *Myt3* leads to the up-regulation of several chemokines in β-cells that are capable of recruiting immune cells to the graft site which would induce β-cell dysfunction and apoptosis [1, 13, 24, 76-78, 80, 81, 87, 113, 114]. However, the level of induction of these chemokines appeared to be insufficient to drive the recruitment of immune cells to the graft site.

These data suggest that *Myt3* may be necessary for transplanted islet-cell survival *in vivo*, and suggest that immune-cell secreted cytokine-induced *Myt3* suppression maybe a significant contributor to immune-cell mediated islet-cell death. We believe that future efforts need to be targeted at uncovering the mechanisms underlying the effects of *Myt3* suppression on β-cell apoptosis and determining whether the maintenance of *Myt3* levels during β-cell immune-assault can reduce β-cell death and dysfunction.

Chapter 5: Conclusions and future directions

5.1 Overall conclusions

According to the International Diabetes Federation if we were to collect all diabetic patients in the same place it would be the third most populous country in the world behind China and India. The unprecedented growth in patients worldwide is having a significant impact on the global economy and complications associated with the disease are greatly affecting the longevity and quality of life for those living with diabetes. Thus, efforts need to be taken to understand the mechanisms that are driving the onset and progression of the disease and that ultimately finding a cure for the hundreds of millions that are suffering with the disease is paramount.

Diabetes is a complex disease with a host of factors driving the various forms of the disease but in all cases is defined by an insufficient capacity of the body's β-cells to secrete sufficient insulin to maintain glucose homeostasis [1, 4, 46, 260]. It is clear that prevention of diabetes depends on maintenance of β-cell mass and insulin secretory capacity. For this reason, a great deal of recent effort has focused on finding ways to enhance β-cell survival, prevent β-cell death and stimulate β-cell mass replacement [113, 212, 261-263]. Additional work is being done to generate glucose-responsive insulin-secreting cells from more abundant cell types like embryonic stem cells and hepatocytes [5, 6, 35, 264]. Despite the promising advances that have been made to date, there are likely additional targets and pathways that are yet to be identified that may further enhance our ability to understand how the tissues involved in glucose homeostasis develop, how diabetes onset occurs and how the disease progresses.

There is a growing body of evidence highlighting the importance of proper spatial and temporal regulation of gene expression for the development and function of endocrine cells, and more specifically β-cells [173-175]. Thus, the identification of transcription factors that are specifically expressed in islets is a promising approach to provide novel targets for the treatment of diabetes. To highlight this fact we previously identified the transcription factor *Myt3* as being highly expressed in adult islets [8], and work studying the effects of *Myt1* suppression in the developing pancreas suggested that *Myt3* could compensate for this loss and may be important for the normal function of mature endocrine cells [11]. The work presented in this dissertation was designed to study how *Myt3* is regulated and to elucidate its role in islet development, function and survival.

We have demonstrated that *Myt3* expression is low during early pancreas development but is highly expressed in maturing and adult endocrine cells suggesting that *Myt3* may be important for the formation and/or the function of mature islets. Part of the process that is necessary for the formation of functional islets is the Ngn3-dependent delamination and subsequent clustering of endocrine precursor cells into islet-like structures adjacent to the pancreatic ducts [125, 137]. Our data demonstrate that Myt3 protein first appears in endocrine cells at ~E18.5 during the period when endocrine cells cluster together into islet-like structures. We also show that ectopic expression of *Ngn3* is capable of inducing the expression of *Myt3* suggesting that it may be important for the formation of mature islets downstream of Ngn3.

We next sought to determine how Ngn3 regulates the expression of *Myt3* and what *Myt3* might be doing during this developmental period. Our data show that exogenously over-expressed *Ngn3* promotes a more open and active chromatin state around the *Myt3* promoter,

through an increase in the enrichment of the activating H3K4me1 and H3K27ac marks, with a concomitant decrease in repressive H3K27me3 enrichment levels. These data suggest that Ngn3-dependent changes to the histone modification state around the *Myt3* promoter may allow it to become activated by other transcription factors. Ngn3 also increases the expression of key maturation factors, such as *Pdx1, Neurod1* and *Mafa,* which drives the formation of fully functional endocrine cells [125, 265]. We performed chromatin immunoprecipitation and luciferase experiments to determine if these transcription factors act downstream of *Ngn3* to promote *Myt3* expression. We show that the *Myt3* promoter is bound and directly regulated by Foxa2, Pdx1 and Neurod1.

As mentioned above the migration of endocrine cell clusters away from the pancreatic ducts is an important step in the islet maturation process and we have shown that Myt3 is present in endocrine cells at this time. The regulation of *Myt3* expression by Ngn3 and transcription factors important for β-cell maturation, along with the fact that it is expressed in cells with redistributed E-cadherin, a marker of migrating cells, suggested that *Myt3* might be important for the migration of islet cells during development. To study the role of *Myt3* in regulating islet-cell migration we cultured whole islets for seven days on 804G. Under normal conditions this procedure results in the expansion of islet area, which we have shown is largely due to cell migration onto the matrix. We present data that confirms that the migration of islet-cells onto 804G is dependent on integrin-β1 signalling and show suppression of *Myt3* dramatically impairs the ability of islet-cells to migrate onto 804G via the regulation of *Tgfbi*. These data were obtained using adult islets in an *in vitro* setting but indicate that *Myt3* may have a role to play in the formation of islets. Evidence is accumulating suggesting that disruption of cell/matrix interactions and migration can have

detrimental effects on the specification of endocrine cells [266], the establishment of islet architecture and morphology [148, 267], and proper islet function [268]. *Myt3* expression is initiated only after endocrine cells are thought to largely be specified, therefore loss of *Myt3* is thus unlikely to impair specification of the major hormone producing endocrine cell types (i.e. α, β, δ, ε and PP) but it may disrupt migration of islet-like clusters away from ducts or alter the establishment of islet architecture which could have detrimental effects on islet function.

In addition to a potential role in islet development our gene expression and protein data indicated that *Myt3* might also be necessary in adult islets. As discussed above we demonstrated that the transcription factors Pdx1, Foxa2 and Neurod1, which are expressed in mature islets, all regulate the expression of *Myt3*. Both *Pdx1* and *Neurod1* are glucose responsive transcription factors [190, 207] and as such we sought to determine if *Myt3* expression was likewise regulated by glucose exposure. Glucose was able to increase the expression of *Myt3* in a dose and time dependent manner, the delay in increased expression likely resulting from a need to recruit additional transcription factors, or to a more restrictive epigenetic landscape that needs to be altered to facilitate increased gene expression. Islets not only alter gene expression but also secrete insulin in response to elevated glucose levels and we were interested in determining if, like other glucose responsive genes, *Myt3* was involved in the regulation of insulin secretion. *Myt3* suppression did not induce any changes in glucose-induced insulin secretion both in the presence and absence of extracellular matrix. The secretion of insulin is dependent on the ability of β-cells to redistribute their F-actin network at the plasma membrane in order to facilitate access to the membrane for insulin secretory granules [232, 255]. Despite being unable to regulate F-actin organization in an

ECM-dependent fashion, *Myt3* suppression did not affect glucose-mediated F-actin reorganization, which is likely part of the reason why no insulin secretion defects are observed in our sh*Myt3*-transduced islets.

In addition to responding to fluctuations in circulating glucose levels, pancreatic islets are also the target of immune-mediated pro-inflammatory signalling in both T1D and T2D [24, 76, 77, 95-101]. Studies examining the signalling events downstream of cytokine exposure in islets demonstrated that *Myt3* is suppressed by cytokines in an Nfκb-dependent manner [13] and we have confirmed that exposure of islets to a cytokine cocktail of Il-1β, Tnfα and Ifnγ suppresses the expression of *Myt3* in a dose and time dependent manner. The cytokine-induced suppression of *Myt3* is likely to also play an important role *in vivo* since immune infiltration in a mouse model of T1D lead to a concomitant decrease in the expression level of *Myt3* suggesting that it may be an important regulatory factor downstream of cytokine exposure in the development of diabetes. Prolonged exposure to cytokines in the context of both T1D and T2D results in increasing β-cell dysfunction and apoptosis [1, 208]. We have already established that *Myt3* suppression is not involved in the regulation of islet function; therefore we sought to determine whether *Myt3* might be a mediator of cytokine-induced apoptosis. Our data clearly show that *Myt3* suppression leads to increased apoptosis in islets and MIN6 cells, suggesting that Il-1β, Tnfα and Ifnγ-induced *Myt3* repression may be a significant factor in cytokine-induced β-cell apoptosis. We further demonstrate that adenoviral-mediated *Myt3* over-expression largely prevents cytokine-induced apoptosis in islets. In agreement with *Myt3* having a pro-survival role in β-cells, suppression of *Myt3* resulted in a significant reduction in the expression of pro-survival genes such as *Pdx1, Il-6, Bcl-xl, c-Iap2,* and *Igfr1*. These genes regulate cell survival in part

by prevention of cytochrome-c release [115], inhibiting caspase activity [210], and controlling Akt signalling [212, 213]. These data are an important step in clarifying the regulatory networks responsible for β-cell survival and suggest that *Myt3* may be an interesting therapeutic target for improving β-cell survival in diabetic patients and islet graft recipients.

While these studies point to a potential role for *Myt3* in regulating islet survival they fail to address the long-term consequences of *Myt3* ablation on islet survival in an *in vivo* setting. To address this we performed syngeneic islet transplants using sh*Myt3*-transduced islets and monitored graft function and survival over time. Contrary to our expectations *Myt3* suppression had no effect on graft function either under random fed or acute glucose challenge conditions. We propose that this result is likely due to the use of 300 islets in an optimal transplant in which only 40-50% of cells within a given islet are transduced. This would leave on the order of 175-200 islet equivalents intact which is a sufficient number of cells remaining to maintain normoglycaemia. Despite this apparent failure of *Myt3* suppression to have any effect on graft function we were able to establish that there is a significant reduction in the number of transduced cells remaining in the graft five weeks post-transplant.

Collectively, the data presented in this disseration are an important step in clarifying the regulatory networks responsible for β-cell development, function and survival, and point to *Myt3* as a potential therapeutic target for improving functional β-cell mass.

5.2 Future directions

In this dissertation we have shown that *Myt3* is the predominant MYT family member in islets and that it regulates the expression of key β-cell genes, while controlling insulin content, cell migration, and apoptosis *in vitro*. These studies have provided the first insights into the role of *Myt3* in islets and have provided a framework from which to further characterise how *Myt3*, and the pathways it regulates, are involved in regulating islet function and survival *in vivo*. The goal is to identify the environmental signals that regulate its activity, determine which target genes it regulates, determine its *in vivo* function and identify how it could be employed to improve islet function and survival in the context of diabetes. Based on the evidence presented in this dissertation, we **hypothesise** that *Myt3* is likely to facilitate the development and maintenance of mature endocrine cells and prevent apoptosis *in vivo*.

As a first step in improving our understanding of the role of *Myt3* in islets we need to identify the signals that control the expression and the intracellular localisation of Myt3. We have already determined some of the transcription factors that are important for its expression and have shown that environmental signals, such as glucose and cytokines, can affect its expression. What is less clear is how these environmental signals alter *Myt3* expression and uncovering these pathways will be an important step in any attempts to maintain *Myt3* expression levels for the purposes of improving islet survival. Another important area of Myt3 regulation that needs to be addressed is its cellular distribution. We have presented evidence that shows Myt3 in islets is predominantly cytoplasmic with only a fraction of total Myt3 localising to the nucleus (Figure 2.3). This suggests that Myt3 cellular distribution is one mechanism employed by cells to regulate its activity and the identification

of the signals that mediate this process will be an important step in increasing Myt3 activity which we have demonstrated is capable of alleviating some of the detrimental effects of cytokine exposure (Figure 2.10 and 3.5).

In conjunction with determining the mechanisms controlling *Myt3* itself, it is necessary to identify the genes that *Myt3* is regulating since it is unlikely that it is directly responsible for affecting changes in the various pathways in which it has been implicated. The MYT family is reported to function as both repressors and activators, with repression being mediated by interaction with Sin3b while their activation potential is likely due to the acidic and central domains [164, 269, 270], providing support for the need to identify Myt3 cofactors to uncover how Myt3 is mediating changes in gene expression. Furthermore, a potential bipartite binding motif (AAA(G/C)TTT) has been identified for Myt3 in *in vitro* studies [164, 165] and several of the genes whose expression is regulated by Myt3, including *gastrin*, *ghrelin*, *Ccl2* and *Cxcl10* harbour this motif within their regulatory regions. This motif is unlikely to be a true binding site *in vivo* and as such an unbiased, genome wide approach will be necessary to uncover the true Myt3 binding sites which will be essential to assess the consequences of *Myt3* misexpression.

Suppression of *Myt3* expression in isolated islets results in a significant increase in the level of apoptosis and reduces the expression of key β-cell transcription factors and pro-survival genes while increasing the expression of pro-inflammatory chemokines. We expected this to negatively affect graft function and survival in a syngeneic islet transplant model, however, this turned out not be the case. An approach that attempts to maintain or improve islet function and survival via the up-regulation of *Myt3* is likely to achieve greater results. We believe that over-expression of *Myt3* in suboptimal syngeneic or optimal

allogeneic transplant models will improve long-term graft function because in addition to the protection from cytokine-induced apoptosis observed in *Myt3* over-expressing islets *in vitro,* preliminary results not presented in this thesis indicate that *Myt3* over-expression increases gastrin expression by 23-fold ($p<0.01$). Interestingly, gastrin co-administration with Egf dramatically improves syngeneic islet transplant survival in NOD mice [271], and promotes regeneration of islets and restores normoglycaemia following alloxan treatment [272] suggesting that a combination of *Myt3* over-expression and administration of Egf or dipeptidyl peptidase-4 inhibitors (DPP-4i), which raise serum Glp-1 and Gip levels [273, 274], will have an even more pronounced affect on graft function and survival.

Several transcription factors that are necessary for early pancreatic and endocrine cell specification are also required for β-cell maturation, and the active maintenance of β-cells in a mature state [151, 176-180]. We show that Myt3 protein first appears in endocrine cells at ~E18.5 during the period of islet maturation, and is also expressed in mature α-, β-, δ-, and PP-cell types. Furthermore, suppression of *Myt3* reduces the expression of several transcription factors responsible for β-cell maturation, including *Mafa* and *Pdx1*, and *Myt3* misexpression also alters the expression of *Gast* and *Ghr*, neither of which are typically expressed in mature β-cells [275, 276]. To determine if *Myt3* is necessary for the establishment or maintenance of endocrine cell identity or maturation state it will be necessary to alter the expression of *Myt3* in both developing and mature endocrine cells. The use of a conditional knockout mouse model would be ideal, however this strategy is not a viable option with the currently available mice and is further complicated by the compensation of the other MYT family members (Dr Guoqiang Gu, personal communication). As such we propose to generate strongly activating and strongly repressing

Myt3 transgenes that will modify the endogenous activity of Myt3 and at the same time prevent compensation by the other MYT family members. Using a pancreas specific and inducible Cre-LoxP system we will be able to assess the effects of *Myt3* misexpression during endocrine cell specification and in the maintenance of endocrine identity and function.

Understanding the mechanisms and transcriptional networks that control β-cell function, and how these are influenced by immune attack in T1D and T2D, is critical to developing novel approaches for treating diabetes. These experiments will define the role of *Myt3* in the regulation of islet function, and determine if *Myt3* is essential for β-cell maturation, function and survival. These data will provide the first *in vivo* support for our hypothesis that *Myt3* is essential for these processes and may implicate it as a novel therapeutic target or inform novel approaches to treat T1D and T2D.

Bibliography

1. van Belle TL, Coppieters KT, Herrath von MG (2011) Type 1 diabetes: etiology, immunology, and therapeutic strategies. Physiological reviews 91:79–118. doi: 10.1152/physrev.00003.2010

2. Prentki M, Nolan CJ (2006) Islet beta cell failure in type 2 diabetes. The Journal of clinical investigation 116:1802–1812. doi: 10.1172/JCI29103

3. Csorba TR, Lyon AW, Hollenberg MD (2010) Autoimmunity and the pathogenesis of type 1 diabetes. Crit Rev Clin Lab Sci 47:51–71. doi: 10.3109/10408361003787171

4. Stumvoll M, Goldstein BJ, van Haeften TW (2005) Type 2 diabetes: principles of pathogenesis and therapy. Lancet 365:1333–1346. doi: 10.1016/S0140-6736(05)61032-X

5. Rezania A, Bruin JE, Arora P, et al. (2014) Reversal of diabetes with insulin-producing cells derived in vitro from human pluripotent stem cells. Nature Biotechnology 32:1121–1133. doi: 10.1038/nbt.3033

6. Kawasaki H, Mizuguchi T, Oshima H, et al. (2008) Efficient transformation of small hepatocytes into insulin-expressing cells by forced expression of Pdx1. Journal of Hepato-Biliary-Pancreatic Surgery 15:403–409. doi: 10.1007/s00534-007-1318-2

7. Edlund H (2002) Pancreatic organogenesis--developmental mechanisms and implications for therapy. Nature Reviews Genetics 3:524–532. doi: 10.1038/nrg841

8. Hoffman BG, Zavaglia B, Witzsche J, et al. (2008) Identification of transcripts with enriched expression in the developing and adult pancreas. Genome Biology 9:R99. doi: 10.1186/gb-2008-9-6-r99

9. Jensen J (2004) Gene regulatory factors in pancreatic development. Developmental dynamics : an official publication of the American Association of Anatomists 229:176–200. doi: 10.1002/dvdy.10460

10. Bernardo AS, Hay CW, Docherty K (2008) Pancreatic transcription factors and their role in the birth, life and survival of the pancreatic beta cell. Molecular and Cellular Endocrinology 294:1–9. doi: 10.1016/j.mce.2008.07.006

11. Wang S, Zhang J, Zhao A, et al. (2007) Loss of Myt1 function partially compromises endocrine islet cell differentiation and pancreatic physiological function in the mouse. Mechanisms of Development 124:898–910. doi: 10.1016/j.mod.2007.08.004

12. Yang J, Siqueira MF, Behl Y, et al. (2008) The transcription factor ST18 regulates proapoptotic and proinflammatory gene expression in fibroblasts. The FASEB Journal 22:3956–3967. doi: 10.1096/fj.08-111013

13. Cardozo AK, Heimberg H, Heremans Y, et al. (2001) A comprehensive analysis of cytokine-induced and nuclear factor-kappa B-dependent genes in primary rat pancreatic beta-cells. The Journal of biological chemistry 276:48879–48886. doi: 10.1074/jbc.M108658200

14. Ashcroft FM, Rorsman P (2012) Diabetes mellitus and the β cell: the last ten years. Cell 148:1160–1171. doi: 10.1016/j.cell.2012.02.010

15. Aguiree F, Brown A, Cho NH, et al. (2013) IDF Diabetes Atlas : sixth edition. International Diabetes Federation

16. Canadian Diabetes Association Clinical Practice Guidelines Expert Committee (2013) Canadian Diabetes Association 2013 Clinical Practice Guidelines for the Prevention and Management of Diabetes in Canada. Canadian Journal of Diabetes 37:S1–S212. doi: 10.1016/S1499-2671(13)00192-5

17. Brownlee M (2005) The pathobiology of diabetic complications: a unifying mechanism. Diabetes 54:1615–1625.

18. Yagihashi S, Mizukami H, Sugimoto K (2011) Mechanism of diabetic neuropathy: Where are we now and where to go? J Diabetes Investig 2:18–32. doi: 10.1111/j.2040-1124.2010.00070.x

19. Atkinson MA (2012) The pathogenesis and natural history of type 1 diabetes. Cold Spring Harbor Perspectives in Medicine. doi: 10.1101/cshperspect.a007641

20. Noble JA, Erlich HA (2012) Genetics of type 1 diabetes. Cold Spring Harbor Perspectives in Medicine 2:a007732. doi: 10.1101/cshperspect.a007732

21. Jeker LT, Bour-Jordan H, Bluestone JA (2012) Breakdown in peripheral tolerance in type 1 diabetes in mice and humans. Cold Spring Harbor Perspectives in Medicine 2:a007807. doi: 10.1101/cshperspect.a007807

22. Roep BO, Peakman M (2012) Antigen targets of type 1 diabetes autoimmunity. Cold Spring Harbor Perspectives in Medicine 2:a007781. doi: 10.1101/cshperspect.a007781

23. Pietropaolo M, Towns R, Eisenbarth GS (2012) Humoral autoimmunity in type 1 diabetes: prediction, significance, and detection of distinct disease subtypes. Cold Spring Harbor Perspectives in Medicine. doi: 10.1101/cshperspect.a012831

24. Delovitch TL, Singh B (1997) The nonobese diabetic mouse as a model of autoimmune diabetes: immune dysregulation gets the NOD. Immunity 7:727–738.

25. Bach J-F, Chatenoud L (2012) The hygiene hypothesis: an explanation for the increased frequency of insulin-dependent diabetes. Cold Spring Harbor Perspectives in Medicine 2:a007799. doi: 10.1101/cshperspect.a007799

26. Coppieters KT, Boettler T, Herrath von M (2012) Environmental triggers of type 1 diabetes. Cold Spring Harbor Perspectives in Medicine 2:a007682. doi: 10.1101/cshperspect.a007682

27. Rodriguez-Calvo T, Herrath von MG (2015) Enterovirus infection and type 1 diabetes: closing in on a link? Diabetes 64:1503–1505. doi: 10.2337/db14-1931

28. Richardson SJ, Willcox A, Bone AJ, et al. (2009) The prevalence of enteroviral capsid protein vp1 immunostaining in pancreatic islets in human type 1 diabetes. Diabetologia 52:1143–1151. doi: 10.1007/s00125-009-1276-0

29. Banting FG, Best CH, Collip JB, et al. (1922) Pancreatic Extracts in the Treatment of Diabetes Mellitus. Can Med Assoc J 12:141–146.

30. Holmes D (2015) Diabetes: Artificial pancreas--first head-to-head comparison of dual-hormone and single-hormone systems. Nature reviews Endocrinology 11:63. doi: 10.1038/nrendo.2014.221

31. Barnard KD, Kubiak T, Hermanns N, Heinemann L (2015) Patient-reported outcomes and continuous glucose monitoring: can we do better with artificial pancreas devices? Diabetes Care 38:e70. doi: 10.2337/dc14-3044

32. Shapiro AM, Lakey JR, Ryan EA, et al. (2000) Islet transplantation in seven patients with type 1 diabetes mellitus using a glucocorticoid-free immunosuppressive regimen. The New England journal of medicine 343:230–238. doi: 10.1056/NEJM200007273430401

33. Pepper AR, Gala-Lopez B, Ziff O, Shapiro AJ (2013) Current status of clinical islet transplantation. World J Transplant 3:48–53. doi: 10.5500/wjt.v3.i4.48

34. Bruin JE, Kieffer TJ (2012) Differentiation of Human Embryonic Stem Cells into Pancreatic Endocrine Cells. In: Stem Cells and Cancer Stem Cells, Volume 12. Springer Netherlands, Dordrecht, pp 191–206

35. Hebrok M (2012) Generating β cells from stem cells-the story so far. Cold Spring Harbor Perspectives in Medicine 2:a007674. doi: 10.1101/cshperspect.a007674

36. Gagliani N, Jofra T, Valle A, et al. (2013) Transplant Tolerance to Pancreatic Islets Is Initiated in the Graft and Sustained in the Spleen. American Journal of Transplantation 13:1963–1975. doi: 10.1111/ajt.12333

37. Montane J, Obach M, Alvarez S, et al. (2014) CCL22 prevents rejection of mouse islet allografts and induces donor-specific tolerance. Cell Transplant. doi: 10.3727/096368914X685149

38. Chatenoud L, Warncke K, Ziegler A-G (2012) Clinical immunologic interventions for the treatment of type 1 diabetes. Cold Spring Harbor Perspectives in Medicine. doi: 10.1101/cshperspect.a007716

39. Yoo H-W, Shin Y-L, Seo E-J, Kim G-H (2002) Identification of a novel mutation in the GLUT2 gene in a patient with Fanconi-Bickel syndrome presenting with neonatal diabetes mellitus and galactosaemia. Eur J Pediatr 161:351–353. doi: 10.1007/s00431-002-0931-y

40. Servitja JM, Ferrer J (2004) Transcriptional networks controlling pancreatic development and beta cell function. Diabetologia 47:597–613. doi: 10.1007/s00125-004-1368-9

41. Liu L, Furuta H, Minami A, et al. (2007) A novel mutation, Ser159Pro in the NeuroD1/BETA2 gene contributes to the development of diabetes in a Chinese potential MODY family. Mol Cell Biochem 303:115–120. doi: 10.1007/s11010-007-9463-0

42. Plengvidhya N, Boonyasrisawat W, Chongjaroen N, et al. (2009) Mutations of maturity-onset diabetes of the young (MODY) genes in Thais with early-onset type 2 diabetes mellitus. Clin Endocrinol (Oxf) 70:847–853. doi: 10.1111/j.1365-2265.2008.03397.x

43. Sachdeva MM, Claiborn KC, Khoo C, et al. (2009) Pdx1 (MODY4) regulates pancreatic beta cell susceptibility to ER stress. Proceedings of the National Academy of Sciences of the United States of America 106:19090–19095. doi: 10.1073/pnas.0904849106

44. Carbone I, Cotellessa M, Barella C, et al. (2002) A novel hepatocyte nuclear factor-1beta (MODY-5) gene mutation in an Italian family with renal dysfunctions and early-onset diabetes. Diabetologia 45:153–154. doi: 10.1007/s001250200019

45. Servitja J-M, Pignatelli M, Maestro MA, et al. (2009) Hnf1alpha (MODY3) controls tissue-specific transcriptional programs and exerts opposed effects on cell growth in pancreatic islets and liver. Molecular and Cellular Biology 29:2945–2959. doi: 10.1128/MCB.01389-08

46. Anık A, Çatlı G, Abacı A, Böber E (2015) Maturity-onset diabetes of the young (MODY): an update. J Pediatr Endocrinol Metab 28:251–263. doi: 10.1515/jpem-2014-0384

47. Halban PA, Polonsky KS, Bowden DW, et al. (2014) β-cell failure in type 2 diabetes: postulated mechanisms and prospects for prevention and treatment. Diabetes Care 37:1751–1758. doi: 10.2337/dc14-0396

48. Kahn SE (2003) The relative contributions of insulin resistance and beta-cell dysfunction to the pathophysiology of Type 2 diabetes. Diabetologia 46:3–19. doi: 10.1007/s00125-002-1009-0

49. Shah P, Vella A, Basu A, et al. (2000) Lack of suppression of glucagon contributes to postprandial hyperglycemia in subjects with type 2 diabetes mellitus. J Clin Endocrinol Metab 85:4053–4059. doi: 10.1210/jcem.85.11.6993

50. Reaven GM, Chen YD, Golay A, et al. (1987) Documentation of hyperglucagonemia throughout the day in nonobese and obese patients with noninsulin-dependent diabetes mellitus. J Clin Endocrinol Metab 64:106–110. doi: 10.1210/jcem-64-1-106

51. Bonnefond A, Froguel P, Vaxillaire M (2010) The emerging genetics of type 2 diabetes. Trends in Molecular Medicine 16:407–416. doi: 10.1016/j.molmed.2010.06.004

52. Dupuis J, Langenberg C, Prokopenko I, et al. (2010) New genetic loci implicated in fasting glucose homeostasis and their impact on type 2 diabetes risk. Nature Genetics 42:105–116. doi: 10.1038/ng.520

53. Gloyn AL, Braun M, Rorsman P (2009) Type 2 diabetes susceptibility gene TCF7L2 and its role in beta-cell function. Diabetes 58:800–802. doi: 10.2337/db09-0099

54. Samuel VT, Petersen KF, Shulman GI (2010) Lipid-induced insulin resistance: unravelling the mechanism. Lancet 375:2267–2277. doi: 10.1016/S0140-6736(10)60408-4

55. Ozcan U, Cao Q, Yilmaz E, et al. (2004) Endoplasmic reticulum stress links obesity, insulin action, and type 2 diabetes. Science 306:457–461. doi: 10.1126/science.1103160

56. Hagberg CE, Mehlem A, Falkevall A, et al. (2012) Targeting VEGF-B as a novel treatment for insulin resistance and type 2 diabetes. Nature 490:426–430. doi: 10.1038/nature11464

57. Butler AE, Janson J, Bonner-Weir S, et al. (2003) Beta-cell deficit and increased beta-cell apoptosis in humans with type 2 diabetes. Diabetes 52:102–110.

58. Dankner R, Chetrit A, Shanik MH, et al. (2009) Basal-state hyperinsulinemia in healthy normoglycemic adults is predictive of type 2 diabetes over a 24-year follow-up: a preliminary report. Diabetes Care 32:1464–1466. doi: 10.2337/dc09-0153

59. Mehran AE, Templeman NM, Brigidi GS, et al. (2012) Hyperinsulinemia drives diet-induced obesity independently of brain insulin production. Cell Metabolism 16:723–737. doi: 10.1016/j.cmet.2012.10.019

60. Thomas HE, McKenzie MD, Angstetra E, et al. (2009) Beta cell apoptosis in diabetes. Apoptosis 14:1389–1404. doi: 10.1007/s10495-009-0339-5

61. Maedler K, Sergeev P, Ris F, et al. (2002) Glucose-induced beta cell production of IL-1beta contributes to glucotoxicity in human pancreatic islets. The Journal of clinical investigation 110:851–860. doi: 10.1172/JCI15318

62. Zhou R, Tardivel A, Thorens B, et al. (2010) Thioredoxin-interacting protein links oxidative stress to inflammasome activation. Nature Immunology 11:136–140. doi: 10.1038/ni.1831

63. Robertson RP, Harmon J, Tran PO, et al. (2003) Glucose toxicity in beta-cells: type 2 diabetes, good radicals gone bad, and the glutathione connection. Diabetes 52:581–587.

64. Kim J-W, You Y-H, Ham D-S, et al. (2009) Suppression of peroxisome proliferator-activated receptor gamma-coactivator-1alpha normalizes the glucolipotoxicity-induced decreased BETA2/NeuroD gene transcription and improved glucose tolerance in diabetic rats. Endocrinology 150:4074–4083. doi: 10.1210/en.2009-0241

65. Harmon JS, Stein R, Robertson RP (2005) Oxidative stress-mediated, post-translational loss of MafA protein as a contributing mechanism to loss of insulin gene expression in glucotoxic beta cells. The Journal of biological chemistry 280:11107–11113. doi: 10.1074/jbc.M410345200

66. Poitout V, Robertson RP (2002) Minireview: Secondary beta-cell failure in type 2 diabetes--a convergence of glucotoxicity and lipotoxicity. Endocrinology 143:339–342. doi: 10.1210/endo.143.2.8623

67. Prentki M, Joly E, El-Assaad W, Roduit R (2002) Malonyl-CoA signaling, lipid partitioning, and glucolipotoxicity: role in beta-cell adaptation and failure in the etiology of diabetes. Diabetes 51 Suppl 3:S405–13.

68. Westermark P, Wernstedt C, Wilander E, et al. (1987) Amyloid fibrils in human insulinoma and islets of Langerhans of the diabetic cat are derived from a neuropeptide-like protein also present in normal islet cells. Proceedings of the National Academy of Sciences of the United States of America 84:3881–3885.

69. Kahn SE, D'Alessio DA, Schwartz MW, et al. (1990) Evidence of cosecretion of islet amyloid polypeptide and insulin by beta-cells. Diabetes 39:634–638.

70. Kahn SE, Andrikopoulos S, Verchere CB (1999) Islet amyloid: a long-recognized but underappreciated pathological feature of type 2 diabetes. Diabetes 48:241–253.

71. Marzban L, Park K, Verchere CB (2003) Islet amyloid polypeptide and type 2 diabetes. Exp Gerontol 38:347–351.

72. Westwell-Roper C, Dai DL, Soukhatcheva G, et al. (2011) IL-1 blockade attenuates islet amyloid polypeptide-induced proinflammatory cytokine release and pancreatic islet graft dysfunction. Journal of immunology (Baltimore, Md : 1950) 187:2755–2765. doi: 10.4049/jimmunol.1002854

73. Westwell-Roper C, Dunne A, Kim ML, et al. (2013) Activating the NLRP3 inflammasome using the amyloidogenic peptide IAPP. Methods Mol Biol 1040:9–18. doi: 10.1007/978-1-62703-523-1_2

74. Westwell-Roper CY, Ehses JA, Verchere CB (2014) Resident macrophages mediate islet amyloid polypeptide-induced islet IL-1β production and β-cell dysfunction. Diabetes 63:1698–1711. doi: 10.2337/db13-0863

75. Westwell-Roper CY, Chehroudi CA, Denroche HC, et al. (2015) IL-1 mediates amyloid-associated islet dysfunction and inflammation in human islet amyloid polypeptide transgenic mice. Diabetologia 58:575–585. doi: 10.1007/s00125-014-3447-x

76. Kay TW, Thomas HE, Harrison LC, Allison J (2000) The beta cell in autoimmune diabetes: many mechanisms and pathways of loss. Trends in endocrinology and metabolism: TEM 11:11–15.

77. Eizirik DL, Colli ML, Ortis F (2009) The role of inflammation in insulitis and beta-cell loss in type 1 diabetes. Nature reviews Endocrinology 5:219–226. doi: 10.1038/nrendo.2009.21

78. Suk K, Kim S, Kim YH, et al. (2001) IFN-gamma/TNF-alpha synergism as the final effector in autoimmune diabetes: a key role for STAT1/IFN regulatory factor-1 pathway in pancreatic beta cell death. Journal of immunology (Baltimore, Md : 1950) 166:4481–4489.

79. Grunnet LG, Mandrup-Poulsen T (2011) Cytokines and type 1 diabetes: a numbers game. Diabetes 60:697–699. doi: 10.2337/db10-1782

80. Kim S, Kim HS, Chung KW, et al. (2007) Essential role for signal transducer and activator of transcription-1 in pancreatic beta-cell death and autoimmune type 1 diabetes of nonobese diabetic mice. Diabetes 56:2561–2568. doi: 10.2337/db06-1372

81. Eizirik DL, Mandrup-Poulsen T (2001) A choice of death--the signal-transduction of immune-mediated beta-cell apoptosis. Diabetologia 44:2115–2133. doi: 10.1007/s001250100021

82. Dupraz P, Cottet S, Hamburger F, et al. (2000) Dominant negative MyD88 proteins inhibit interleukin-1beta /interferon-gamma -mediated induction of nuclear factor kappa B-dependent nitrite production and apoptosis in beta cells. The Journal of biological chemistry 275:37672–37678. doi: 10.1074/jbc.M005150200

83. Gilmore TD (1999) The Rel/NF-kappaB signal transduction pathway: introduction. Oncogene 18:6842–6844. doi: 10.1038/sj.onc.1203237

84. Saklatvala J, Dean J, Finch A (1999) Protein kinase cascades in intracellular signalling by interleukin-I and tumour necrosis factor. Biochem Soc Symp 64:63–77.

85. Tau G, Rothman P (1999) Biologic functions of the IFN-gamma receptors. Allergy 54:1233–1251.

86. Eizirik DL, Sandler S, Welsh N, et al. (1994) Cytokines suppress human islet function irrespective of their effects on nitric oxide generation. The Journal of clinical investigation 93:1968–1974. doi: 10.1172/JCI117188

87. Ortis F, Pirot P, Naamane N, et al. (2008) Induction of nuclear factor-kappaB and its downstream genes by TNF-alpha and IL-1beta has a pro-apoptotic role in pancreatic beta cells. Diabetologia 51:1213–1225. doi: 10.1007/s00125-008-0999-7

88. Reddy SA, Huang JH, Liao WS (1997) Phosphatidylinositol 3-kinase in interleukin 1 signaling. Physical interaction with the interleukin 1 receptor and requirement in NFkappaB and AP-1 activation. The Journal of biological chemistry 272:29167–29173.

89. Stark GR, Kerr IM, Williams BR, et al. (1998) How cells respond to interferons. Annu Rev Biochem 67:227–264. doi: 10.1146/annurev.biochem.67.1.227

90. Rath PC, Aggarwal BB (1999) TNF-induced signaling in apoptosis. J Clin Immunol 19:350–364.

91. Hoffmann A, Leung TH, Baltimore D (2003) Genetic analysis of NF-kappaB/Rel transcription factors defines functional specificities. The EMBO journal 22:5530–5539. doi: 10.1093/emboj/cdg534

92. Hayden MS, Ghosh S (2008) Shared principles in NF-kappaB signaling. Cell 132:344–362. doi: 10.1016/j.cell.2008.01.020

93. Hayden MS, Ghosh S (2004) Signaling to NF-kappaB. Genes & Development 18:2195–2224. doi: 10.1101/gad.1228704

94. Papaccio G, Graziano A, d'Aquino R, et al. (2005) A biphasic role of nuclear transcription factor (NF)-kappaB in the islet beta-cell apoptosis induced by interleukin (IL)-1beta. Journal of Cellular Physiology 204:124–130. doi: 10.1002/jcp.20276

95. Böni-Schnetzler M, Boller S, Debray S, et al. (2009) Free fatty acids induce a proinflammatory response in islets via the abundantly expressed interleukin-1 receptor I. Endocrinology 150:5218–5229. doi: 10.1210/en.2009-0543

96. Maedler K (2008) Beta cells in type 2 diabetes - a crucial contribution to pathogenesis. Diabetes, Obesity and Metabolism 10:408–420. doi: 10.1111/j.1463-1326.2007.00718.x

97. Ehses JA, Perren A, Eppler E, et al. (2007) Increased number of islet-associated macrophages in type 2 diabetes. Diabetes 56:2356–2370. doi: 10.2337/db06-1650

98. Larsen CM, Faulenbach M, Vaag A, et al. (2007) Interleukin-1-receptor antagonist in type 2 diabetes mellitus. The New England journal of medicine 356:1517–1526. doi: 10.1056/NEJMoa065213

99. Böni-Schnetzler M, Ehses JA, Faulenbach M, Donath MY (2008) Insulitis in type 2 diabetes. Diabetes, Obesity and Metabolism 10 Suppl 4:201–204. doi: 10.1111/j.1463-1326.2008.00950.x

100. Ehses JA, Böni-Schnetzler M, Faulenbach M, Donath MY (2008) Macrophages, cytokines and beta-cell death in Type 2 diabetes. Biochemical Society Transactions 36:340–342. doi: 10.1042/BST0360340

101. Donath MY, Böni-Schnetzler M, Ellingsgaard H, Ehses JA (2009) Islet inflammation impairs the pancreatic beta-cell in type 2 diabetes. Physiology (Bethesda, Md) 24:325–331. doi: 10.1152/physiol.00032.2009

102. Schroder K, Zhou R, Tschopp J (2010) The NLRP3 inflammasome: a sensor for metabolic danger? Science 327:296–300. doi: 10.1126/science.1184003

103. Jin C, Flavell RA (2010) Molecular mechanism of NLRP3 inflammasome activation. J Clin Immunol 30:628–631. doi: 10.1007/s10875-010-9440-3

104. Foster SL, Medzhitov R (2009) Gene-specific control of the TLR-induced inflammatory response. Clin Immunol 130:7–15. doi: 10.1016/j.clim.2008.08.015

105. Kawai T, Akira S (2008) Toll-like receptor and RIG-I-like receptor signaling. Annals of the New York Academy of Sciences 1143:1–20. doi: 10.1196/annals.1443.020

106. Talchai C, Xuan S, Lin HV, et al. (2012) Pancreatic β cell dedifferentiation as a mechanism of diabetic β cell failure. Cell 150:1223–1234. doi: 10.1016/j.cell.2012.07.029

107. Dor Y, Glaser B (2013) β-cell dedifferentiation and type 2 diabetes. The New England journal of medicine 368:572–573. doi: 10.1056/NEJMcibr1214034

108. Blum B, Roose AN, Barrandon O, et al. (2014) Reversal of β cell de-differentiation by a small molecule inhibitor of the TGFβ pathway. Elife 3:e02809. doi: 10.7554/eLife.02809

109. Darville MI, Eizirik DL (2006) Notch signaling: a mediator of beta-cell de-differentiation in diabetes? Biochemical and Biophysical Research Communications 339:1063–1068. doi: 10.1016/j.bbrc.2005.11.111

110. Wang Z, York NW, Nichols CG, Remedi MS (2014) Pancreatic β cell dedifferentiation in diabetes and redifferentiation following insulin therapy. Cell Metabolism 19:872–882. doi: 10.1016/j.cmet.2014.03.010

111. Guo S, Dai C, Guo M, et al. (2013) Inactivation of specific β cell transcription factors in type 2 diabetes. The Journal of clinical investigation 123:3305–3316. doi: 10.1172/JCI65390

112. Elmore S (2007) Apoptosis: a review of programmed cell death. Toxicologic pathology 35:495–516. doi: 10.1080/01926230701320337

113. Johnson JD, Luciani DS (2010) Mechanisms of pancreatic beta-cell apoptosis in

diabetes and its therapies. Advances in experimental medicine and biology 654:447–462. doi: 10.1007/978-90-481-3271-3_19

114. Cnop M, Welsh N, Jonas J-C, et al. (2005) Mechanisms of pancreatic beta-cell death in type 1 and type 2 diabetes: many differences, few similarities. Diabetes 54 Suppl 2:S97–107.

115. Carrington EM, McKenzie MD, Jansen E, et al. (2009) Islet beta-cells deficient in Bcl-xL develop but are abnormally sensitive to apoptotic stimuli. Diabetes 58:2316–2323. doi: 10.2337/db08-1602

116. Chipuk JE, Fisher JC, Dillon CP, et al. (2008) Mechanism of apoptosis induction by inhibition of the anti-apoptotic BCL-2 proteins. Proceedings of the National Academy of Sciences of the United States of America 105:20327–20332. doi: 10.1073/pnas.0808036105

117. Cory S, Adams JM (2002) The Bcl2 family: regulators of the cellular life-or-death switch. Nature reviews Cancer 2:647–656. doi: 10.1038/nrc883

118. Edlich F, Banerjee S, Suzuki M, et al. (2011) Bcl-x(L) retrotranslocates Bax from the mitochondria into the cytosol. Cell 145:104–116. doi: 10.1016/j.cell.2011.02.034

119. Martinou J-C, Youle RJ (2011) Mitochondria in Apoptosis: Bcl-2 Family Members and Mitochondrial Dynamics. Developmental Cell 21:92–101. doi: 10.1016/j.devcel.2011.06.017

120. Alejandro EU, Johnson JD (2008) Inhibition of Raf-1 alters multiple downstream pathways to induce pancreatic beta-cell apoptosis. The Journal of biological chemistry 283:2407–2417. doi: 10.1074/jbc.M703612200

121. Plesner A, Liston P, Tan R, et al. (2005) The X-linked inhibitor of apoptosis protein enhances survival of murine islet allografts. Diabetes 54:2533–2540.

122. Srinivasan S, Bernal-Mizrachi E, Ohsugi M, Permutt MA (2002) Glucose promotes pancreatic islet beta-cell survival through a PI 3-kinase/Akt-signaling pathway. American journal of physiology Endocrinology and metabolism 283:E784–93. doi: 10.1152/ajpendo.00177.2002

123. Ryan EA, Lakey JR, Rajotte RV, et al. (2001) Clinical outcomes and insulin secretion after islet transplantation with the Edmonton protocol. Diabetes 50:710–719.

124. Cleaver O, MacDonald RJ (2010) Developmental molecular biology of the pancreas. Pancreatic Cancer. doi: 10.1007/978-0-387-77498-5_4

125. Pan FC, Wright C (2011) Pancreas organogenesis: from bud to plexus to gland. Developmental Dynamics 240:530–565. doi: 10.1002/dvdy.22584

126. Herrera PL (2000) Adult insulin- and glucagon-producing cells differentiate from two independent cell lineages. Development (Cambridge, England) 127:2317–2322.

127. Herrera PL, Nepote V, Delacour A (2002) Pancreatic cell lineage analyses in mice. Endocrine 19:267–278. doi: 10.1385/ENDO:19:3:267

128. Larsson LI (1998) On the development of the islets of Langerhans. Microsc Res Tech 43:284–291. doi: 10.1002/(SICI)1097-0029(19981115)43:4<284::AID-JEMT2>3.0.CO;2-0

129. Piper K, Brickwood S, Turnpenny LW, et al. (2004) Beta cell differentiation during early human pancreas development. The Journal of endocrinology 181:11–23.

130. Polak M, Bouchareb-Banaei L, Scharfmann R, Czernichow P (2000) Early pattern of differentiation in the human pancreas. Diabetes 49:225–232.

131. Hara A, Kadoya Y, Kojima I, Yamashina S (2007) Rat pancreatic islet is formed by unification of multiple endocrine cell clusters. Developmental dynamics : an official publication of the American Association of Anatomists 236:3451–3458. doi: 10.1002/dvdy.21359

132. Gradwohl G, Dierich A, LeMeur M, Guillemot F (2000) neurogenin3 is required for the development of the four endocrine cell lineages of the pancreas. Proceedings of the National Academy of Sciences of the United States of America 97:1607–1611.

133. Gu G, Dubauskaite J, Melton DA (2002) Direct evidence for the pancreatic lineage: NGN3+ cells are islet progenitors and are distinct from duct progenitors. Development (Cambridge, England) 129:2447–2457.

134. Lee JC, Smith SB, Watada H, et al. (2001) Regulation of the pancreatic pro-endocrine gene neurogenin3. Diabetes 50:928–936.

135. Lynn FC, Smith SB, Wilson ME, et al. (2007) Sox9 coordinates a transcriptional network in pancreatic progenitor cells. Proceedings of the National Academy of Sciences of the United States of America 104:10500–10505. doi: 10.1073/pnas.0704054104

136. Oliver-Krasinski JM, Kasner MT, Yang J, et al. (2009) The diabetes gene Pdx1 regulates the transcriptional network of pancreatic endocrine progenitor cells in mice. The Journal of clinical investigation 119:1888–1898. doi: 10.1172/JCI37028

137. Gouzi M, Kim YH, Katsumoto K, et al. (2011) Neurogenin3 initiates stepwise delamination of differentiating endocrine cells during pancreas development. Developmental Dynamics 240:589–604. doi: 10.1002/dvdy.22544

138. Metzger DE, Gasperowicz M, Otto F, et al. (2012) The transcriptional co-repressor Grg3/Tle3 promotes pancreatic endocrine progenitor delamination and β-cell differentiation. Development 139:1447–1456. doi: 10.1242/dev.072892

139. Habener JF, Kemp DM, Thomas MK (2005) Minireview: transcriptional regulation in pancreatic development. Endocrinology 146:1025–1034. doi: 10.1210/en.2004-1576

140. Naya FJ, Huang HP, Qiu Y, et al. (1997) Diabetes, defective pancreatic morphogenesis, and abnormal enteroendocrine differentiation in BETA2/neuroD-deficient mice. Genes & Development 11:2323–2334.

141. Collombat P, Hecksher-Sørensen J, Serup P, Mansouri A (2006) Specifying pancreatic endocrine cell fates. Mechanisms of Development 123:501–512. doi: 10.1016/j.mod.2006.05.006

142. Sussel L, Kalamaras J, Hartigan-O'Connor DJ, et al. (1998) Mice lacking the homeodomain transcription factor Nkx2.2 have diabetes due to arrested differentiation of pancreatic beta cells. Development (Cambridge, England) 125:2213–2221.

143. Sander M, Sussel L, Conners J, et al. (2000) Homeobox gene Nkx6.1 lies downstream of Nkx2.2 in the major pathway of beta-cell formation in the pancreas. Development (Cambridge, England) 127:5533–5540.

144. Collombat P, Hecksher-Sørensen J, Krull J, et al. (2007) Embryonic endocrine pancreas and mature β cells acquire α and PP cell phenotypes upon Arx misexpression. Journal of Clinical Investigation 117:961–970. doi: 10.1172/JCI29115

145. Collombat P, Mansouri A, Hecksher-Sørensen J, et al. (2003) Opposing actions of Arx and Pax4 in endocrine pancreas development. Genes & Development 17:2591–2603. doi: 10.1101/gad.269003

146. Kesavan G, Lieven O, Mamidi A, et al. (2014) Cdc42/N-WASP signaling links actin dynamics to pancreatic β cell delamination and differentiation. Development 141:685–696. doi: 10.1242/dev.100297

147. Kim HJ, Schleiffarth JR, Jessurun J, et al. (2005) Wnt5 signaling in vertebrate pancreas development. BMC Biol 3:23. doi: 10.1186/1741-7007-3-23

148. Greiner TU, Kesavan G, Ståhlberg A, Semb H (2009) Rac1 regulates pancreatic islet morphogenesis. BMC Developmental Biology 9:2. doi: 10.1186/1471-213X-9-2

149. Miller K, Kim A, Kilimnik G, et al. (2009) Islet formation during the neonatal development in mice. PloS one 4:e7739. doi: 10.1371/journal.pone.0007739

150. Aramata S, Han S-I, Kataoka K (2007) Roles and regulation of transcription factor MafA in islet beta-cells. Endocrine journal 54:659–666.

151. Zhang C, Moriguchi T, Kajihara M, et al. (2005) MafA is a key regulator of glucose-stimulated insulin secretion. Molecular and Cellular Biology 25:4969–4976. doi:

10.1128/MCB.25.12.4969-4976.2005

152. Gu C, Stein GH, Pan N, et al. (2010) Pancreatic β Cells Require NeuroD to Achieve and Maintain Functional Maturity. Cell Metabolism 11:298–310. doi: 10.1016/j.cmet.2010.03.006

153. Aguayo-Mazzucato C, Zavacki AM, Marinelarena A, et al. (2013) Thyroid hormone promotes postnatal rat pancreatic β-cell development and glucose-responsive insulin secretion through MAFA. Diabetes 62:1569–1580. doi: 10.2337/db12-0849

154. Jermendy A, Toschi E, Aye T, et al. (2011) Rat neonatal beta cells lack the specialised metabolic phenotype of mature beta cells. Diabetologia 54:594–604. doi: 10.1007/s00125-010-2036-x

155. Szabat M, Lynn FC, Hoffman BG, et al. (2012) Maintenance of β-cell maturity and plasticity in the adult pancreas: developmental biology concepts in adult physiology. Diabetes 61:1365–1371. doi: 10.2337/db11-1361

156. Szabat M, Luciani DS, Piret JM, Johnson JD (2009) Maturation of adult beta-cells revealed using a Pdx1/insulin dual-reporter lentivirus. Endocrinology 150:1627–1635. doi: 10.1210/en.2008-1224

157. Rutter GA, Pullen TJ, Hodson DJ, Martinez-Sanchez A (2015) Pancreatic β-cell identity, glucose sensing and the control of insulin secretion. The Biochemical journal 466:203–218. doi: 10.1042/BJ20141384

158. Johnson JH, Newgard CB, Milburn JL, et al. (1990) The high Km glucose transporter of islets of Langerhans is functionally similar to the low affinity transporter of liver and has an identical primary sequence. The Journal of biological chemistry 265:6548–6551.

159. Unger RH (1991) Diabetic hyperglycemia: link to impaired glucose transport in pancreatic beta cells. Science 251:1200–1205.

160. Prentki M, Matschinsky FM, Madiraju SRM (2013) Metabolic signaling in fuel-induced insulin secretion. Cell Metabolism 18:162–185. doi: 10.1016/j.cmet.2013.05.018

161. Dean PM, Matthews EK (1970) Electrical activity in pancreatic islet cells: effect of ions. J Physiol (Lond) 210:265–275.

162. Ribalet B, Beigelman PM (1980) Calcium action potentials and potassium permeability activation in pancreatic beta-cells. Am J Physiol 239:C124–33.

163. Porte D, Pupo AA (1969) Insulin responses to glucose: evidence for a two pool system in man. The Journal of clinical investigation 48:2309–2319. doi: 10.1172/JCI106197

164. Bellefroid EJ, Bourguignon C, Hollemann T, Ma Q (1996) X-MyT1, a Xenopus C2HC-type zinc finger protein with a regulatory function in neuronal differentiation. Cell

165. Yee KS, Yu VC (1998) Isolation and characterization of a novel member of the neural zinc finger factor/myelin transcription factor family with transcriptional repression activity. The Journal of biological chemistry 273:5366–5374.

166. Kim JG, Armstrong RC, Agoston DV, et al. (1997) Myelin transcription factor 1 (Myt1) of the oligodendrocyte lineage, along with a closely related CCHC zinc finger, is expressed in developing neurons in the mammalian central nervous system. Journal of neuroscience research 50:272–290.

167. Kim JG, Hudson LD (1992) Novel member of the zinc finger superfamily: A C2-HC finger that recognizes a glia-specific gene. Molecular and Cellular Biology 12:5632–5639.

168. Romm E, Nielsen JA, Kim JG, Hudson LD (2005) Myt1 family recruits histone deacetylase to regulate neural transcription. Journal of Neurochemistry 93:1444–1453. doi: 10.1111/j.1471-4159.2005.03131.x

169. Silverstein RA, Ekwall K (2005) Sin3: a flexible regulator of global gene expression and genome stability. Current Genetics 47:1–17. doi: 10.1007/s00294-004-0541-5

170. Alland L, Muhle R, Hou H, et al. (1997) Role for N-CoR and histone deacetylase in Sin3-mediated transcriptional repression. Nature 387:49–55. doi: 10.1038/387049a0

171. Kutlu B, Cardozo AK, Darville MI, et al. (2003) Discovery of gene networks regulating cytokine-induced dysfunction and apoptosis in insulin-producing INS-1 cells. Diabetes 52:2701–2719.

172. Sarkar SA, Kutlu B, Velmurugan K, et al. (2009) Cytokine-mediated induction of anti-apoptotic genes that are linked to nuclear factor kappa-B (NF-kappaB) signalling in human islets and in a mouse beta cell line. Diabetologia 52:1092–1101. doi: 10.1007/s00125-009-1331-x

173. Zhang T-J, Hoffman BG, Ruiz de Algara T, Helgason CD (2006) SAGE reveals expression of Wnt signalling pathway members during mouse prostate development. Gene Expression Patterns 6:310–324. doi: 10.1016/j.modgep.2005.07.005

174. Hoffman BG, Williams KL, Tien AH, et al. (2005) Identification of novel genes and transcription factors involved in spleen, thymus and immunological development and function. Genes Immun 7:101–112. doi: 10.1038/sj.gene.6364270

175. Hoffman BG, Zavaglia B, Beach M, Helgason CD (2008) Expression of Groucho/TLE proteins during pancreas development. BMC Developmental Biology 8:81. doi: 10.1186/1471-213X-8-81

176. Gao N, White P, Doliba N, et al. (2007) Foxa2 controls vesicle docking and insulin secretion in mature Beta cells. Cell Metabolism 6:267–279. doi: 10.1016/j.cmet.2007.08.015

177. Gauthier BR, Wiederkehr A, BaquiE M, et al. (2009) PDX1 deficiency causes mitochondrial dysfunction and defective insulin secretion through TFAM suppression. Cell Metabolism 10:110–118. doi: 10.1016/j.cmet.2009.07.002

178. Johnson JD, Ahmed NT, Luciani DS, et al. (2003) Increased islet apoptosis in Pdx1+/- mice. The Journal of clinical investigation 111:1147–1160. doi: 10.1172/JCI16537

179. Schisler JC, Jensen PB, Taylor DG, et al. (2005) The Nkx6.1 homeodomain transcription factor suppresses glucagon expression and regulates glucose-stimulated insulin secretion in islet beta cells. Proceedings of the National Academy of Sciences 102:7297–7302. doi: 10.1073/pnas.0502168102

180. Aramata S, Han S-I, Yasuda K, Kataoka K (2005) Synergistic activation of the insulin gene promoter by the beta-cell enriched transcription factors MafA, Beta2, and Pdx1. Biochimica et biophysica acta 1730:41–46. doi: 10.1016/j.bbaexp.2005.05.009

181. Babu DA, Deering TG, Mirmira RG (2007) A feat of metabolic proportions: Pdx1 orchestrates islet development and function in the maintenance of glucose homeostasis. Mol Genet Metab 92:43–55. doi: 10.1016/j.ymgme.2007.06.008

182. Gao N, LeLay J, Vatamaniuk MZ, et al. (2008) Dynamic regulation of Pdx1 enhancers by Foxa1 and Foxa2 is essential for pancreas development. Genes & Development 22:3435–3448. doi: 10.1101/gad.1752608

183. Gao N, Gao N, Le Lay J, et al. (2010) Foxa1 and Foxa2 Maintain the Metabolic and Secretory Features of the Mature β-Cell. Molecular Endocrinology 24:1594–1604. doi: 10.1210/me.2009-0513

184. Gamsjaeger R, Gamsjaeger R, Gamsjaeger, et al. (2008) Structural and biophysical analysis of the DNA binding properties of myelin transcription factor 1. The Journal of biological chemistry 283:5158–5167. doi: 10.1074/jbc.M703772200

185. Hoffman BG, Robertson G, Zavaglia B, et al. (2010) Locus co-occupancy, nucleosome positioning, and H3K4me1 regulate the functionality of FOXA2-, HNF4A-, and PDX1-bound loci in islets and liver. Genome Research 20:1037–1051. doi: 10.1101/gr.104356.109

186. Miyazaki J, Araki K, Yamato E, et al. (1990) Establishment of a pancreatic beta cell line that retains glucose-inducible insulin secretion: special reference to expression of glucose transporter isoforms. Endocrinology 127:126–132. doi: 10.1210/endo-127-1-126

187. Yoshida T, Hanahan D (1994) Murine pancreatic ductal adenocarcinoma produced by in vitro transduction of polyoma middle T oncogene into the islets of Langerhans. Am J Pathol 145:671–684.

188. Luo J, Deng Z-L, Luo X, et al. (2007) A protocol for rapid generation of recombinant adenoviruses using the AdEasy system. Nature protocols 2:1236–1247. doi: 10.1038/nprot.2007.135

189. Hagman DK, Hays LB, Parazzoli SD, Poitout V (2005) Palmitate Inhibits Insulin Gene Expression by Altering PDX-1 Nuclear Localization and Reducing MafA Expression in Isolated Rat Islets of Langerhans. Journal of Biological Chemistry 280:32413–32418. doi: 10.1074/jbc.M506000200

190. Andrali SS, Qian Q, Ozcan S (2007) Glucose mediates the translocation of NeuroD1 by O-linked glycosylation. The Journal of biological chemistry 282:15589–15596. doi: 10.1074/jbc.M701762200

191. Cai T, Chen X, Wang R, et al. (2011) Expression of Insulinoma-Associated 2 (INSM2) in Pancreatic Islet Cells Is Regulated by the Transcription Factors Ngn3 and NeuroD1. Endocrinology 152:1961–1969. doi: 10.1210/en.2010-1065

192. Gasa R, Mrejen C, Lynn FC, et al. (2008) Induction of pancreatic islet cell differentiation by the neurogenin-neuroD cascade. Differentiation 76:381–391. doi: 10.1111/j.1432-0436.2007.00228.x

193. Bernstein BE, Humphrey EL, Erlich RL, et al. (2002) Methylation of histone H3 Lys 4 in coding regions of active genes. Proceedings of the National Academy of Sciences 99:8695–8700. doi: 10.1073/pnas.082249499

194. Heintzman ND, Hon GC, Hawkins RD, et al. (2009) Histone modifications at human enhancers reflect global cell-type-specific gene expression. Nature 459:108–112. doi: 10.1038/nature07829

195. Heintzman ND, Stuart RK, Hon G, et al. (2007) Distinct and predictive chromatin signatures of transcriptional promoters and enhancers in the human genome. Nature Genetics 39:311–318. doi: 10.1038/ng1966

196. Santos-Rosa H, Schneider R, Bannister AJ, et al. (2002) Active genes are tri-methylated at K4 of histone H3. Nature 419:407–411. doi: 10.1038/nature01080

197. Andrali SS, Sampley ML, Vanderford NL, Ozcan S (2008) Glucose regulation of insulin gene expression in pancreatic beta-cells. The Biochemical journal 415:1–10. doi: 10.1042/BJ20081029

198. Vanderford NL, erford, Andrali SS, Ozcan S (2007) Glucose induces MafA expression in pancreatic beta cell lines via the hexosamine biosynthetic pathway. The Journal of biological chemistry 282:1577–1584. doi: 10.1074/jbc.M605064200

199. Macfarlane WM, Macfarlane WM, Campbell SC, et al. (2000) Glucose regulates islet amyloid polypeptide gene transcription in a PDX1- and calcium-dependent manner. The Journal of biological chemistry 275:15330–15335. doi: 10.1074/jbc.M908045199

200. Cardozo AK, Kruhøffer M, Leeman R, et al. (2001) Identification of novel cytokine-induced genes in pancreatic beta-cells by high-density oligonucleotide arrays. Diabetes 50:909–920.

201. Brissova M, Shiota M, Nicholson WE, et al. (2002) Reduction in pancreatic transcription factor PDX-1 impairs glucose-stimulated insulin secretion. The Journal of biological chemistry 277:11225–11232. doi: 10.1074/jbc.M111272200

202. Hotamisligil GS (2010) Endoplasmic reticulum stress and the inflammatory basis of metabolic disease. Cell 140:900–917. doi: 10.1016/j.cell.2010.02.034

203. Cunha DA, Ladrière L, Ortis F, et al. (2009) Glucagon-like peptide-1 agonists protect pancreatic beta-cells from lipotoxic endoplasmic reticulum stress through upregulation of BiP and JunB. Diabetes 58:2851–2862. doi: 10.2337/db09-0685

204. Matsushita F, Kameyama T, Marunouchi T (2002) NZF-2b is a novel predominant form of mouse NZF-2/MyT1, expressed in differentiated neurons especially at higher levels in newly generated ones. Mechanisms of Development 118:209–213.

205. Gu G, Wells JM, Dombkowski D, et al. (2004) Global expression analysis of gene regulatory pathways during endocrine pancreatic development. Development (Cambridge, England) 131:165–179. doi: 10.1242/dev.00921

206. Schuit F, Schuit F, Flamez D, et al. (2002) Glucose-regulated gene expression maintaining the glucose-responsive state of beta-cells. Diabetes 51 Suppl 3:S326–32.

207. Macfarlane WM, McKinnon CM, Felton-Edkins ZA, et al. (1999) Glucose stimulates translocation of the homeodomain transcription factor PDX1 from the cytoplasm to the nucleus in pancreatic beta-cells. The Journal of biological chemistry 274:1011–1016.

208. Ehses JA, Ellingsgaard H, Böni-Schnetzler M, Donath MY (2009) Pancreatic islet inflammation in type 2 diabetes: from alpha and beta cell compensation to dysfunction. Arch Physiol Biochem 115:240–247. doi: 10.1080/13813450903025879

209. Henry C, Close A-F, Buteau J (2014) A critical role for the neural zinc factor ST18 in pancreatic β-cell apoptosis. The Journal of biological chemistry 289:8413–8419. doi: 10.1074/jbc.M114.554915

210. Liston P, Fong WG, Korneluk RG (2003) The inhibitors of apoptosis: there is more to life than Bcl2. Oncogene 22:8568–8580. doi: 10.1038/sj.onc.1207101

211. Ellingsgaard H, Hauselmann I, Schuler B, et al. (2011) Interleukin-6 enhances insulin secretion by increasing glucagon-like peptide-1 secretion from L cells and alpha cells. Nature Medicine 17:1481–1489. doi: 10.1038/nm.2513

212. Cornu M, Yang J-Y, Jaccard E, et al. (2009) Glucagon-like peptide-1 protects beta-cells against apoptosis by increasing the activity of an IGF-2/IGF-1 receptor autocrine loop. Diabetes 58:1816–1825. doi: 10.2337/db09-0063

213. Ueki K, Okada T, Hu J, et al. (2006) Total insulin and IGF-I resistance in pancreatic beta cells causes overt diabetes. Nature Genetics 38:583–588. doi: 10.1038/ng1787

214. Choi S-E, Choi K-M, Yoon I-H, et al. (2004) IL-6 protects pancreatic islet beta cells from pro-inflammatory cytokines-induced cell death and functional impairment in vitro and in vivo. Transpl Immunol 13:43–53. doi: 10.1016/j.trim.2004.04.001

215. Miettinen PJ, Huotari M, Koivisto T, et al. (2000) Impaired migration and delayed differentiation of pancreatic islet cells in mice lacking EGF-receptors. Development (Cambridge, England) 127:2617–2627.

216. Tennant BR, Islam R, Kramer MM, et al. (2012) The transcription factor *Myt3* acts as a pro-survival factor in β-cells. PloS one 7:e51501. doi: 10.1371/journal.pone.0051501

217. Ichikawa T, Nakazato K, Keller PJ, et al. (2013) Live imaging of whole mouse embryos during gastrulation: migration analyses of epiblast and mesodermal cells. PloS one 8:e64506. doi: 10.1371/journal.pone.0064506

218. Srinivasan S, Wang F, Glavas S, et al. (2003) Rac and Cdc42 play distinct roles in regulating PI(3,4,5)P3 and polarity during neutrophil chemotaxis. The Journal of cell biology 160:375–385. doi: 10.1083/jcb.200208179

219. Barber MA, Welch HCE (2006) PI3K and RAC signalling in leukocyte and cancer cell migration. Bull Cancer 93:E44–52.

220. Chan AY, Coniglio SJ, Chuang Y-Y, et al. (2005) Roles of the Rac1 and Rac3 GTPases in human tumor cell invasion. Oncogene 24:7821–7829. doi: 10.1038/sj.onc.1208909

221. Vicente-Manzanares M, Horwitz AR (2011) Cell migration: an overview. Methods Mol Biol 769:1–24. doi: 10.1007/978-1-61779-207-6_1

222. Kuang H-B, Miao C-L, Guo W-X, et al. (2009) Dickkopf-1 enhances migration of HEK293 cell by beta-catenin/E-cadherin degradation. Frontiers in bioscience (Landmark edition) 14:2212–2220.

223. Ridley AJ, Schwartz MA, Burridge K, et al. (2003) Cell migration: integrating signals from front to back. Science 302:1704–1709. doi: 10.1126/science.1092053

224. Evers EE, Zondag GC, Malliri A, et al. (2000) Rho family proteins in cell adhesion and cell migration. Eur J Cancer 36:1269–1274.

225. Huttenlocher A, Horwitz AR (2011) Integrins in cell migration. Cold Spring Harbor perspectives in biology 3:a005074. doi: 10.1101/cshperspect.a005074

226. Horwitz R, Webb D (2003) Cell migration. Curr Biol 13:R756–9.

227. Rohatgi R, Ma L, Miki H, et al. (1999) The interaction between N-WASP and the Arp2/3 complex links Cdc42-dependent signals to actin assembly. Cell 97:221–231.

228. Kurisu S, Takenawa T (2009) The WASP and WAVE family proteins. Genome Biology 10:226. doi: 10.1186/gb-2009-10-6-226

229. Ridley AJ (2006) Rho GTPases and actin dynamics in membrane protrusions and vesicle trafficking. Trends in cell biology 16:522–529. doi: 10.1016/j.tcb.2006.08.006

230. Zhang W, Wu Y, Liping du, et al. (2005) Activation of the Arp2/3 complex by N-WASp is required for actin polymerization and contraction in smooth muscle. American journal of physiology Cell physiology 288:C1145–60. doi: 10.1152/ajpcell.00387.2004

231. Aplin AE, Howe A, Alahari SK, Juliano RL (1998) Signal transduction and signal modulation by cell adhesion receptors: the role of integrins, cadherins, immunoglobulin-cell adhesion molecules, and selectins. Pharmacol Rev 50:197–263.

232. Bosco D, Meda P, Halban PA, Rouiller DG (2000) Importance of cell-matrix interactions in rat islet beta-cell secretion in vitro: role of alpha6beta1 integrin. Diabetes 49:233–243.

233. Wang R, Li J, Lyte K, et al. (2005) Role for beta1 integrin and its associated alpha3, alpha5, and alpha6 subunits in development of the human fetal pancreas. Diabetes 54:2080–2089.

234. Hara M, Wang X, Kawamura T, et al. (2003) Transgenic mice with green fluorescent protein-labeled pancreatic beta-cells. American journal of physiology Endocrinology and metabolism 284:E177–83. doi: 10.1152/ajpendo.00321.2002

235. Luciani DS, White SA, Widenmaier SB, et al. (2013) Bcl-2 and Bcl-xL suppress glucose signaling in pancreatic β-cells. Diabetes 62:170–182. doi: 10.2337/db11-1464

236. Langhofer M, Hopkinson SB, Jones JC (1993) The matrix secreted by 804G cells contains laminin-related components that participate in hemidesmosome assembly in vitro. Journal of Cell Science 105 (Pt 3):753–764.

237. Luciani DS, Ao P, Hu X, et al. (2007) Voltage-gated Ca(2+) influx and insulin

secretion in human and mouse beta-cells are impaired by the mitochondrial Na(+)/Ca(2+) exchange inhibitor CGP-37157. Eur J Pharmacol 576:18–25. doi: 10.1016/j.ejphar.2007.07.055

238. Trapnell C, Roberts A, Goff L, et al. (2012) Differential gene and transcript expression analysis of RNA-seq experiments with TopHat and Cufflinks. Nature protocols 7:562–578. doi: 10.1038/nprot.2012.016

239. Hammar E, Parnaud G, Bosco D, et al. (2004) Extracellular matrix protects pancreatic beta-cells against apoptosis: role of short- and long-term signaling pathways. Diabetes 53:2034–2041.

240. Steer SA, Scarim AL, Chambers KT, Corbett JA (2006) Interleukin-1 stimulates beta-cell necrosis and release of the immunological adjuvant HMGB1. PLoS medicine 3:e17. doi: 10.1371/journal.pmed.0030017

241. Ortis F, Cardozo AK, Crispim D, et al. (2006) Cytokine-induced proapoptotic gene expression in insulin-producing cells is related to rapid, sustained, and nonoscillatory nuclear factor-kappaB activation. Mol Endocrinol 20:1867–1879. doi: 10.1210/me.2005-0268

242. Donath MY, Størling J, Berchtold LA, et al. (2008) Cytokines and beta-cell biology: from concept to clinical translation. Endocrine Reviews 29:334–350. doi: 10.1210/er.2007-0033

243. Wei MC, Zong WX, Cheng EH, et al. (2001) Proapoptotic BAX and BAK: a requisite gateway to mitochondrial dysfunction and death. Science 292:727–730. doi: 10.1126/science.1059108

244. Rountree AM, Neal AS, Lisowski M, et al. (2014) Control of insulin secretion by cytochrome C and calcium signaling in islets with impaired metabolism. The Journal of biological chemistry 289:19110–19119. doi: 10.1074/jbc.M114.556050

245. Parnaud G, Hammar E, Rouiller DG, et al. (2006) Blockade of beta1 integrin-laminin-5 interaction affects spreading and insulin secretion of rat beta-cells attached on extracellular matrix. Diabetes 55:1413–1420.

246. Riopel M, Krishnamurthy M, Li J, et al. (2011) Conditional β1-integrin-deficient mice display impaired pancreatic β cell function. The Journal of pathology 224:45–55. doi: 10.1002/path.2849

247. Saleem S, Li J, Yee S-P, et al. (2009) beta1 integrin/FAK/ERK signalling pathway is essential for human fetal islet cell differentiation and survival. The Journal of pathology 219:182–192. doi: 10.1002/path.2577

248. Cai EP, Casimir M, Schroer SA, et al. (2012) In vivo role of focal adhesion kinase in regulating pancreatic β-cell mass and function through insulin signaling, actin dynamics, and granule trafficking. Diabetes 61:1708–1718. doi: 10.2337/db11-1344

249. Kalwat MA, Thurmond DC (2013) Signaling mechanisms of glucose-induced F-actin remodeling in pancreatic islet β cells. Experimental & Molecular Medicine 45:e37. doi: 10.1038/emm.2013.73

250. Kalwat MA, Yoder SM, Wang Z, Thurmond DC (2013) A p21-activated kinase (PAK1) signaling cascade coordinately regulates F-actin remodeling and insulin granule exocytosis in pancreatic β cells. Biochemical Pharmacology 85:808–816. doi: 10.1016/j.bcp.2012.12.003

251. Han B, Qi S, Hu B, et al. (2011) TGF-beta i promotes islet beta-cell function and regeneration. Journal of immunology 186:5833–5844. doi: 10.4049/jimmunol.1002303

252. Kim M-O, Yun S-J, Kim I-S, et al. (2003) Transforming growth factor-beta-inducible gene-h3 (beta(ig)-h3) promotes cell adhesion of human astrocytoma cells in vitro: implication of alpha6beta4 integrin. Neurosci Lett 336:93–96.

253. Ferguson JW, Thoma BS, Mikesh MF, et al. (2003) The extracellular matrix protein betaIG-H3 is expressed at myotendinous junctions and supports muscle cell adhesion. Cell Tissue Res 313:93–105. doi: 10.1007/s00441-003-0743-z

254. Han B, Luo H, Raelson J, et al. (2014) TGFBI (βIG-H3) is a diabetes-risk gene based on mouse and human genetic studies. Human Molecular Genetics 23:4597–4611. doi: 10.1093/hmg/ddu173

255. Rondas D, Tomas A, Halban PA (2011) Focal adhesion remodeling is crucial for glucose-stimulated insulin secretion and involves activation of focal adhesion kinase and paxillin. Diabetes 60:1146–1157. doi: 10.2337/db10-0946

256. Shang D, Liu Y, Yang P, et al. (2012) TGFBI-promoted adhesion, migration and invasion of human renal cell carcinoma depends on inactivation of von Hippel-Lindau tumor suppressor. Urology 79:966.e1–7. doi: 10.1016/j.urology.2011.12.011

257. Nummela P, Lammi J, Soikkeli J, et al. (2012) Transforming growth factor beta-induced (TGFBI) is an anti-adhesive protein regulating the invasive growth of melanoma cells. Am J Pathol 180:1663–1674. doi: 10.1016/j.ajpath.2011.12.035

258. Wen G, Partridge MA, Li B, et al. (2011) TGFBI expression reduces in vitro and in vivo metastatic potential of lung and breast tumor cells. Cancer Lett 308:23–32. doi: 10.1016/j.canlet.2011.04.010

259. Clemente-Casares X, Tsai S, Huang C, Santamaria P (2012) Antigen-specific therapeutic approaches in Type 1 diabetes. Cold Spring Harbor Perspectives in Medicine 2:a007773. doi: 10.1101/cshperspect.a007773

260. Greeley SAW, Tucker SE, Worrell HI, et al. (2010) Update in neonatal diabetes. Curr Opin Endocrinol Diabetes Obes 17:13. doi: 10.1097/MED.0b013e328334f158

261. Dror V, Nguyen V, Walia P, et al. (2007) Notch signalling suppresses apoptosis in adult human and mouse pancreatic islet cells. Diabetologia 50:2504–2515. doi: 10.1007/s00125-007-0835-5

262. Luciani DS, Gwiazda KS, Yang T-LB, et al. (2009) Roles of IP3R and RyR Ca2+ channels in endoplasmic reticulum stress and beta-cell death. Diabetes 58:422–432. doi: 10.2337/db07-1762

263. Aiping du, Hunter CS, Murray J, et al. (2009) Islet-1 is required for the maturation, proliferation, and survival of the endocrine pancreas. Diabetes 58:2059–2069. doi: 10.2337/db08-0987

264. Fodor A, Harel C, Fodor L, et al. (2007) Adult rat liver cells transdifferentiated with lentiviral IPF1 vectors reverse diabetes in mice: an ex vivo gene therapy approach. Diabetologia 50:121–130. doi: 10.1007/s00125-006-0509-8

265. Juhl K, Sarkar SA, Wong R, et al. (2008) Mouse pancreatic endocrine cell transcriptome defined in the embryonic Ngn3-null mouse. Diabetes 57:2755–2761. doi: 10.2337/db07-1126

266. Kesavan G, Sand FW, Greiner TU, et al. (2009) Cdc42-mediated tubulogenesis controls cell specification. Cell 139:791–801. doi: 10.1016/j.cell.2009.08.049

267. Borden P, Houtz J, Leach SD, Kuruvilla R (2013) Sympathetic innervation during development is necessary for pancreatic islet architecture and functional maturation. Cell reports 4:287–301. doi: 10.1016/j.celrep.2013.06.019

268. Wang RN, Rosenberg L (1999) Maintenance of beta-cell function and survival following islet isolation requires re-establishment of the islet-matrix relationship. The Journal of endocrinology 163:181–190.

269. Xu Y, Wang S, Zhang J, et al. (2006) The fringe molecules induce endocrine differentiation in embryonic endoderm by activating cMyt1/cMyt3. Developmental Biology 297:340–349. doi: 10.1016/j.ydbio.2006.04.456

270. Jiang Y, Yu VC, Buchholz F, et al. (1996) A novel family of Cys-Cys, His-Cys zinc finger transcription factors expressed in developing nervous system and pituitary gland. The Journal of biological chemistry 271:10723–10730.

271. Suarez-Pinzon WL, Rabinovitch A (2008) Combination therapy with epidermal growth factor and gastrin delays autoimmune diabetes recurrence in nonobese diabetic mice transplanted with syngeneic islets. Transplant Proc 40:529–532. doi: 10.1016/j.transproceed.2008.01.005

272. Rooman I, Bouwens L (2004) Combined gastrin and epidermal growth factor treatment induces islet regeneration and restores normoglycaemia in C57Bl6/J mice treated with alloxan. Diabetologia 47:259–265. doi: 10.1007/s00125-003-1287-1

273. Suarez-Pinzon WL, Rabinovitch A (2011) Combination therapy with a dipeptidyl peptidase-4 inhibitor and a proton pump inhibitor induces β-cell neogenesis from adult human pancreatic duct cells implanted in immunodeficient mice. Cell Transplant 20:1343–1349. doi: 10.3727/096368910X557263

274. Suarez-Pinzon WL, Power RF, Yan Y, et al. (2008) Combination therapy with glucagon-like peptide-1 and gastrin restores normoglycemia in diabetic NOD mice. Diabetes 57:3281–3288. doi: 10.2337/db08-0688

275. Suissa Y, Magenheim J, Stolovich-Rain M, et al. (2013) Gastrin: a distinct fate of neurogenin3 positive progenitor cells in the embryonic pancreas. PloS one 8:e70397. doi: 10.1371/journal.pone.0070397

276. Wierup N, Sundler F, Heller RS (2014) The islet ghrelin cell. Journal of Molecular Endocrinology 52:R35–49. doi: 10.1530/JME-13-0122